Charles University in Prague

Faculty of Science

Department of Organic and Nuclear Chemistry

Mgr. Jiří Míšek

On Azahelicenes: Synthesis, Resolution, Properties and Applications

Ph.D. Thesis

Supervisor:

RNDr. Ivo Starý, CSc.

Institute of Organic Chemistry and Biochemistry, v.v.i.

ÚOCHB AV ČR

Academy of Sciences of the Czech Republic

Prague, 2008

Acknowledgement

Declaration

The Thesis was worked out at the Institute of Organic Chemistry and Biochemistry, v.v.i., Academy of Sciences of the Czech Republic, from 2004 to 2008.

"I hereby declare that I have done this Thesis independently while noting all resources used, as well as all co-authors."

Prague, 20th September 2008

....
                                    Signature

Table of Contents

1   Introduction

Helix is a ubiquitous structural feature occurring from galaxies up to atomic world (Figure 1.1). Since the fundamental work of Watson and Crick showing the helix to be a basic structural concept of DNA[1], a great interest in the field of molecular helical structures has emerged. Helices have also showed to be crucial structures in other biologically important molecules like proteins possessing both structural and functional properties. These findings have stimulated chemical community to emulate nature and create artificial helices with different structures and functions[2-6].

a)   b)   c)
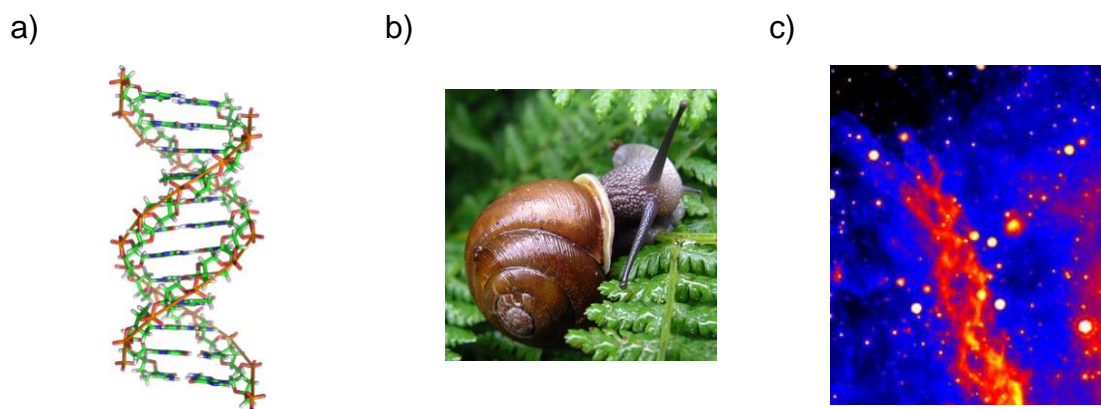
Figure 1.1 Examples of helices in nature: a) DNA double helix. b) Snail's helical shell c) Helical Nebula galaxy

Helix itself can exist in the right- and the left-handed form. It is therefore chiral. Helical chirality of small organic molecules is known but a main attention in the area of molecular chirality has been paid to compounds with central, axial or planar chirality. Syntheses and applications of such enantiomerically pure molecules are well established both in academia and industry. In contrast to this, chemistry of small helically chiral molecules remains underdeveloped, despite the fact that the research in this direction is growing rapidly. Typical examples of small helically chiral molecules are helicenes[7-9], compounds consisting of aromatic or heteroaromatic rings which are all (minimum five) angularly arranged so as to give helically shaped molecules. [6]helicene, the first member of the helicene family, was synthesised by Newman et al. in 1956[10] (Figure 1.2). This pivotal work showed that these molecules with a twisted polyaromatic scaffold are accessible

and stable enough even to be resolved into their enantiomers signed with prefixes *P* (right-handed helix) and *M* (left-handed helix). It is also worth mentioning that the IUPAC Recommendations 1998 include helicene in "Fused ring and bridged fused ring nomenclature". Prefixes (penta, hexa, hepta, etc.) denote number of fused rings. Newman's simplified nomenclature where the number of rings is indicated by the number in brackets instead of the prefix is also commonly used in the literature.

(P)

(M)
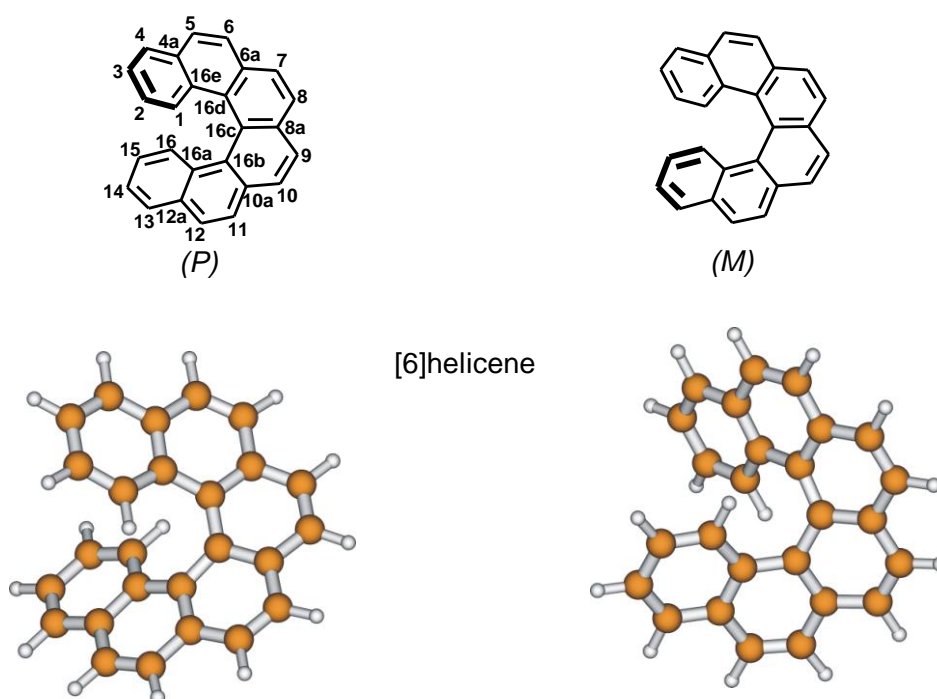
[6]helicene

Figure 1.2 Structures and models of *(P)*- and *(M)*-[6]helicene.

1.1 Synthesis of helicenes

Since the first Newman's synthesis of [6]helicene[10], a variety of different synthetic approaches have been developed. Mallory et al. introduced a photochemical rearrangement - oxidation sequence converting stilbenes to phenantrenes[11]. This methodology was later used by Martin et al. to construct helicenes from suitable stilbene derivatives[12]. This photochemical approach was further generalised by Katz et al. employing propyleneoxide as an additive suppressing undesired side reactions caused by HI that is generated during

photochemical reaction[13]. Iodine in a stoichiometric amount was showed to be better oxidant than air itself (Scheme 1.1).

entry 1

entry 2
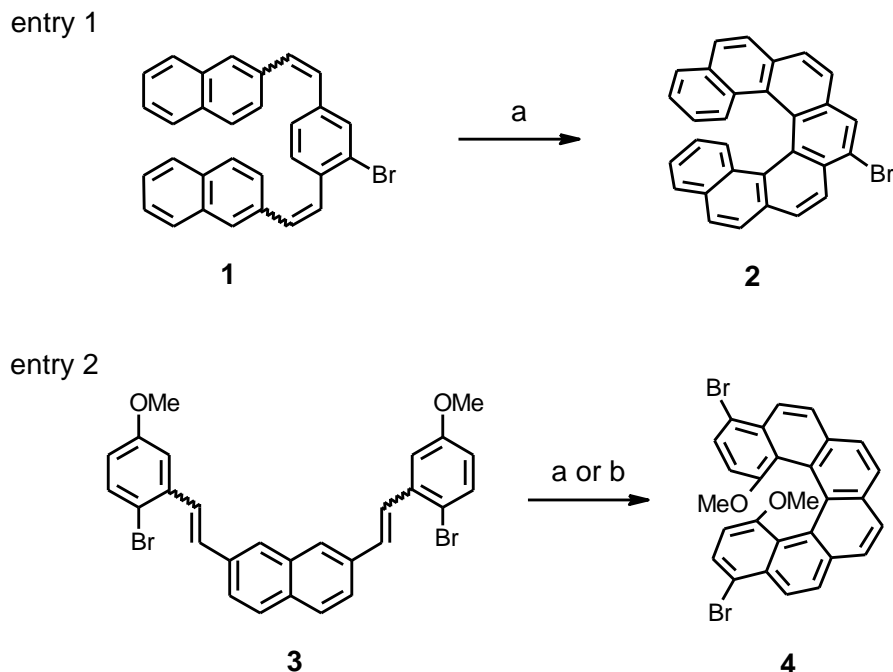
Scheme 1.1 Reagents and conditions:

(a) air, hv, I_2 (cat.), benzene, 66 %.

(b) air, hv, I_2 (cat.), benzene, <4 %.

(c) I_2 (2.0 eq.), propylene oxide (190 eq.), hv, benzene, 71 %.

Although the use of this method allowed preparing a number of interesting helicene derivatives, it still suffers from drawbacks disqualifying it to be a general approach. The main disadvantages are a high dilution necessary for the photochemical reaction and limited presence of heteroatoms and functional groups. Katz et al presented a non-photochemical strategy based on Diels-Alder reaction resulting in helicene quinones, which have oxygen atoms in the positions enabling further functionalization of a helicene skeleton[14–21] (Scheme 1.2, entry 1). The first non-photochemical preparation of [7]helicene **9** was described by Gingras et al. using a carbenoid coupling strategy[22,23] (Scheme 1.2, entry 2). A related strategy was used by Rajca et al. for the synthesis of heterohelicene **11**[24]. This synthetic route enables an iterative extension of the helicene scaffold allowing the preparation of up to hetero[11]helicene (Scheme 1.2, entry 3). Another approach

to [5]helicene **13** relied on radical cyclisation was reported by Harrowven[25] (Scheme 1.2, entry 4).

entry 1

5   **6**   **7**

entry 2

8   **9**

entry 3

10   **11**

entry 4

12   **13**
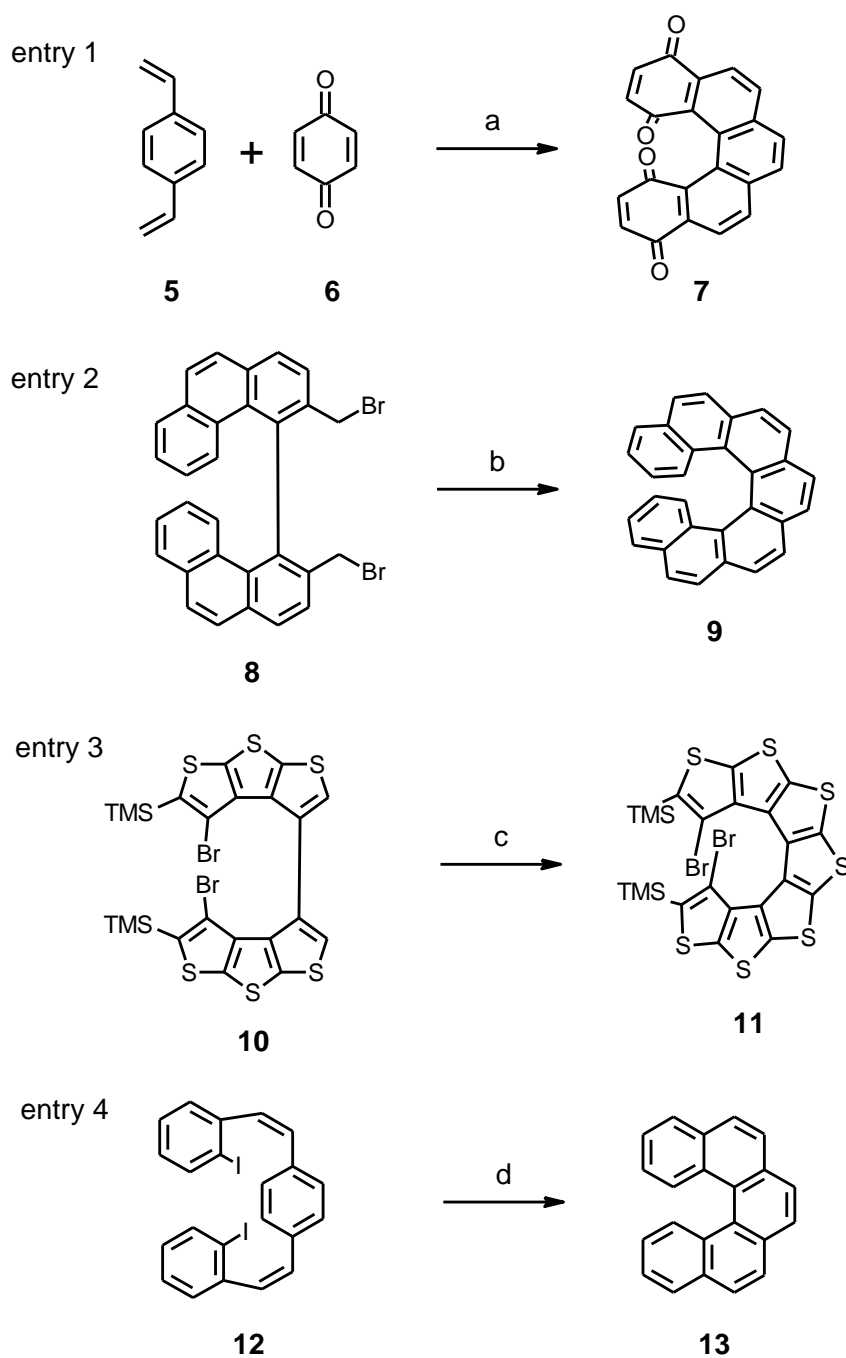
Scheme 1.2 Reagents and conditions:

(a) reflux, toluene, 50 %.

(b) LiHMDS (excess), THF/HMPA, 0 °C, 75 %.

(c) 1. LDA, Et$_2$O; 2. (PhSO$_2$)$_2$S, 40 %.

(d) Bu$_3$SnH, AIBN, 58 %.

An important breakthrough in this field was reported by our laboratory[26]. The novel strategy for the synthesis of helicene molecules is based on transition metal catalyzed [2+2+2] cyclotrimerisation of appropriate triynes. This atom-economical transformation (three new cycles are formed within one step) is performed under very mild conditions thus allowing the presence of various functional groups. Generality of this methodology was demonstrated by the synthesis of different substituted [5], [6] and [7]helicenes in good to excellent yields (Scheme 1.3).
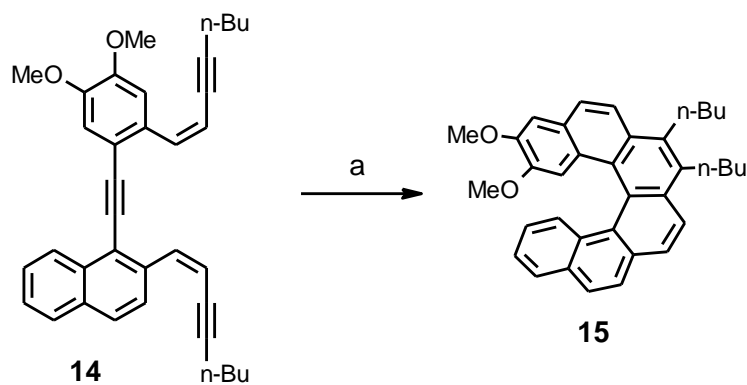
Scheme 1.3 Reagents and conditions:
(a) Ni(COD)$_2$, PPh$_3$, THF, rt, 61 %.

An increasing interest in the efficient and practical preparation of helicenes can be exemplified by the fact that during last 5 years more than 10 new or improved synthetic strategies have emerged. Naming the most important, Nozaki et al. used Pd catalyzed N- and O-arylation to construct hetero[7]helicenes[27] (Scheme 1.4, entry 1), Collins et al. employed ring closing metathesis[28] (Scheme 1.4, entry 2), base mediated rearrangement of tetraynes to the [5]helicene derivatives was reported by Wang et al.[29] (Scheme 1.4, entry 3) and Friedel-Crafts reaction of difluoroalkenes leading to methyl substituted [5] and [6]helicene was utilized by Ichikawa et al.[30] (Scheme 1.4, entry 4).

entry1

16

a

17

entry 2

18

b

19

entry 3

Ph

Ph

tBu   tBu

20

c

tBu

Ph
Ph

tBu

21

10
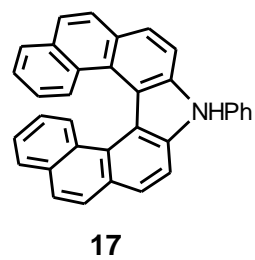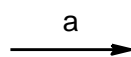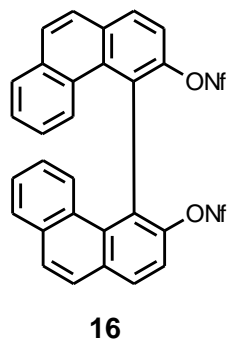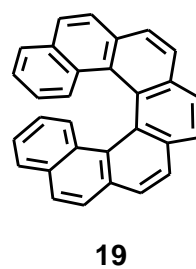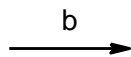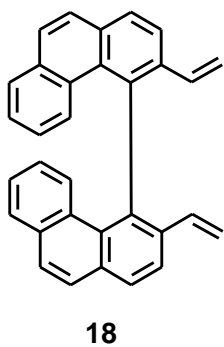
entry 4

22   **23**
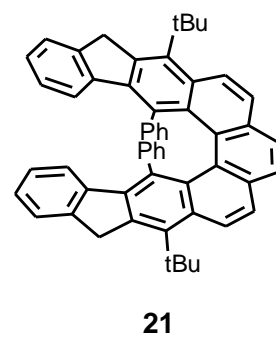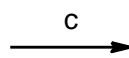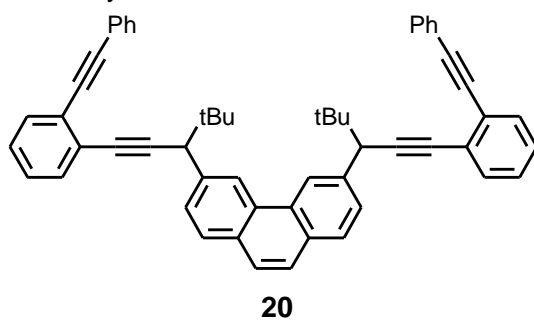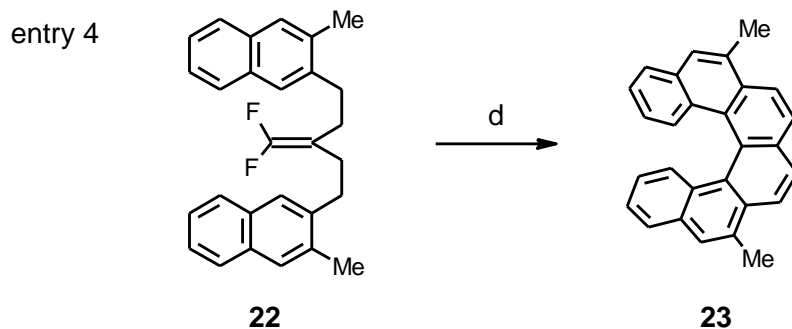
Scheme 1.4 Reagents and conditions:

(a) PhNH$_2$, [Pd$_2$(dba)$_3$]·CHCl$_3$, xantphos, xylene, 100°C, 94 %.

(b) Grubbs 2nd, CH$_2$Cl$_2$, 40°C, 80 %.

(c) KOtBu, toluene, reflux, 47 %.

(d) 1. FSO$_3$H·SbF$_5$, (CF$_3$)$_2$CHOH/CH$_2$Cl$_2$, 0°C, 62 %.

     2. Ph$_3$CBF$_4$, (CH$_2$Cl)$_2$, reflux, 86 %.

1.2   Synthesis of azahelicenes

The first azahelicene reported in the literature was 1-aza[6]helicene prepared by Martin et al. in 1975[31]. The classic photochemical cyclisation, however, provided only very low yield and neither spectral data nor other details are available in the original article. One year later, Schuster reported an approach to diazaderivative **25**[32] (Scheme 1.5).


24   **25**
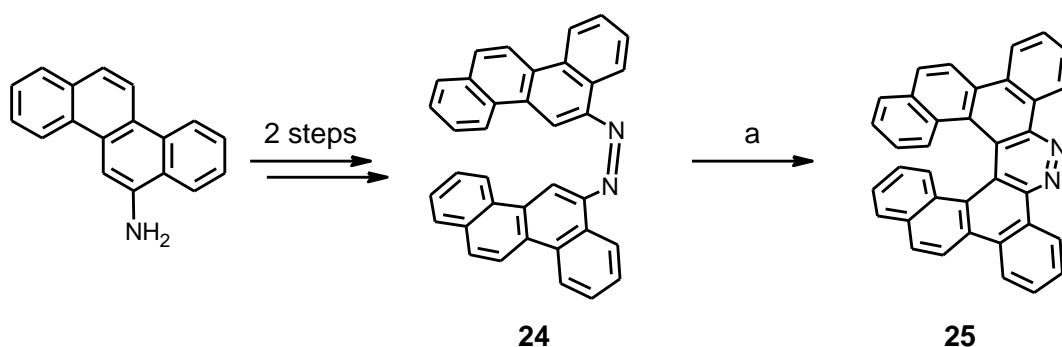
Scheme 1.5 Reagents and conditions:

(a) H$_2$SO$_4$, quant.

More than one decade later, another attempts to introduce nitrogen atom to the helicene skeleton occurred. During elaboration on proton sponges, Staab et al. synthesised diaza[6]helicene **27** using Pd catalyzed cross-coupling as a key step[33] (Scheme 1.6, entry 1). Diederich et al. showed that photocyclisation can be successfully employed in the preparation of the helicene derivative **29** containing several pyridine rings[34] (Scheme 1.6, entry 2).

entry 1

26   a   **27**

entry 2

28   b   **29**
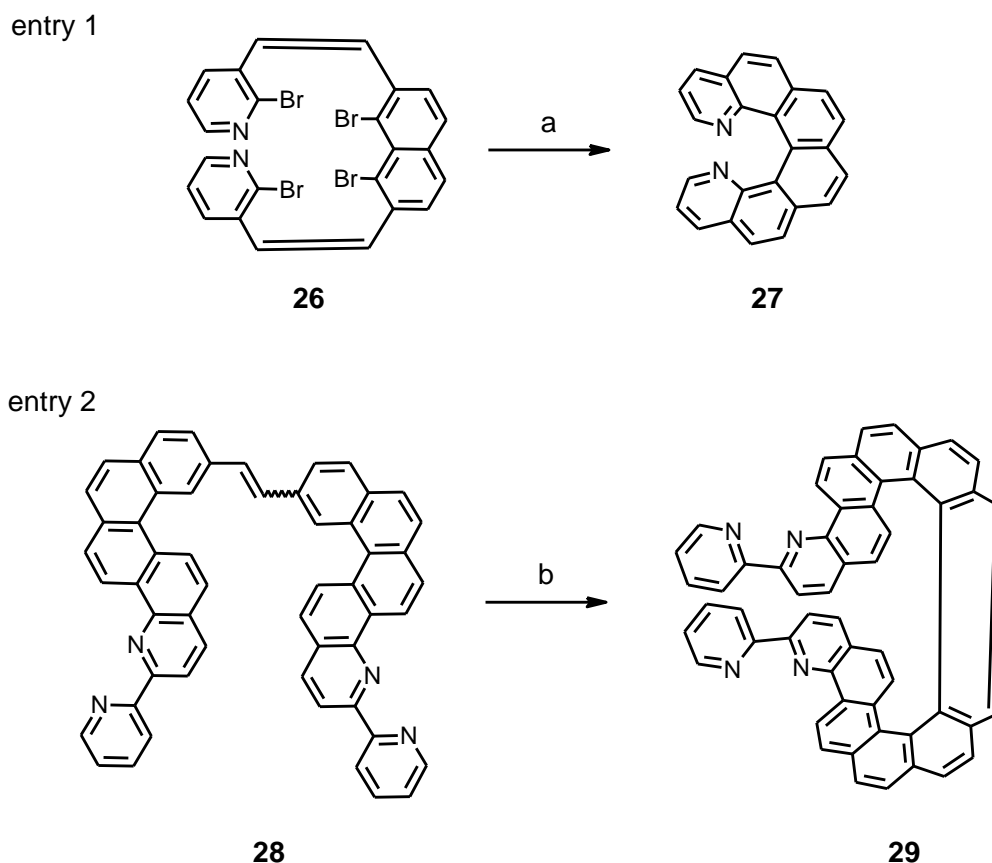
Scheme 1.6 Reagents and conditions:
(a) Pd(PPh$_3$)$_4$, Me$_3$SnSnMe$_3$, toluene, reflux, 52 %.
(b) I$_2$, hv, toluene, rt, 35 %.

Most of the following syntheses of azahelicenes have relied on this photochemical approach. A number of different azahelicenes was synthesised using this methodology even though some derivatives are not accessible because the presence of nitrogen in specific positions might affect an electronic nature of

the substrate so that the photochemical reaction can lead to either undesired product or it is suppressed at all[35] (Scheme 1.7).

entry 1

30   a   **31**

entry 2

32   a   **33**

entry 3

34   a   **35**
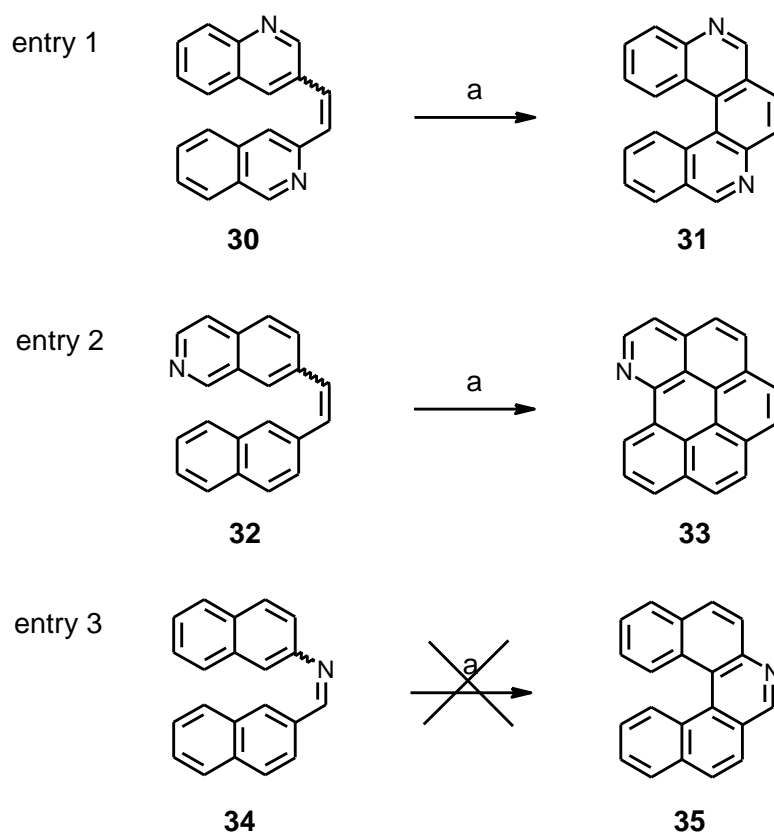
Scheme 1.7 Reagents and conditions:
(a) air, hv, EtOAc, rt, 98 % for **31**, 98 % for **33**.

Recupero et al. have studied extensively synthesis of pentacyclic mono- and diazahelicenes[36]. Apart from the photochemical reaction, other methods were developed or improved by this group in order to prepare azahelicenes with the nitrogen atom in different positions. However a rather limited success was achieved regarding yields (Scheme 1.8).

entry 1

36   a →   **37**

entry 2

38   b →   **39**
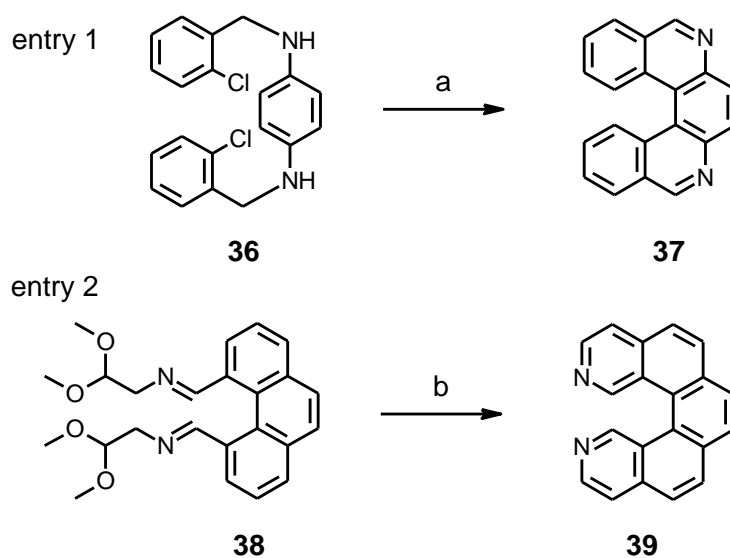
Scheme 1.8   Reagents and conditions:

(a) 1. NaNH$_2$, THF, reflux, 25 %, 2. MnO$_2$, CHCl$_3$, rt, 4 %.

(b) P$_2$O$_5$, H$_2$SO$_4$, reflux, 3 %.

Branda et al. used photocyclisation for the preparation of [7]helicene **41** containing two terminal benzyloxypyridine rings that were later transformed into pyridones and utilized for self-assembly studies[37](Scheme 1.9, entry 1). Friedel-Crafts acylation was employed by Venkataraman et al. for the synthesis of the nitrogen containing helicene **43**[38] (Scheme 1.9, entry 2).

entry 1

40   a →   **41**

entry 2

42 → b → **43**
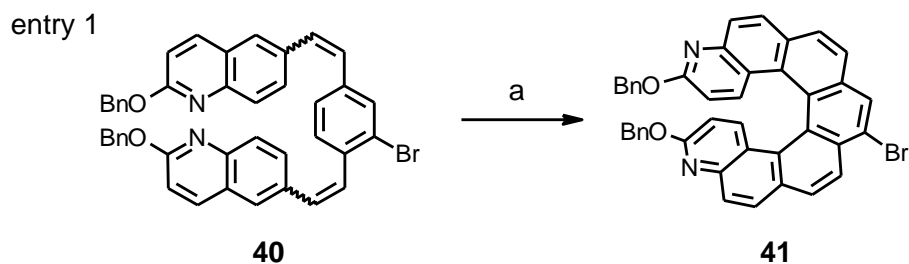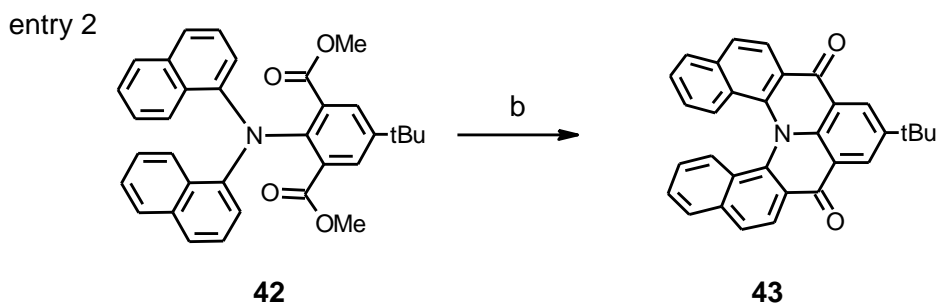
Scheme 1.9 Reagents and conditions:

(a) I_2, propylene oxide, hv, benzene, 63 %.

(b) 1. NaOH, H_2O/EtOH, reflux. 2. $(COCl)_2$, CH_2Cl_2, reflux.

3. $SnCl_4$, CH_2Cl_2, reflux, 57 % (overall).

Recently, Hassine et al. reported the preparation of 3-aza-14-methoxy[6]helicene **45**[39] (Scheme 1.10, entry 1) and Harrowven utilized the radical strategy also for the preparation of aza[5]helicene derivative **47**[40] (Scheme 1.10, entry 2).

entry 1

44 → a → **45**

entry 2

46 → b → **47**
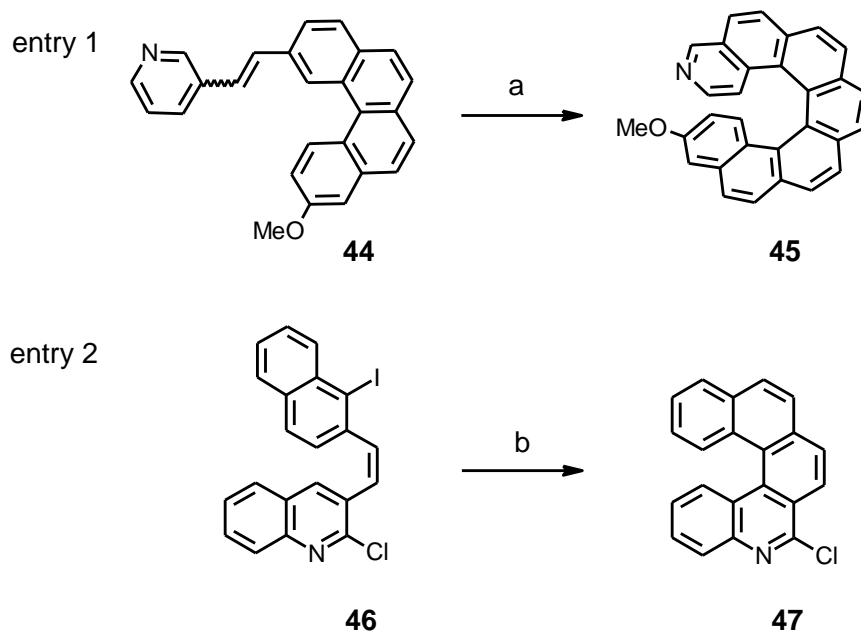
Scheme 1.10 Reagents and conditions:

(a) I_2, propylene oxide, hv, cyclohexane, 53 %.

(b) Bu_3SnH, VAZO, toluene, 90 °C, 75 %.

1.3 Nonracemic helicenes

Another major challenge in helicene chemistry is the preparation of individual enantiomers. Newman's first synthesis of racemic [6]helicene **73** was already accompanied by its resolution into enantiomers using repeated cocrystalisation with TAPA[10]. This method relies on the formation of a CT complex by π- π stacking of unfunctionalized [6]helicene **73** with TAPA. Since TAPA was available in both enantiomers, both enantiomeric forms of [6]helicene were obtained and characterized. Despite the tedious resolution procedure and low yield, it remains an important landmark in helicene chemistry (Scheme1.11).

rac-[6]helicene **73**   *(M)*-(-)-[6]helicene **73**
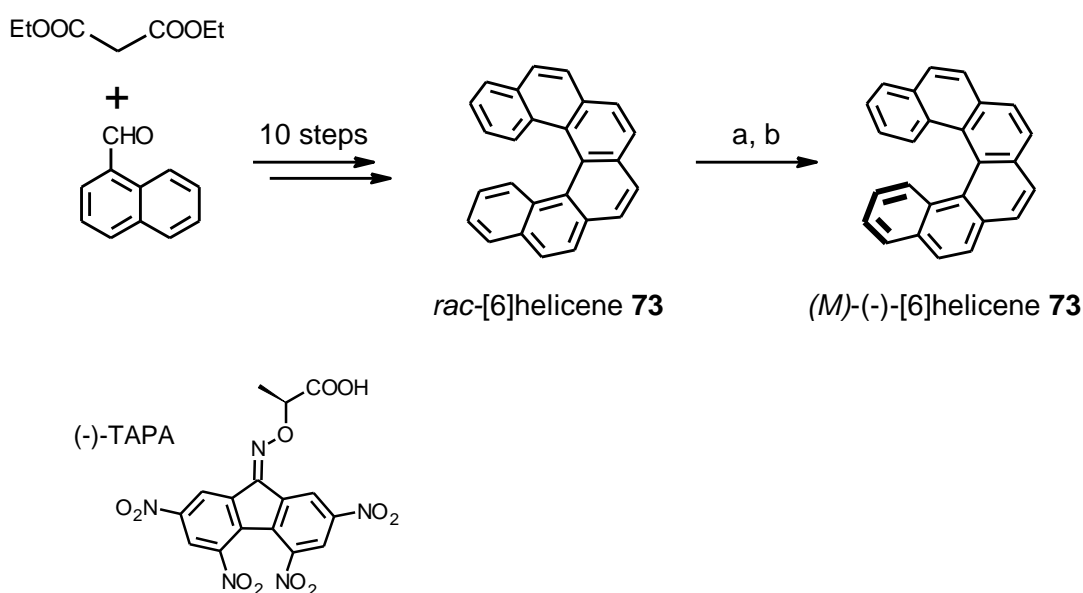
(-)-TAPA

Scheme 1.11 Reagents and conditions:
(a) 3 x cocrystallisation with (-)-TAPA, EtOH, benzene, 22 %.
(b) 8 x recrystallisation from EtOH/benzene, 2 %.

Most of the methods for the preparation of enantiomerically pure helicenes reported to date are based on resolution of a racemic material. In the past it was mainly connected to Katz's Diels-Alder approach to helicenes since this synthetic methodology allowed preparation of helicenes in larger quantities and with suitable functionalities. This can be exemplified by the resolution of helicene **48**. The starting racemic bisquinone **48** was converted to diastereoizomeric (-)-camphanoyl esters **49** that were separated on silica gel and final oxidative cleavage of

camphanoyl auxiliary afforded both enantiomers of bisquinone **48** in more than 97 % ee[17]. Another route to nonracemic helicenes is based on a diastereoselective formation of a helical scaffold starting from an optically pure substrate. Stara et al. published the transformation of the optically pure axially chiral quarternary ammonium salt **50** into [5]helicene **13** with complete transfer of axial-to-helical chirality[41].

entry 1

rac-**48**

49

= R*

(*P*)-(+)-**48** and (*M*)-(-)-**48**

entry 2

(*S*)-(+)-**50**

(*R,3R*)-(+)-**51**

(*P*)-(+)-**13**
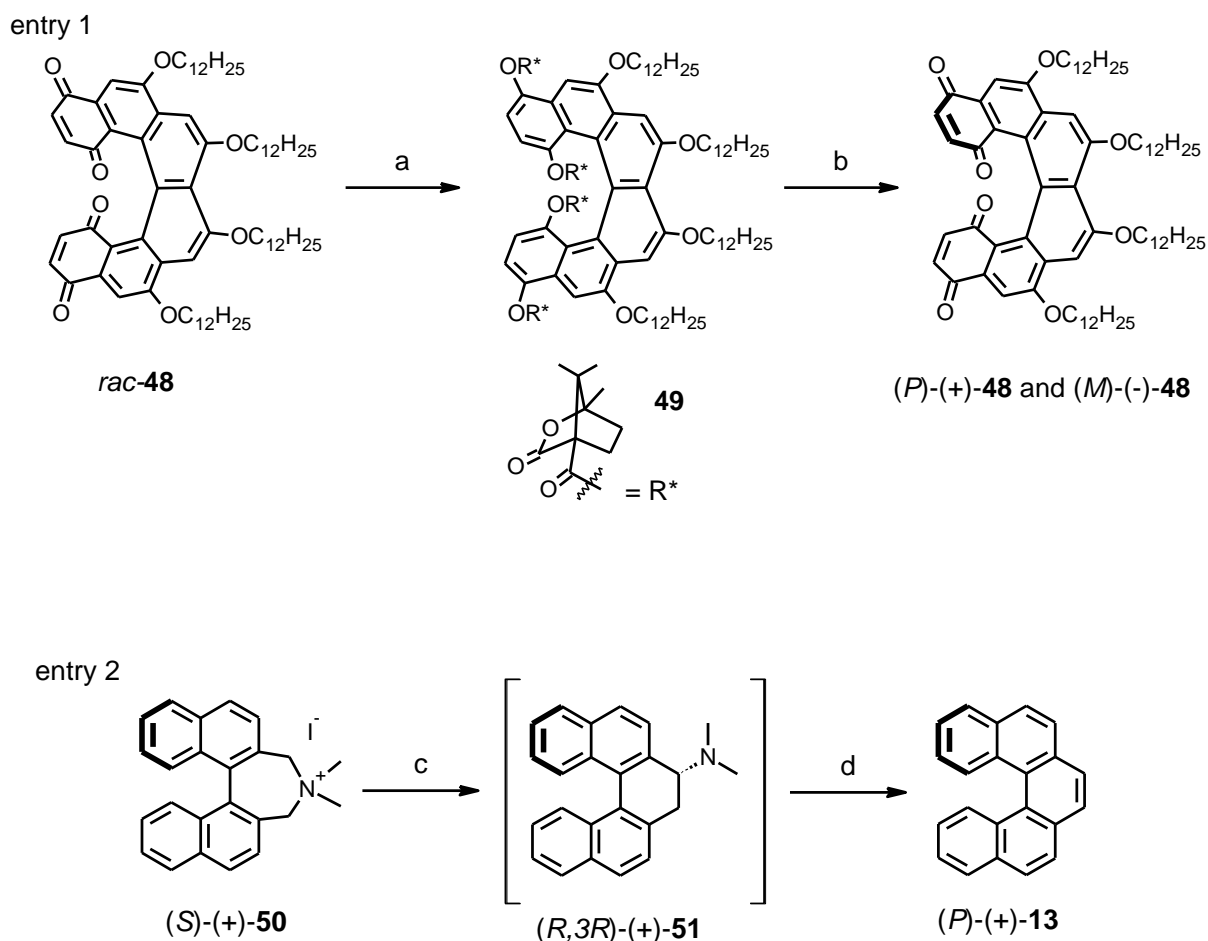
Scheme 1.12 Reagents and conditions:

(a) 1. $Na_2S_2O_3$, THF, rt. 2. (1*S*)-(-)-camphanoyl chloride, Et₃N, THF, reflux. 3. silica gel chromatography, 85 % of (-)-**49**, 83 % of (+)-**49** (overall).

(b) 1. MeLi, THF, -78°C. 2. chloranil, benzene, rt, 95 % (overall).

(c) n-BuLi, THF, -20 °C, not isolated.

(d) MCPBA, CHCl₃, -20 °C, 95 %, >99 % op.

Chiral sulfoxide auxiliary was used by Carreño et al. in diastereoselective Diels-Alder cyclisation leading to the helicene-like compound **54**[42–44]. Interestingly, **54** can be selectively transformed either to (*M*)-**55** or (*P*)-**56** (Scheme 1.13, entry 1). Karikomi et al. developed a method for the synthesis of chiral [5]helicene derivatives using an aromatic oxy-Cope rearrangement strategy. Under treatment of the derivative **57** with KHMDS, oxy-Cope rearrangement proceeded leading to the pentacyclic fused-ring derivative **58** that can be transformed in four steps to the optically pure [5]helicene derivative[45] (Scheme 1.13, entry 2). The chiral oxazoline auxiliary was exploited by Tanaka et al. in the preparation of (*P*)-hetero[7]helicene **62**[46]. A key step of the synthesis is stereoselective Stille cross-coupling leading to the intermediate **61** that is converted in four steps to helicene **62** (Scheme 1.13, entry 3).

entry 1

entry 2

(1R,2S,4S)-57

(4aS,14dR)-58

entry 3
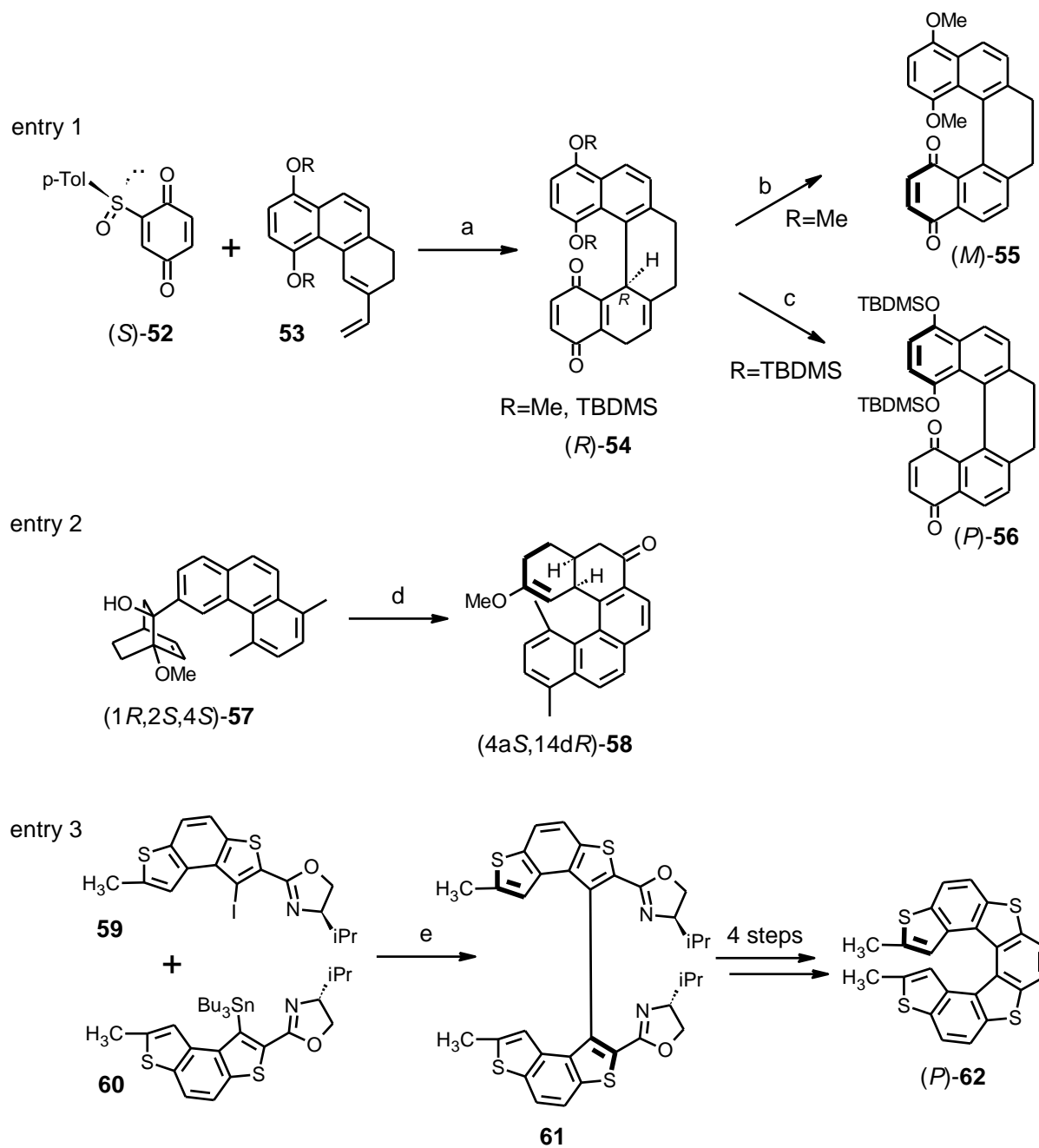
Scheme 1.13 Reagents and conditions:

(a) CH$_2$Cl$_2$, -20 ^{o}C, not isolated.

(b) CAN, CH$_2$Cl$_2$, rt, 67 %, 90 % ee.

(c) DDQ, benzene, rt, 88 %, >96 % ee.

(d) KHMDS, 18-crown-6, THF, 0 ^{o}C, 47 %.

(e) PdCl$_2$(PPh$_3$)$_2$, THF, 65 ^{o}C, 68 %, dr 2.9:1.

In another example of central-to-helical chirality transfer, Stara et al. used triyne bearing chiral carbon for diastereoselective [2+2+2] cyclotrimerisation[47]. This method provided helicene-like molecules in up to 99 % de (Scheme 1.14).

(S)-(-)-**63**

(P,S)-(+)-**64**
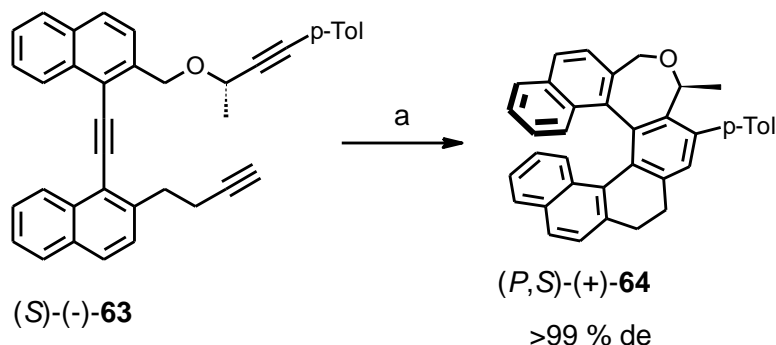
>99 % de

Scheme 1.14 Reagents and conditions:

(a) CpCo(CO)$_2$, PPh$_3$, dioxane, 120 $^{\circ}$C, 66 %, >99 % de.

Stara et al. also reported the first catalytic enantioselective synthesis of tetrahydro[6]helicene **67** using Ni(0) catalyzed [2+2+2] cyclotrimerisation of triyne in the presence of BOP as a chiral ligand[48] (Scheme 1.15, entry 1). This approach was further improved by Tanaka et al. when chiral Rh(I) catalyst was utilized for [2+2+2] cyclotrimerisation leading to helicene derivative **69** with up to 85 % ee[49] (Scheme 1.15, entry 2).

entry 1

66

(*S*)-(-)-BOP =

a

(P)-(+)-**67**

54 % ee

entry 2

68

(*R,R*)-Me-Duphos =

b

(M)-(-)-**69**

85 % ee
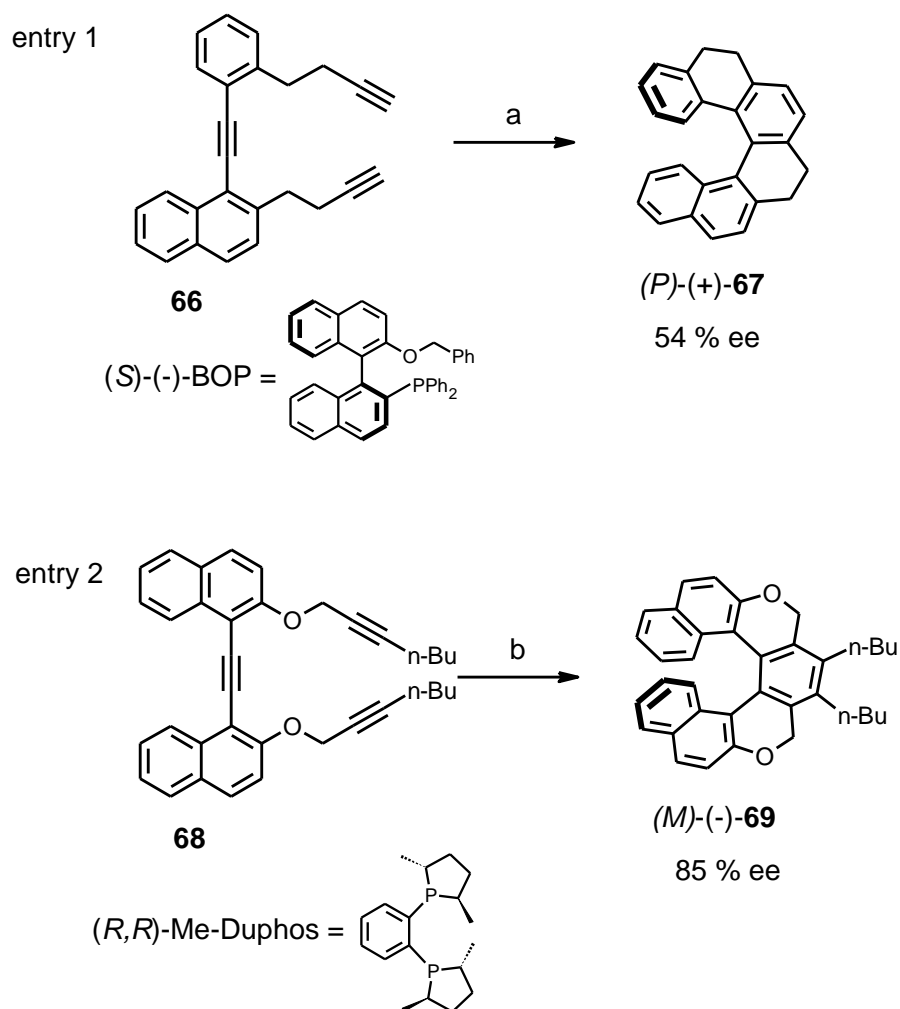
Scheme 1.15 Reagents and conditions:

(a) Ni(COD)$_2$, (*S*)-(-)-BOP, THF, -20 $^{\circ}$C, 81 %.

(b) [Rh(COD)$_2$]BF$_4$, (*R,R*)-Me-Duphos, CH$_2$Cl$_2$, 40 $^{\circ}$C, 71 %.

As far as azahelicenes are concerned, the first azahelicene synthesis (see above) was intended to be carried out in an asymmetric manner using circularly polarised light as a source of chirality during photocyclisation[31]. Unfortunately, yield was very poor and enantioselectivity negligible. Further methods are predominantly based on resolving racemic materials and exploiting methods developed for simple carbohelicenes. Diazahelicene **25** prepared by Schuster et al. was resolved according to the Newman's procedure using cocrystalisation with TAPA[32]. Venkataraman et al. separated helicene enantiomers through

camphenate diastereoisomers using chromatography and subsequent cleavage of the chiral auxiliary[38] (Figure 1.3).

70
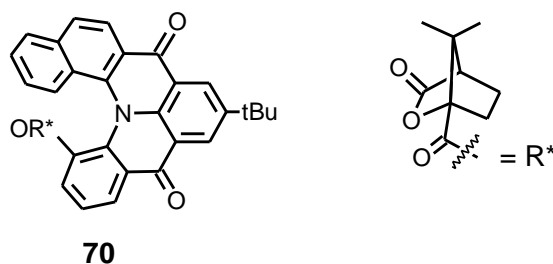
Figure 1.3 Diastereoisomeric esters of azahelicene **70** used for its enantiomers separation

The diazahelicenium dye **71** was synthesized and resolved by Lacour. Chiral sulfoxide was attached to the helicenium and after the chromatographic separation the sulfoxide moiety was cleaved utilising Pummerer-like chemistry[50].

[*rac*-**71**][BF$_4$]   **72**

[*(P)*-**71**][PF$_6$]   > 98 % ee

[*(M)*-**71**][PF$_6$]   > 98 % ee
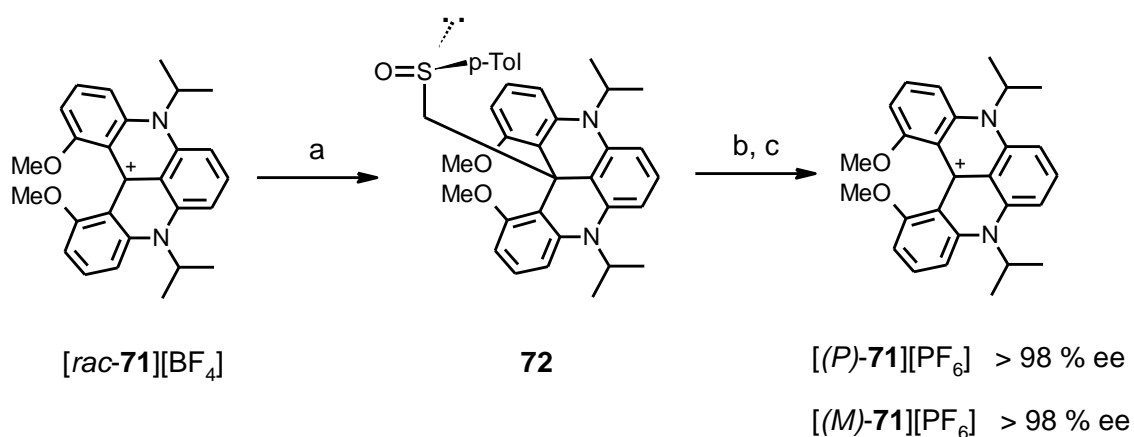
Scheme 1.16 Reagents and conditions:

(a) (+)-(*R*)-methyl-*p*-tolylsulfoxide, LDA, THF, 0 °C,

(b) silica gel chromatography, (-)-(*R,M*)-**72** 43 %, >98 % de, (+)-(*R,P*)-**72** 41%, >98 % de.

(c) aq. HPF$_6$, acetone, rt, 80 %.

Despite the fact that various azahelicene derivatives were prepared, the resolution into enantiomers or the asymmetric synthesis remain practically unexplored. One of the reasons is that most derivatives are pentacyclic and thus

configurationally unstable. The presence of nitrogen can also bring difficulties during the asymmetric synthesis. It is surprising that up to these days no procedure is reported using benefit of basic nitrogen for diastereoisomeric salt crystallisation.

1.4 Configurational stability of helicenes

Helicenes are known to undergo thermal racemisation. This phenomenon was first described by Goedicke et al. in 1970[51]. Since that, racemisation of helicenes was studied extensively both experimentally[52, 53] and theoretically[54−56]. It has been shown that helicenes racemise via nonchiral C_s transiton state (TS) where two terminal rings both are pseudoparallel (Figure 1.4).

*(P)-(+)-***73**   *(M)-(-)-***73**

C_s TS

$\Delta G^{\neq}$

(M)
C_2 GS

(P)
C_2 GS
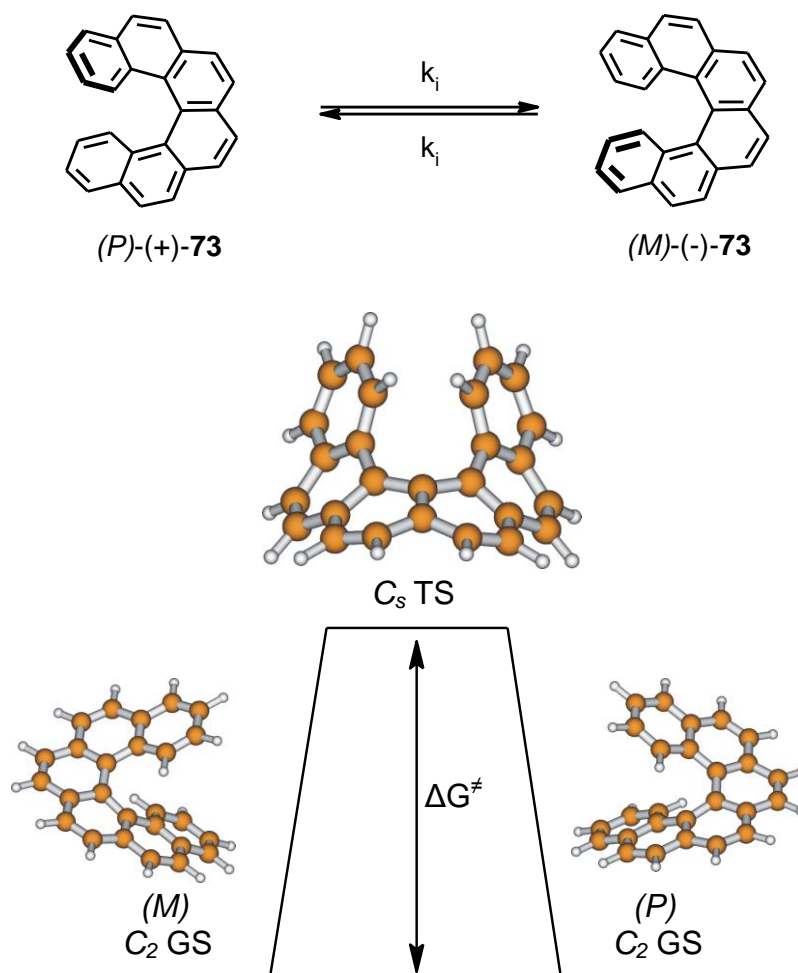
Figure 1.4 Mechanism of racemisation of [6]helicene.

The height of the racemisation barrier is strongly dependent on the number of benzene rings. The more rings, the higher the barrier. This rule is valid in the series from [5]helicene to [7]helicene. Further ring expansion does not affect the barrier significantly: The racemisation barriers of [7]helicene, [8]helicene and [9]helicene differs only slightly (Figure 1.5).
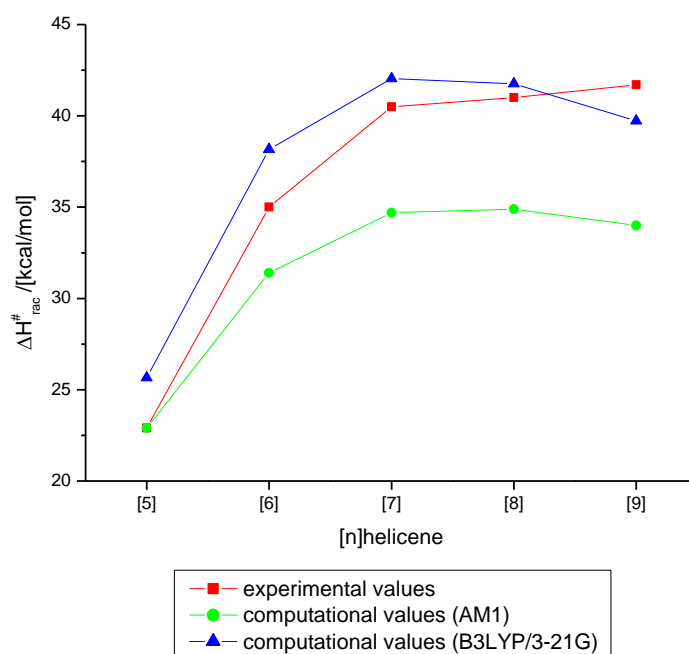
Figure 1.5 Racemisation barriers in the [n]helicene series. Comparison of experimental[52, 53] and calculated values[54].

An explanation for this behaviour was suggested by Janke et al. on the basis of quantum chemical calculations. The C_s symmetrical TS become an intermediate and two new equivalent TSs appear instead[54] (Figure 1.6). The racemisation reaction coordinate for [8]helicene and higher homologues in fact comprises double racemisation of a [7]helicene substructure.
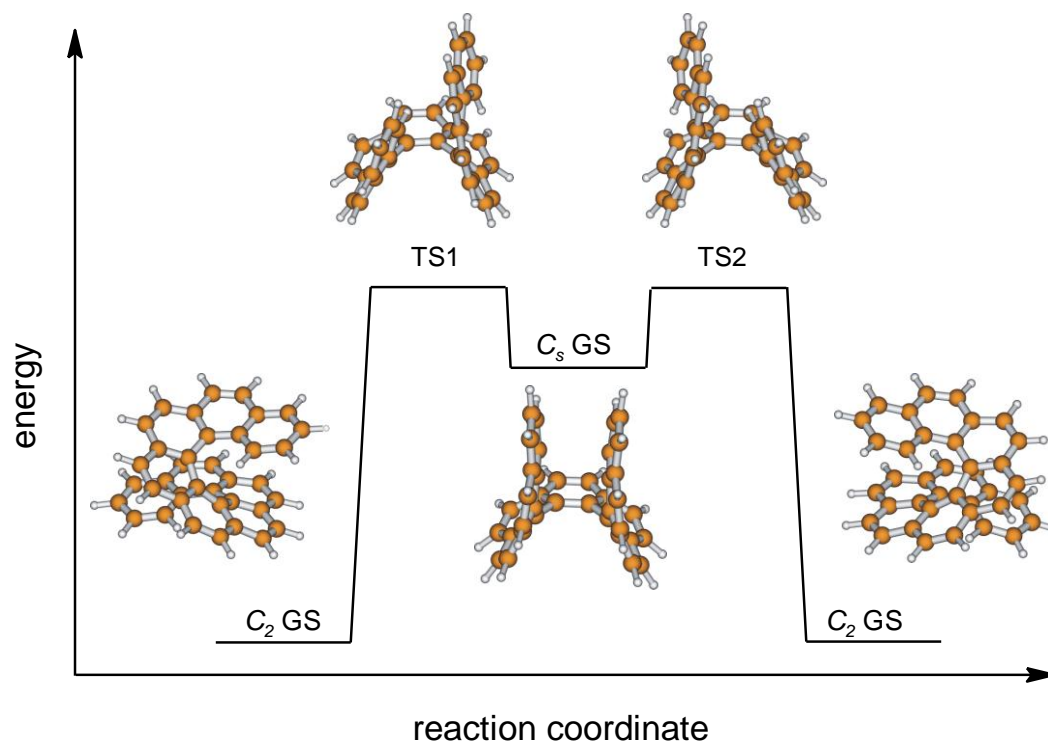
Figure 1.6 Scheme of the reaction coordinate for racemisation of [9]helicene.

The same authors also investigated a role of the methyl substituent in the helicene scaffold on the racemisation barrier[54]. Their results indicate that only substitution in the most crowded position 1 significantly increases the barrier. For example, 1-methyl[6]helicene has the same height of the racemisation barrier as the nearest higher helicene homologue ([7]helicene). The influence of nitrogen on racemisation has not been so far examined.

1.5   Application of helicenes

Despite the fact that helicenes possess a unique topology and electronic properties and thus new applications can be envisaged in asymmetric synthesis, chiral sensing or material chemistry, this branch of chemistry remains underdeveloped. One of the reasons might be lack of a simple, modular and general approach to the synthesis of optically pure helicene derivatives. However, as mentioned above, several promising synthetic strategies have recently appeared and the further progress might be expected.

The first use of helicenes in asymmetric synthesis was reported by Martin et al.[57]. Optically pure 2-cyano[7]helicene **74** was used as a stoichiometric reagent in asymmetric epoxidation of styrene derivatives with hydrogen peroxide (Scheme 1.17, entry 1). Reetz et al. utilised bis(diphenylphosphino)helicene **75** as a ligand for rhodium catalyzed hydrogenation of itaconate[58](Scheme 1.17, entry 2). Only modest ee was observed. Unsubstituted [5]helicene **13** and [6]helicene **73** were used by Soai et al. as chiral inductors in asymmetric autocatalytic amplification[59](Scheme 1.17, entry 3). As low ee of helicene as 0.13 % can induce up to 56 % ee of the resulting alcohol. The role of helicene is to create an initial tiny enantiomeric excess of resulting alcoxide that is then amplified independently on the helicene molecule. Another example where a helicene derivative serves as a truly chiral catalyst is enantioselective addition of diethylzinc to benzaldehyde reported by Katz et al.[60](Scheme 1.17, entry 4). Using 5-HELOL **76**, up to 81 % ee was achieved.

entry 1

H$_2$O$_2$

Ph

(P)-(+)-**74**

NC

Ph R O

100 % ee

(84 %)

entry 2

MeOOC COOMe

[Rh(COD)$_2$][BF$_4$], H$_2$

Ph$_2$P
Ph$_2$P

(M)-(-)-**75**

MeOOC S COOMe

39 % ee

(54 %)

entry 3

CHO

t-Bu

i-Pr$_2$Zn

(P)-(+)-**73**

OH

S

t-Bu

95 % ee

(95 %)

entry 4

CHO

Et$_2$Zn

OH

MeO

OMe

MeO OMe

MeO HO

(P,P)-(+)-**76**

OH

S

81 % ee

(93 %)
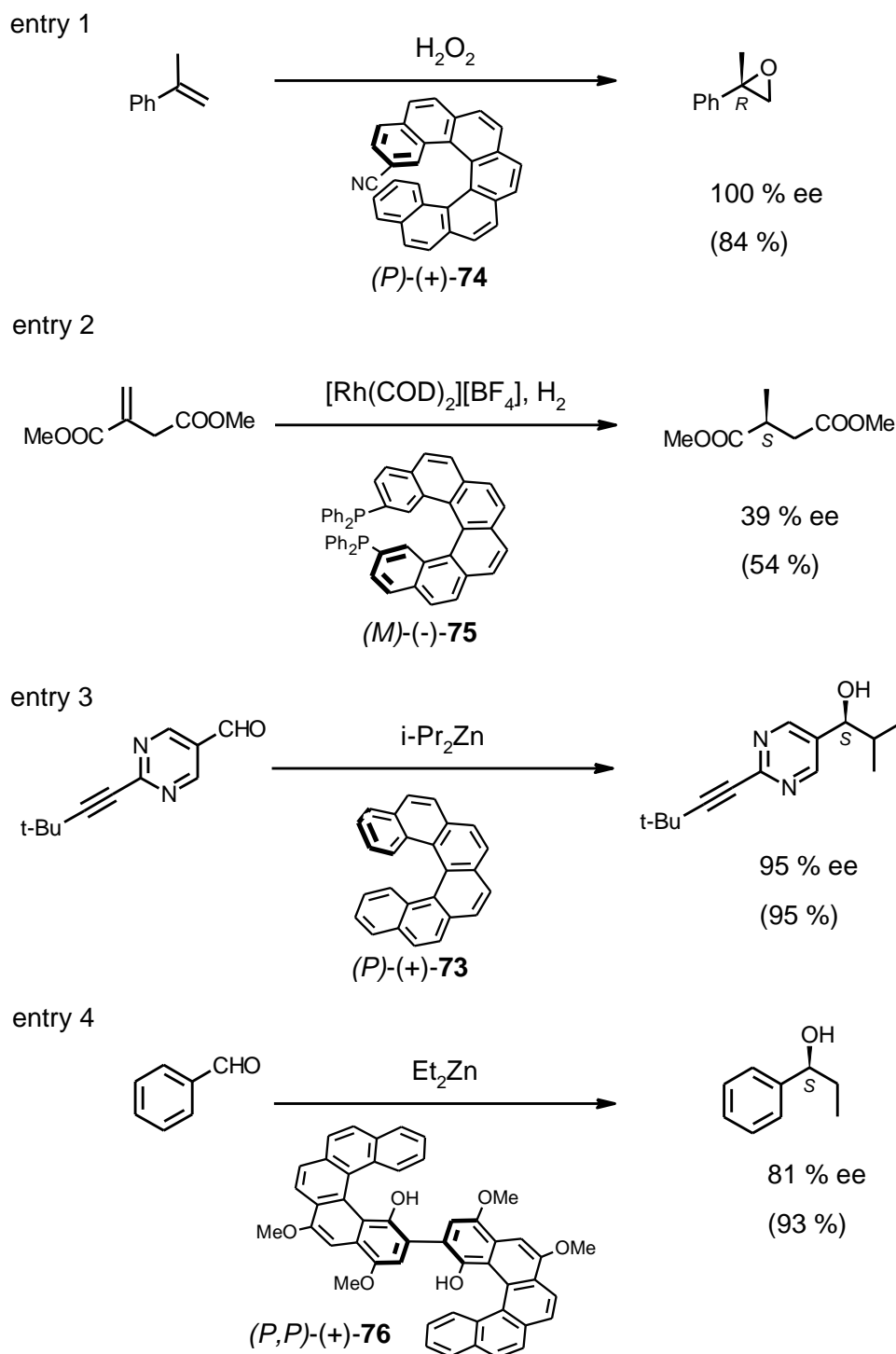
Scheme 1.17 Applications of helicenes in asymmetric synthesis.

In this context it is worth mentioning that supramolecular approaches to asymmetric catalysis relying on helical chirality have recently appeared. A classic example is the Feringa's use of DNA as a chiral environment for the copper catalysed enantioselective transformation[61–64] (Scheme 1.18, entry 1). It was

proved that the helix of double stranded DNA is responsible for enantioselective induction (almost no ee is observed for single stranded DNA) (Scheme 1.18, entry 1). Another case is Yashima's artificial double helix **77** with embedded copper catalyst[65]. Using this catalytic system in cyclopropanation of alkenes with diazo compounds, a linear relationship between the helix-sense excess and ee of the product was observed (Scheme 1.18, entry 2).

entry 1

>99 % endo
up to 99 % ee
(90 %)

entry 2

(+)-**77**

(+)-helix sense excess 81 %

up to 85 % ee
(95 %)
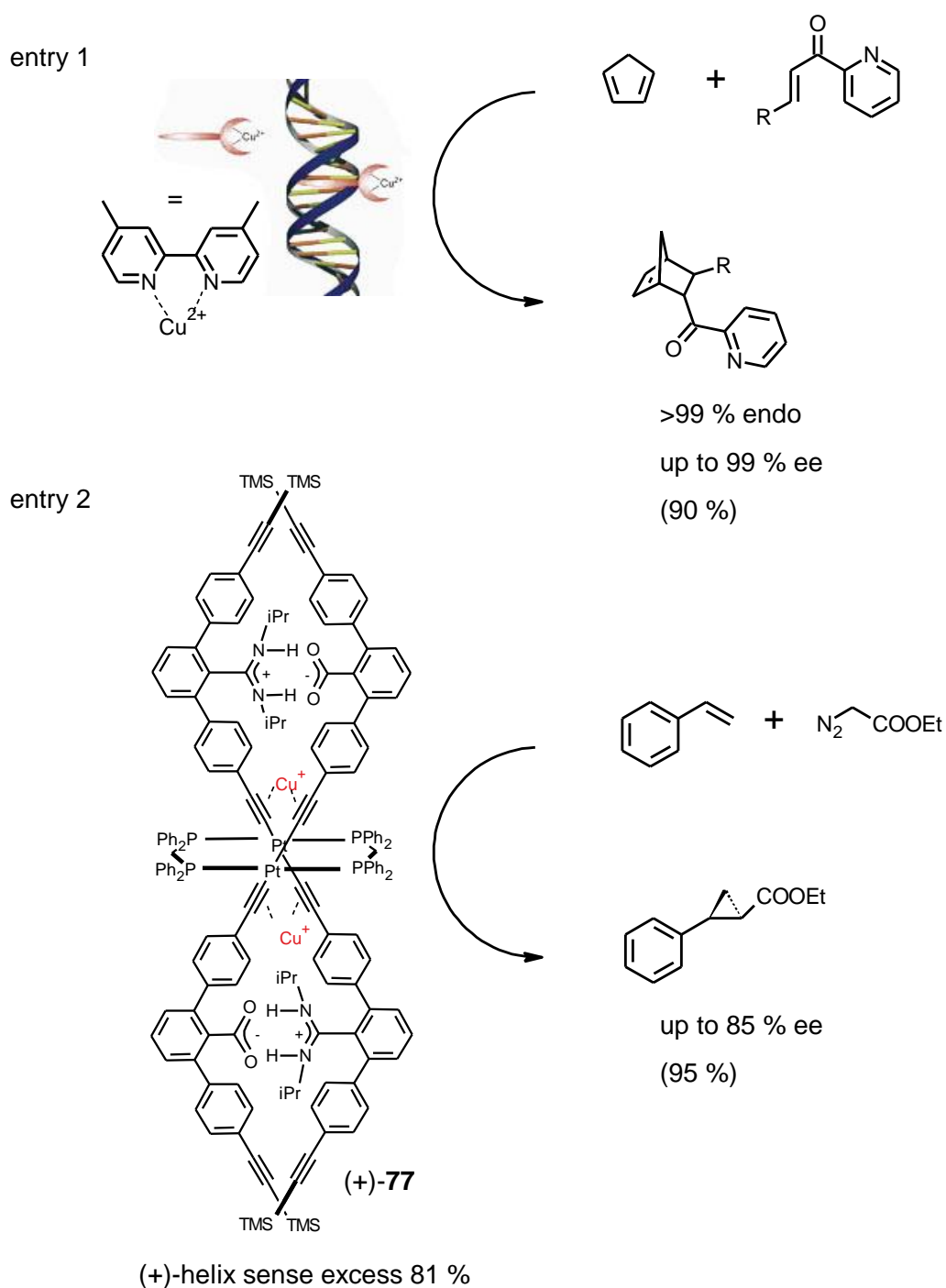
Scheme 1.18 Supramolecular helices as chiral inductors in asymmetric catalysis.

Another field of applications of helicenes is chiral recognition and sensing. Diol **78** was utilised by Reetz et al. as a fluorescent probe for sensing ee of some chiral amines[66] (Figure 1.7). Fluorescence quenching of M-**78** is stronger for *R* enantiomer. 5-HELOL based phosphochloridite **79** was used as a derivatisation agent for chiral alcohols, amines and carboxylic acids[67]. Upon derivatisation of a relevant compound, ee can be easily determined by [13]P NMR. Ee at broad spectrum of chiral substrates can be successfully monitored. Even the derivatives with remote chirality can be analysed using this technique. An intriguing application of the helicene derivative **80** was described by Yamamoto et al[68, 69]. The crown ether modified helicene **80** was utilised for the chiral transport throught a liquid membrane. Several chiral ammonium substrates can be resolved using this method. Recently, Tanaka et al. have reported an interesting feature of heterohelicene **81**[70]. Its (*P*)-(+) optical isomer can selectively interact with left-handed Z-DNA. The intensity of the (*P*)-(+)-**81** circular dichroism response is much lower upon mixing with Z-DNA, whereas right handed form of DNA (B-DNA) does not induce this effect. Since Z-DNA has been found to be an important factor in gene expression and cancer development[71], this discovery might stimulate a further research.

entry 1

fluorescent sensor

substrates

(*M*)-(-)-**78**

entry 2

NMR shift reagent

(*P,P*)-(+)-**79**

entry 3

membrane transporter

(*M*)-(-)-**80**

entry 4

DNA recognition

(*P*)-(+)-**81**

A-DNA   B-DNA   Z-DNA

(right handed)   (left handed)
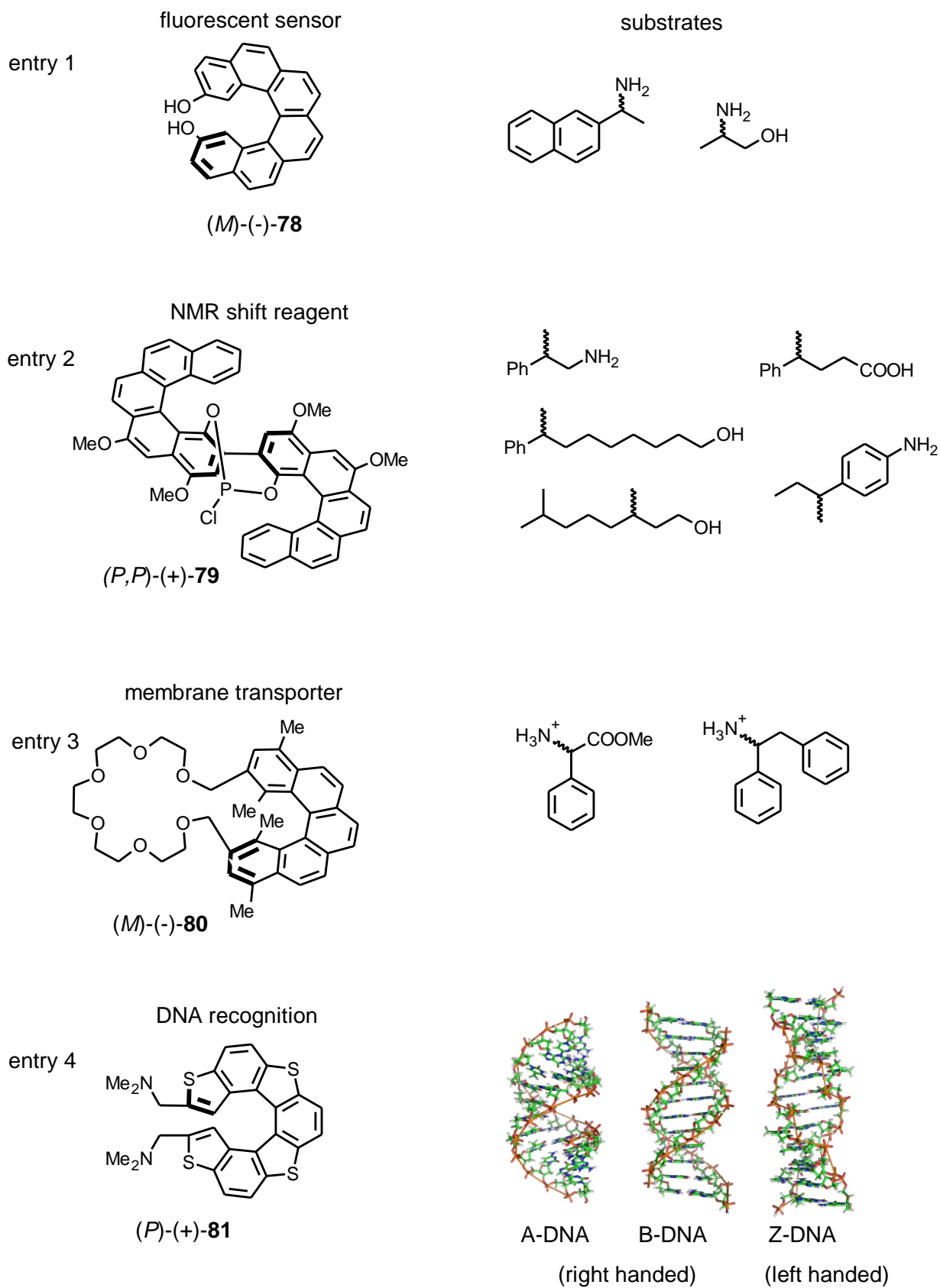
Figure 1.7 Applications of helicenes in chiral sensing.

The third field of applications of helicenes is material chemistry. Although this area is rather unexplored, some promising results have been achieved. For example, huge optical rotation of these molecules is a consequence of chirality spread over the entire π-conjugated scaffold. The possibility of the formation of a noncentrosymmetric environment together with optoelectronic properties makes helicenes good candidates for applications in nonlinear optics[72] and other areas of material science profiting from these properties (organic magnets[73], piezoelectric crystals[74], metamaterials[75] etc.). An interesting example of the utilisation of these unique properties was demonstrated by Katz et al.[76], when they studied a thin solid film of quinone **48**. The detailed investigation of the deposited layer showed that helicenes forms regular columnar aggregates on the surface (Figure 1.8). A nonlinear optical response of the optically pure derivative film was 30 times higher than for the racemic material.

(*M*)-(-)-**48**
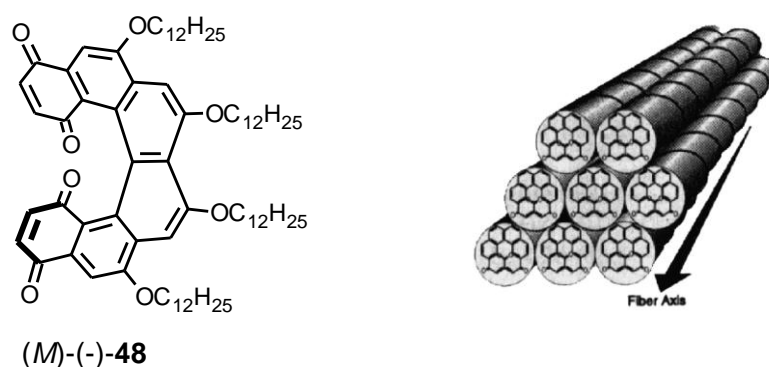
Figure 1.8 Schematic representation of stacked helicene molecules **48** as observed in a Langmuir-Blodgett film (right).

A singular example of the azahelicene use in material chemistry was reported by Venkataraman et al. [77]. These authors showed that azahelicene **82** can be used for generating circularly polarised luminescence (Figure 1.9).
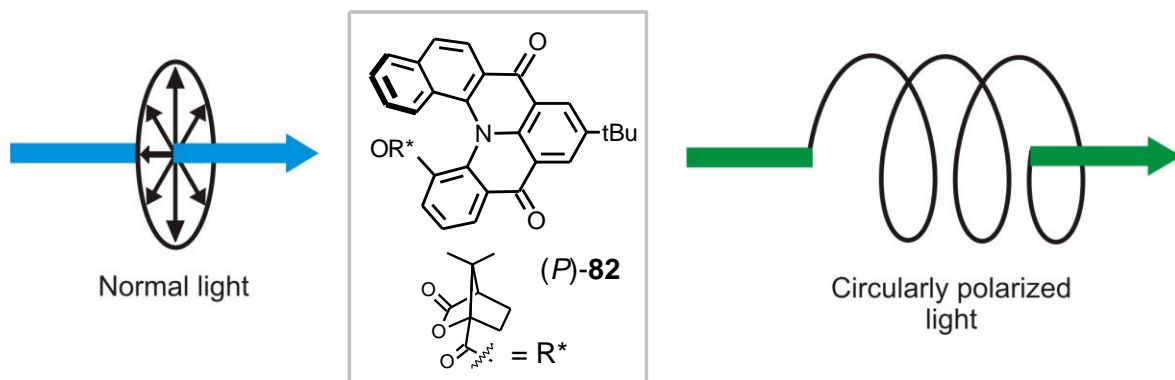
Figure 1.9 Schematic representation of the property of azahelicene (*P*)-**82** to convert normal light to circularly polarised light.

2　Goals

The presence of nitrogen atom(s) in the helicene skeleton might be beneficial for their applications in asymmetric catalysis as chiral ligands or catalysts. Nitrogen atom(s) in the helicene skeleton might also act as fuctional groups in chiral recognition and sensing. Therefore the first aim of this work was to examine if the well established synthetic approach to helicenes using [2+2+2] cyclotrimerisation as the key step, could be also adapted to the synthesis of such molecules. If so, further investigation of these molecules in order to determine their physico-chemical properties and possible applications would be desirable.

In particular, the goals were to:

- Synthesise azahelicenes **83**, **84** and **85** via [2+2+2] cyclotrimerisation of
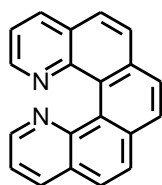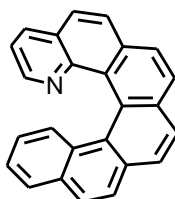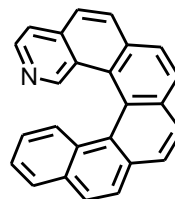
appropriate triynes (Figure 2.1).

Figure 2.1 Target compounds

- Resolve configurationaly stable derivatives into their individual enantiomers.

- Determine racemisation barriers of the azahelicenes in order to determine the impact of nitrogen position on the height of the barrier.

- Test the azahelicenes ability to serve as chiral ligands for transion metals.

- Determine basicity of azahelicenes.

- Aplly azahelicenes in asymmetric transformations.

3   Results and discussion

3.1   Synthesis

Commercially available 2-bromo-3-methylpyridine **86** was chosen as an appropriate starting material for the preparation of the pentacyclic target **83**. Radical benzylic bromination of **86**[78] afforded compound **87** in modest yield 49 % (Scheme 3.1). This reaction was, not surprisingly, complicated by the formation of other brominated products[79]. Varying of temperature and reaction time did not bring any significant improvement in yield. However, this reaction step afforded **87** in acceptable yield and purity.
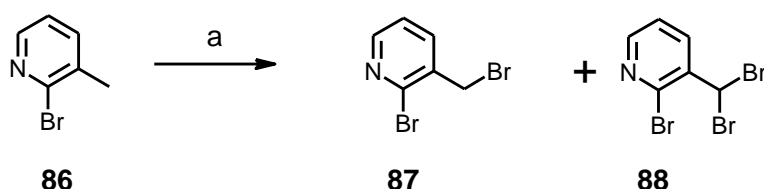
Scheme 3.1 Reagents and conditions:
(a) NBS, AIBN, K_2CO_3, CCl_4, reflux, 49 % of **87**, 23 % of **88**.

The following reaction was nucleophilic substitution of benzylic bromide with propargyl lithium reagent, which was generated in situ from 1-(triisopropylsilyl)-1-propyne by deprotonation with butyllithium (Scheme 3.2). This step afforded the desired product **89** in satisfactory 48 % yield. Alternative nucleophilic reactions on the pyridine ring are likely the reason for lower yield of the product **89**. Thus, the different reaction set up was suggested in order to improve yield. Originally, the

solution of bromide **87** was slowly added to the precooled solution of lithium reagent (-78 °C). Under the optimised conditions, the lithium reagent solution was slowly added via cannula to a solution of bromide **87** cooled to -78 °C. These conditions avoided a local excess of the lithium reagent during the reaction and reduced undesired reaction channels providing alkyne **89** in 81 % yield.
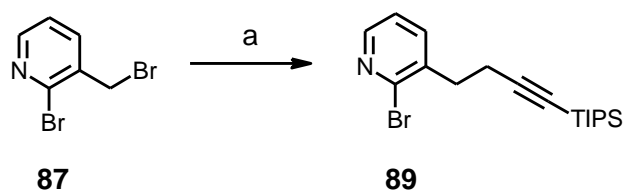
Scheme 3.2 Reagents and conditions:
(a) Li-CH$_2$-C≡C-TIPS, THF, -78 °C, 81 %.

The subsequent step is double Sonogashira cross-coupling of the compound **89** with gaseous acetylene. Using standard coupling conditions, triyne **90** was obtained in good 86 % yield. Desilylation afforded triyne **91** in 77 % yield (Scheme 3.3), which was a suitable substrate for the following cyclisation.
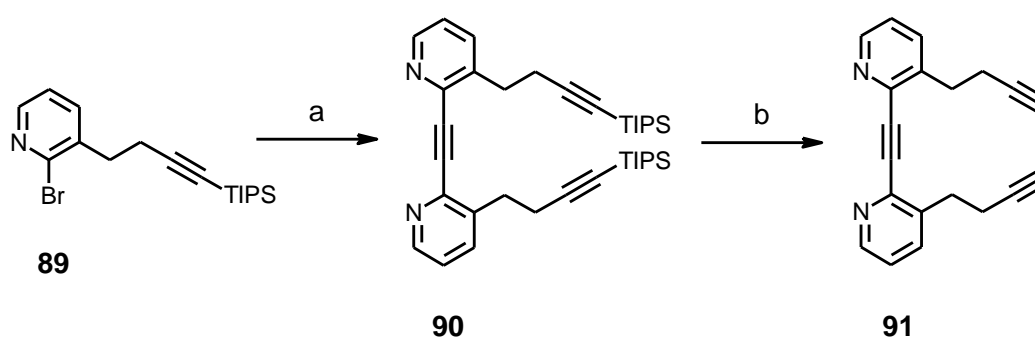
Scheme 3.3 Reagents and conditions:
(a) acetylene, Pd(PPh$_3$)$_4$, CuI, piperidine, 80 °C, 86 %.
(b) n-Bu$_4$NF, THF, rt, 77 %.

Cyclotrimerisation of triyne **91** was performed under standard conditions using CpCo(CO)$_2$ catalysis and irradiation with a halogen lamp (Scheme 3.4). The main role of irradiation is to facilitate dissociation of carbonyls from cobalt and accordingly, to activate catalytic species. Triphenylphosphine in this reaction is beneficial for the stabilisation of a catalytic species. After 1 h at 120°C, the product of cyclisation was isolated in 60 % yield. The starting material was completely consumed and only the desired tetrahydrodiaza[5]helicene **92** was isolated from the reaction mixture as a low molecular weight product.

91   a →   **92**
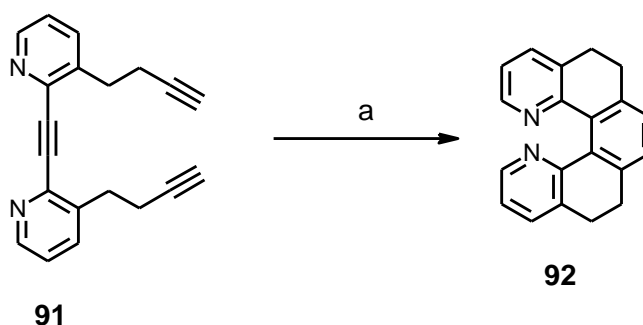
Scheme 3.4 Reagents and conditions:
(a) CpCo(CO)$_2$, PPh$_3$, hv, decane, 140 ^{o}C, 60 %.

The last step of the synthesis is oxidation of tetrahydroderivative **92** to fully aromatic diaza[5]helicene **83**. This showed to be the most problematic part of the entire synthetic sequence. Trityl tetrafluoroborate is a well established reagent for aromatisation and its efficiency was also approved previously on different tetrahydro substrates leading to fully aromatic carbohelicenes[80]. Unfortunately the presence of two nitrogens in the molecule totally suppressed the reaction. Thus, using the standard conditions, starting material was recovered unchanged. Even elevated temperature and prolonged reaction period did not lead to any change of reactivity. Though plethora of other reagents for aromatisation is known[81], neither Pd/C nor DDQ, SeO$_2$ and MnO$_2$ lead to the desired reaction. Harsher conditions, such as neat Pd/C with **92** at 250°C or neat MnO$_2$ with **92** at 250°C lead to either no reaction or total decomposition of starting compound, respectively. Eventually, a successful combination showed to be MnO$_2$ in toluene under microwave irradiation at elevated temperature (150 °C) and pressure (2 bars). This was the

only useful method that provided a fully aromatic product in reasonable yield 41 %. Microwave irradiation was also beneficial for DDQ oxidation. However under similar conditions, yield was slightly lower (37 %) and the reaction provided many side procucts (Scheme 3.5).

92   **83**
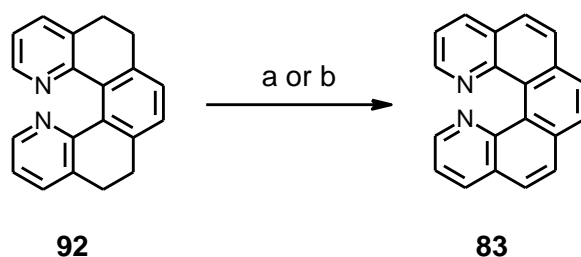
Scheme 3.5 Reagents and conditions:
(a) MnO_2, toluene, microwave irradiation, 150 ^{o}C, 41 %.
(b) DDQ, $(CH_2Cl)_2$, microwave irradiation, 200 ^{o}C, 37 %.

Encouraged by the successful preparation of diaza[5]helicene **83**, the intermediate **89** was used for preparing the target compound **84**. Sonogashira coupling of bromide **89** with the readily available diyne **93**[82] afforded triyne **94** in excellent 90 % yield. After almost quantitative removal of TIPS protecting groups with n-Bu$_4$NF, triyne **95** was subjected to Co(I) catalysed cyclisation. Tetrahydroaza[6]helicene **96** was obtained in good 82 % yield. Subsequently, optimised oxidation conditions as MnO_2/microwaves led to fully aromatic 1-aza[6]helicene **84** in 64% yield (Scheme 3.6).
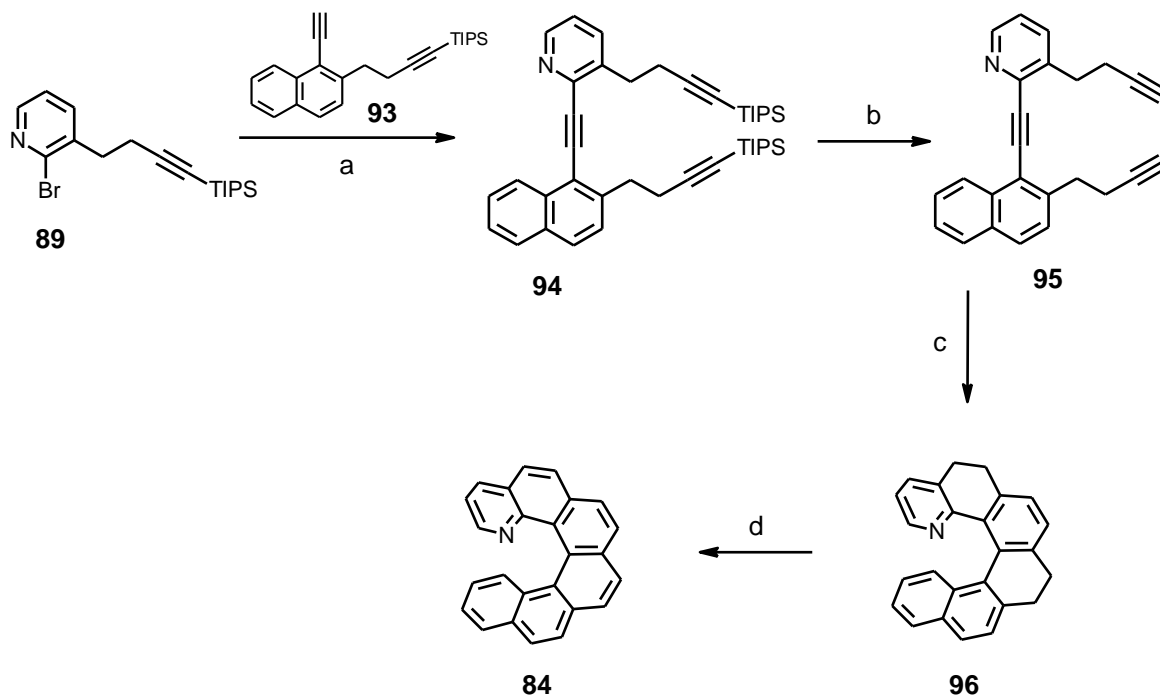
Scheme 3.6   Reagents and conditions:

(a) Pd(PPh$_3$)$_4$, CuI, iPr$_2$NH/toluene, rt, 90 %.

(b) n-Bu$_4$NF, THF, rt, 92 %.

(c) CpCo(CO)$_2$, PPh$_3$, hv, decane, 140 °C, 82 %.

(d) MnO$_2$, toluene, microwave irradiation, 150 °C, 65 %.

The last target compound **85** was prepared starting from commercially availabe 3-bromo-4-methylpyridine **97**. The introduction of the propargyl moiety was performed by deprotonation of the benzylic position and followed by the reaction with TMS protected propargyl bromide (Scheme 3.7). The reaction proceeded well giving **98** in high 93 % yield.

97   3**98**
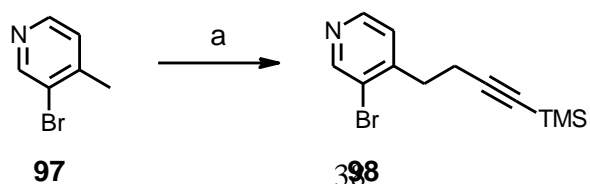
Scheme 3.7 Reagents and conditions:

(a) LDA, THF, 50 ^{o}C, then Br-CH$_2$-C≡C-TMS, 0 ^{o}C, 93 %.

However, bromide in the position 3 at the pyridine ring is not reactive enough for the following Sonogashira cross-coupling. Therefore, the bromine-to-iodine exchange was inevitable (Scheme 3.8). For this purpose the Buchwald's copper catalysed Finkelstein-like halogen exchange reaction was chosen[83]. This method is reported to be relatively mild tolerating a variety of functional groups. However, applying reported conditions only a partial success was achieved. After 24 hours, 21 % conversion was determined by NMR. Further prolongation of the reaction period did not lead to any improvement. Moreover, this transformation is complicated by the fact that the substrate and product are not separable using standard silica gel chromatography. When harsher condition such as microwave irradiation, higher temperature and pressure were applied, the product **89** was obtained in 61 % yield. Unfortunately, reproducibility during the scale up was problematic and, therefore, another more reliable method was needed. Transhalogenation using the halogen-lithium exchange was the alternative reaction to be tried, despite the fact that pyridine can undergo side reactions under such as reaction conditions. Low temperature and a short reaction period during the halogen-lithium exchange should suppress undesired side reactions. The treatment of pyridine **98** with one equivalent of n-BuLi in THF at -78 °C for 30 minutes followed by quenching the reaction with iodine afforded the desired iodide **99** in 42 % yield. No starting material remained in the reaction mixture. The halogen-lithium exchange at -78°C in THF was obviously accompanied by other reactions of an organolithium species and temperature below -100°C is necessary. However, diethyl ether can be used for this purpose at -78°C. Indeed, changing the solvent and keeping otherwise identical conditions led to substantially better 82 % yield.

98 → **99**

a or b or c
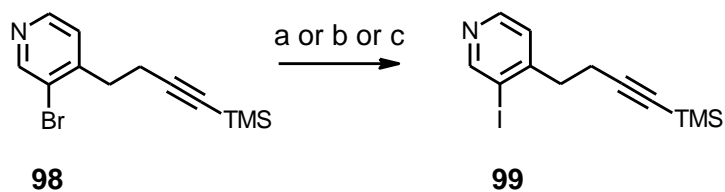
Scheme 3.8 Reagents and conditions:

(a) NaI, CuI, N,N'-dimethyl-1,2-cyclohexanediamine, dioxane, 170 ^{o}C, 61 %.

(b) n-BuLi, THF, -78 ^{o}C, then I_2, -78 ^{o}C, 42 %.

(c) n-BuLi, Et$_2$O, -78 ^{o}C, then I_2, -78 ^{o}C, 82 %.

Having iodide **99** in hand, the further synthetic sequence resembles that one for 1-aza[6]helicene **84**. Sonogashira cross-coupling with diyne **93**, deprotection and cobalt catalysed cyclisation led to the tetrahydro precursor of 2-aza[6]helicene **85**. It is worth mentioning that microwave irradiation during the cyclisation step was also applied. A comfortable reaction set up, THF instead of decane and shortening the reaction period while keeping the same yield are the most obvious advantages of using microwave irradiation. Imidazolium tetrafluoroborate based ionic liquid (1 vol % to THF) was utilised as a magnetic susceptor to increase the microwaves absorption by the reaction medium. The entire synthesis of 2-aza[6]helicene **85** was accomplished by oxidation of the precursor **102** with MnO$_2$ under microwave irradiation conditions (Scheme 3.9).
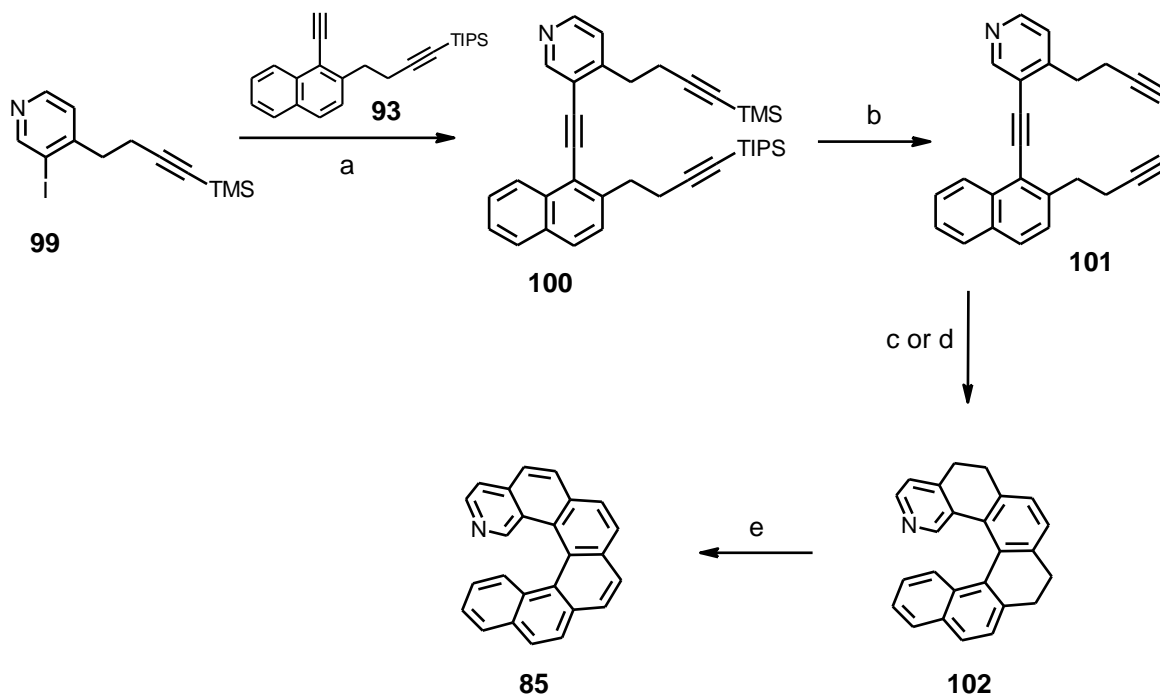
Scheme 3.9 Reagents and conditions:

(a) Pd(PPh$_3$)$_4$, CuI, iPr$_2$NH, rt, 91 %.

(b) n-Bu$_4$NF, THF, rt, 84 %.

(c) CpCo(CO)$_2$, PPh$_3$, hv, decane, 140 $^\circ$C, 89 %.

(d) CpCo(CO)$_2$, PPh$_3$, microwave irradiation, THF, ionic liquid,150 $^\circ$C, 87 %.

(e) MnO$_2$, toluene, microwave irradiation, 130 $^\circ$C, 53 %.

The successful and efficient syntheses of all three target molecules proved the viability of our proposed synthetic strategy. This approach can also be considered modular for the preparation of helicene derivatives containing nitrogen atoms in the aromatic skeleton. It is also the first method that can effectively install the nitrogen atom in the sterically most demanding positions 1 and 2 of the helicene backbone.

To further simplify the azahelicene synthesis and to avoid the aromatisation step, a modified synthetic route starting from commercially available 2-bromonicotinaldehyde **103** was designed (Scheme 3.10). Sonogashira cross-coupling of **103** with gaseous acetylene afforded the desired product **104** in 75 % yield. It is worth noting that THF as a co-solvent was key to success in this specific case. When Et$_3$N was applied as the only solvent, a complicated mixture of products was obtained. Thus, THF might contribute to the better solubility of acetylene in reaction medium and thus push the reaction in the desired direction. The addition of the propargyl Grignard reagent followed by acetylation provided triyne **105** for [2+2+2] cyclotrimerisation in 35 % overall yield. Co(I) cyclisation worked well and the helical intermediate **106** was isolated in good 76 % yield. Interestingly, free homopropargyl alcohols were not compatible with the cyclisation procedure leading to the decomposition of the starting material. Final elimination of acetates was smooth under chosen conditions[84] and provided diaza[5]helicene **83** in good 67 % yield. This improved synthetic strategy allowed to prepare C_2 symmetrical diaza[5]helicene **83** in only four simple steps from the commercially available material.
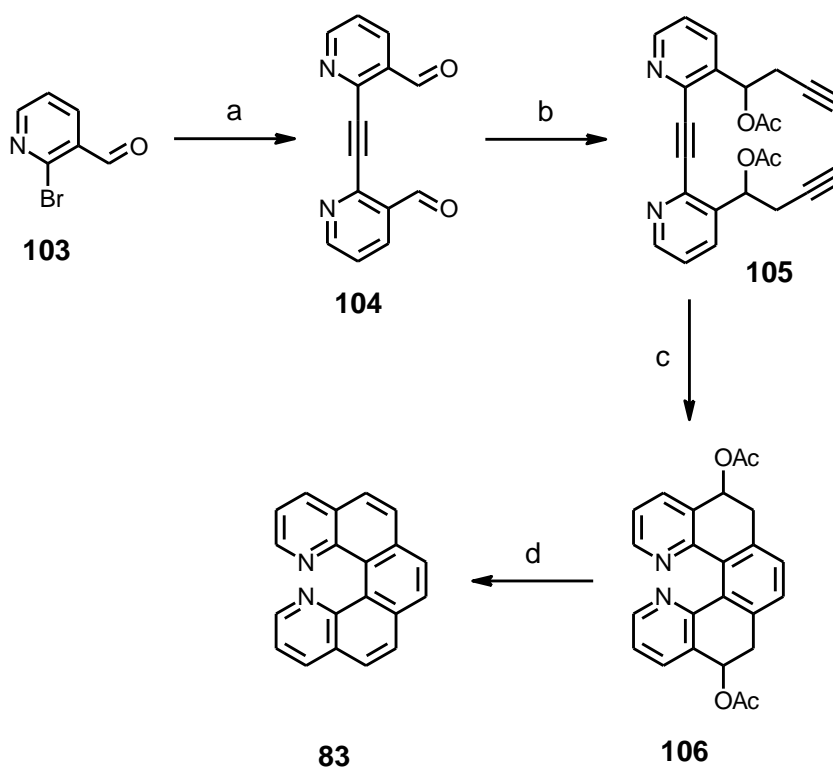
(a) acetylene, Pd(PPh$_3$)$_2$Cl$_2$, CuI, Et$_3$N/THF, 50 °C, 75 %.

(b) BrMg-CH$_2$-C≡CH, Et$_2$O/THF, -78 °C then Ac$_2$O, rt, 35 %.

(c) CpCo(CO)$_2$, PPh$_3$, hv, decane, 140 °C, 76 %.

(d) TfOH/silica gel, 120 °C, 67 %.

Having these azahelicenes in hand, the next step was the resolution of configurationally stable derivatives enantiomers **84** and **85** using chiral HPLC (Chiralcel OD-H column). The difference in retention times of 2-aza[6]helicene enantiomers **85** was large (more than 10 min). Thus, enantiomers of **85** were separated using overloaded analytical column (1.5 mg of racemate per injection) or semipreparative chiral column (EUROCELL 01) (20 mg of racemate per injection).This method allowed the rapid separation of large quantities of 2-aza[6]helicene enantiomers **85** (Scheme 3.10).

(*M*)-(-)-**85**

$[\alpha]^{25}_D$ -3840

(*P*)-(+)-**85**

$[\alpha]^{25}_D$ +3825

rac-**85**

Chiralcel OD-H

heptane-iPrOH
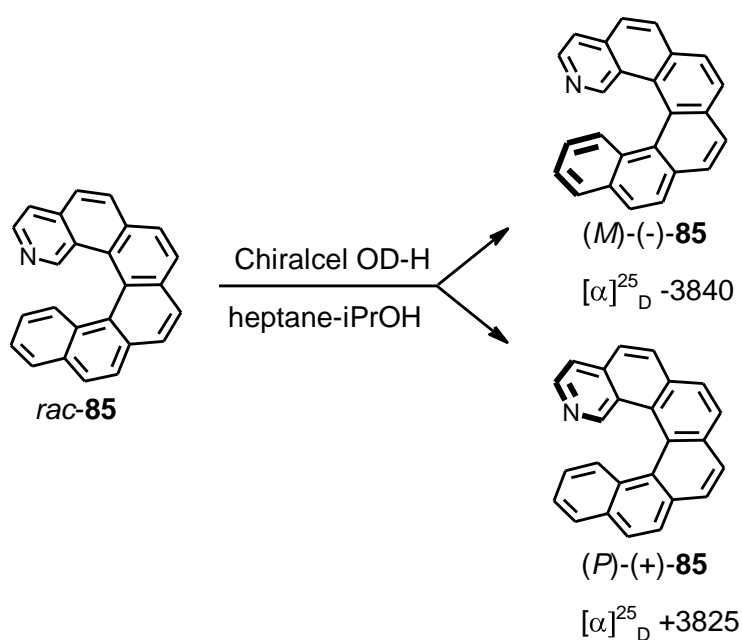
Scheme 3.11 Resolution of 2-aza[6]helicene **85.**

Moving of nitrogen from the position 2 to 1 at 1-aza[6]helicene **84** led to a smaller difference in retention times of individual enantiomers (less than 2 minutes), so chiral HPLC was not applicable for the preparative separation of optical isomers. Therefore crystallisation of diastereomeric salts was tested. After

screening of several chiral acids such as mandelic acid, malic acid, tartaric acid, di-O-toluoyltartaric acid, 10-camphorsulfonic acid, and Mosher's acid, (+)-di-O-benzoyltartaric acid ((+)-DBTA) gave satisfactory results. After optimization, up to 30% of one optically pure enantiomer (from 50% possible) was obtained. Since DBTA is available in both enantiomer forms, both enantiomers of 1-aza[6]helicene **84** were separated (Scheme 3.12). Important criterion for the successful resolution is the excess of DBTA. When a 1:1 mixture of DBTA and helicene was used, no enrichment of helicene enantiomer in the diastereomeric crystals was observed. However, when DBTA applied in an excess the substantial enrichment of one helicene optical isomer in the crystals was achieved. The crystals of a diastereoisomeric salt have stoichiometry 2:1 of DBTA to helicene. This suggests that not only a salt bridge but also a π-π interaction is important for the resolution process.
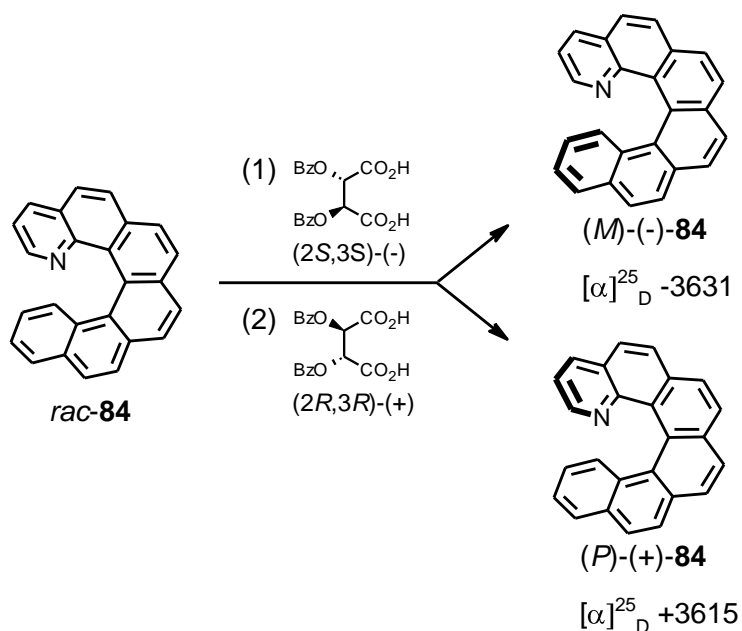
Scheme 3.12 Resolution of 1-aza[6]helicene **84.**

Absolute configuration of enatiomers was assigned by comparison of CD spectra with known CD of [6]helicene **73**[85] whose configuration was determined by X-ray analysis[86]. Notable agreement of CD characteristics of (*P*)-(+)-[6]helicene **73** and (+)-1-aza[6]helicene **84** and (+)-2-aza[6]helicene **85** allowed to unambiguously

ascribe *P* helicity to dextrorotary enantiomer and *M* helicity to laevorotary enantiomers (Figure 3.1).
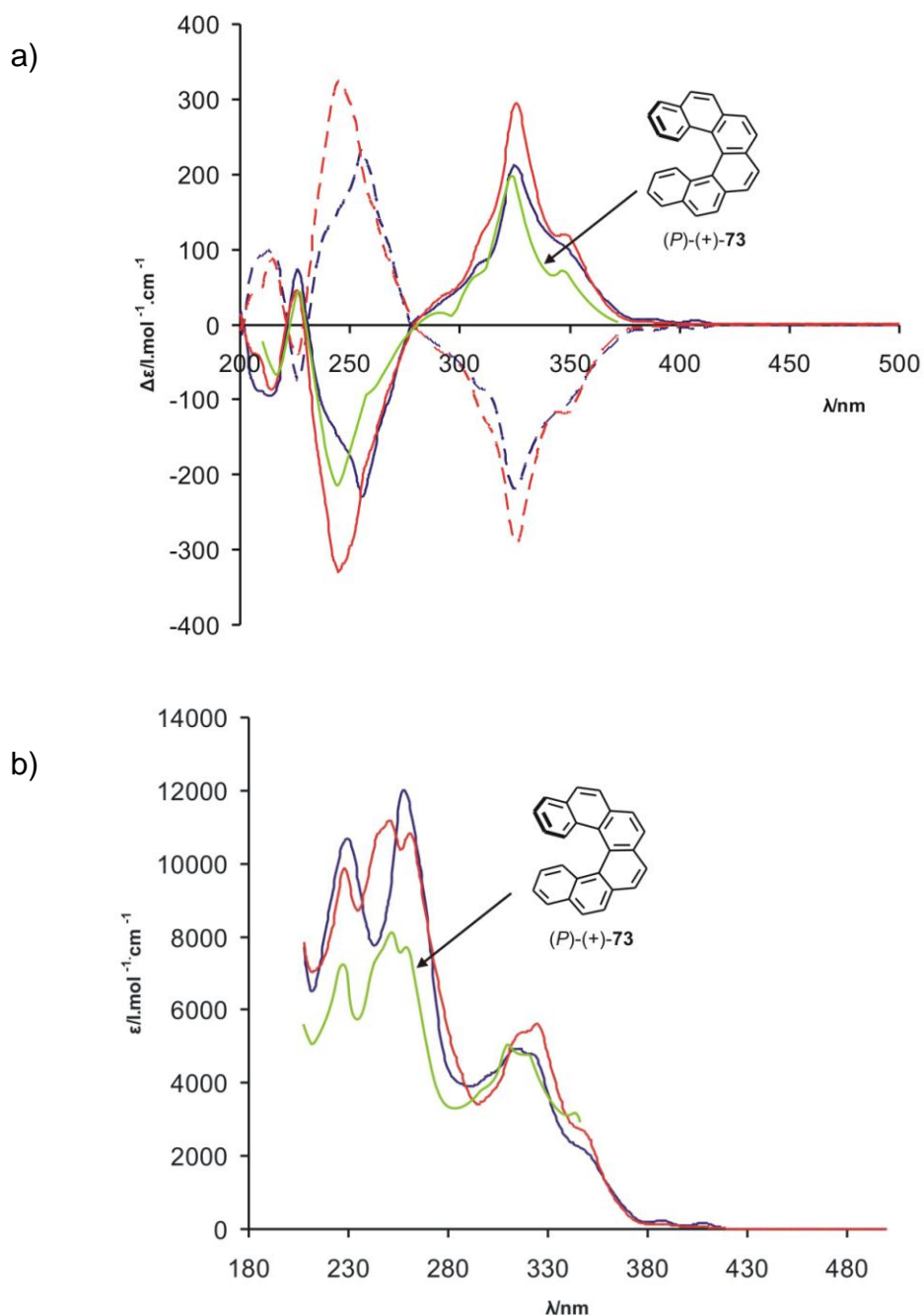
Figure 3.1 a) CD spectra of (*P*)-(+)-1-aza[6]helicene **84** (blue solid line), (*M*)-(-)-1-aza[6]helicene **84** (blue dashed line), (*P*)-(+)-2-aza[6]helicene **85** (red solid line), (*M*)-(-)-2-aza[6]helicene **85** (red dashed line) in acetonitrile (4.70x 10^{-4}M) as well as the spectrum of (*P*)-(+)-[6]helicene **73** (green line) in methanol as reference (1.65x 10^{-5}M). b) UV spectra of 1-aza[6]helicene **84** (blue solid line), 2-aza[6]helicene **85** (red solid line) and [6]helicene **73**[85] (green line).

For complexation and chiral recognition studies in gas phase it was desirable to prepare deuterium labeled azahelicenes. As the most convenient way to introduce deuterium atoms, deprotonation of terminal acetylenes of the intermediate **95** followed by deuteration with D_2O was chosen. After quenching lithium acetylides with D_2O, high degree of deuteration was confirmed by the MS analysis of the reaction mixture. However, a chromatographic purification on silica gel of the desired compound caused almost total lost of deuteration. Acetylenic deuteriums are acidic enough to be exchanged with protons on silica gel. Nevertheless deuteration reaction works well and we suggested in situ cyclisation mediated by $CpCo(CO)_2$ to receive tetrahydroaza[6]helicene [7,8-d_2]-**96**. Subsequent MnO_2 mediated aromatisation procedure afforded aza[6]helicene [7,8-d_2]-**84** with high degree of deuteration (81 %) in 45 % overall yield. Resolution of enantiomers was achieved using chiral HPLC (Chiralcel OD-H column).

95   [7,8-d_2]-**96**

(*P*)-(+)-[7,8-d_2]-**84**
(*M*)-(-)-[7,8-d_2]-**84**
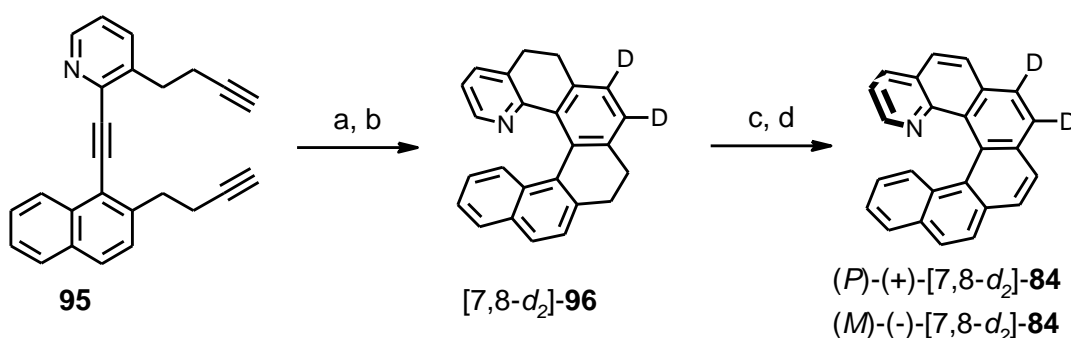
Scheme 3.13   Reagents and conditions:

(a) LDA, THF, -78 °C, then D_2O, rt.

(b) $CpCo(CO)_2$, PPh_3, hv, decane, 140 °C.

(c) MnO_2, toluene, microwave oven, 150 °C, 45 % (overall).

(d) Chiral HPLC (Chiralcel OD-H column)

The last synthetic modification of azahelicene scaffolds was N-oxidation of optically pure (*M*)-(-)-1-aza[6]helicene **84** and (*P*)-(+)-2-aza[6]helicene **85** in order to utilise them in asymmetric catalysis. The classical methodology using MCPBA in CH_2Cl_2 was used[87]. The reaction with (*P*)-(+)-2-aza[6]helicene **85** proceeded

smoothly providing N-oxide **107** in 80 % yield. (*M*)-(-)-1-aza[6]helicene **84** was a less reactive substrate for this reaction and probably due to the steric hindrance of nitrogen in position 1, the corresponding N-oxide **108** was isolated in only 35 % yield (47 % of the starting material was recovered) (Scheme 3.14).

(*P*)-(+)-**85**   (*P*)-(+)-**107**

(*M*)-(-)-**84**   (*M*)-(-)-**108**   (*M*)-(-)-**84**
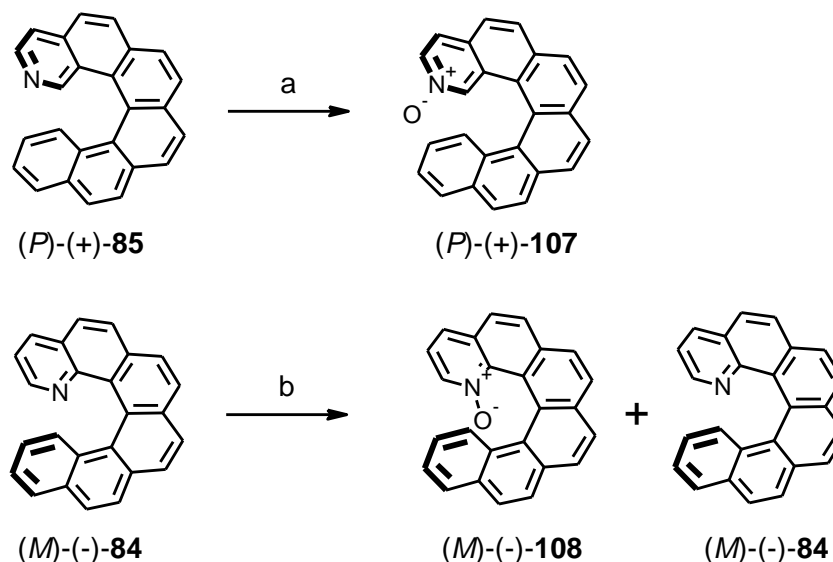
Scheme 3.14   Reagents and conditions:
(a) MCPBA, CH$_2$Cl$_2$, rt, 80 %.
(b) MCPBA, CH$_2$Cl$_2$, rt, 35 % of **108**, 47 % recovery **84**.

3.2   Properties of azahelicenes

3.2.1   X-ray structural analysis

Single crystals of hexacyclic azahelicenes **84** and **85** were successfully grown and subjected to the X-ray analysis. We obtained structures **109** (CCDC 664670) and **110** (CCDC 664671) which are shown in Figure 3.2 together with previously reported [6]helicene[88]. Comparing distances between the position 1 and 16, it is evident that both azahelicenes are more compressed than carbohelicene. This structural difference might be attributed to a less steric demand of the nitrogen electron lone pair in comparison with hydrogen at sp^2 carbon (especially for 1-aza[6]helicene).

a) b) c)

[6]helicene   **110^b**   **109**

Figure 3.2 X-ray crystal structures of a) [6]helicene, b) 2-aza[6]helicene and c) 1-aza[6]helicene

The X-ray analysis of 2-aza[6]helicene **85** offered also information about the stiffness of the helical backbone. The single crystal contains two independent units with different packing of 2-aza[6]helicene **85**. Accordingly, two different molecular geometries of 2-aza[6]helicene **106^a** and **106^b** are observed (Figure 3.3 and 3.4). The distances between the positions 1 and 16 are 3.082 Å for **106^a** and 3.049 Å for **106^b**. The dihedral angles (abcd) that indicate a compression of the helical spring are 36.73° for **106^a** and 34.13° for **106^b**. This shows that the helicene aromatic backbone is not completely rigid and some degree of flexibility might be considered. Such behaviour of the helicene skeleton was already observed in the single crystal of [7]helicene[89]. This fact can have a positive impact for instance in complexation of transition metals or other Lewis acids since azahelicenes might adapt geometry of aromatic skeleton according to the guest.

110ᵃ   **110ᵇ**

Figure 3.3 X-ray structures **110ᵃ** and **110ᵇ** obtained from single crystal of 2-aza[6]helicene **85.**
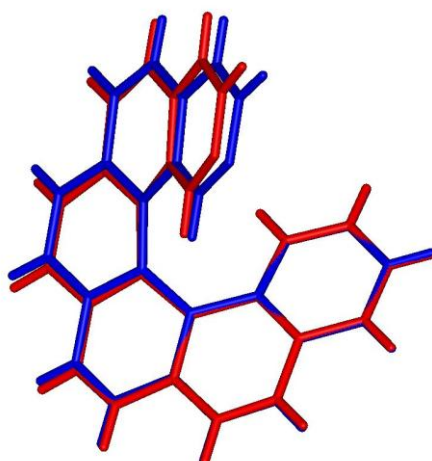
Figure 3.4 Superposition of structures **110ᵃ** and **110ᵇ**.

3.2.2 Configurational stability of aza[6]helicenes 84 and 85

Having optically pure azahelicenes **84** and **85** in hand, kinetic measurements were performed in order to determine racemisation barriers. The first attempt was done as follows: Optically pure 1-aza[6]helicene **84** was dissolved in decanol, the solution was distributed in twenty capped vials and heated with the Rotilabo® heating block to 188 °C. In the course of time, samples were analysed by chiral HPLC to determine enantiomeric excess. This

experimental set up was chosen for several reasons. Decanol as a solvent has reasonable high boiling point (230 °C), solubility of both azahelicenes **84** and **85** was excellent and a direct injection of samples to HPLC is possible. The Rotilabo$^{®}$ heating block can be heated up to 250°C allowing controlling the desired temperature with the high accuracy (±0.1°C). 188 °C is the temperature which was applied in original racemisation experiment for [6]helicene **73** by Martin[52]. However, using these conditions racemisation was too fast to obtain a reliable value of free energy barrier. Therefore, the temperature was eventually reduced to 140 °C. Racemisation of 2-aza[6]helicene **85** was obviously slower and racemisation temperature 188 °C was sufficient enough. Plots of the enantiomers composition towards time are listed below for both azahelicene regioisomers (Figure 3.6). To fit the experimental data to appropriate regression, kinetic analysis of the A↔B equilibration reaction was performed (Figure 3.5). The general regression curve $y = y_0 + ae^{-bx}$ was applied to the data and basic kinetic parameters were calculated. It is necessary to point out that a trial to separate enthalpic and entropic terms of $\Delta G^{\neq}$ was done. Racemisation kinetics was measured at three different temperatures however difference of the barrier values was very small for both azahelicenes within the interval of the accuracy of the method. Therefore no reliable values could be extracted. Nevertheless, these results are in agreement with the previously performed experiments showing the entropic term very small and contributing to $\Delta G^{\neq}$ only marginally[52, 53]. This makes values for 1-aza[6]helicene **84** (measured at 140 °C) and 2-aza[6]helicene **85** (measured at 188 °C) well comparable.

$$M \rightleftharpoons P$$

$$\frac{d[M]}{dt} = -k_i[M] + k_i[P] \qquad\qquad ([P]=100-[M])$$

$$\int_{[M]_0}^{[M]} \frac{d[M]}{[M]-50} = \int_0^t -2k_i dt$$

$$[M] = ([M]_0 - 50)e^{-2k_i t} - 50$$

regression curve

$$y = y_0 + ae^{-bx}$$

half-life of reaction $\qquad\qquad\qquad$ k_i to $\Delta G^{\neq}$ *relation*

$$\tfrac{1}{2}[A]_0 = [A]_0 e^{-2k_i t} \qquad\qquad k_i = \frac{k_b T}{h} e^{-\frac{\Delta G^{\neq}}{RT}}$$

$$t_{1/2} = \frac{\ln 2}{2k_i}$$

$[M]$, $[P]$ – concentrations of M and P optical isomers

k_i - rate constant

$\Delta G^{\neq}$ - Gibbs free energy

k_b - Boltzmann constant (1.380650^{-23} J·K^{-1})

T - temperature

h - gas constant (8.314472 J K^{-1}·mol^{-1})

Figure 3.5 Kinetic analysis of racemisation reaction.

Thermal racemisation of 1-aza[6]helicene at 413 K

Data: 1-aza[6]helicene at 413 K
Model: ExpDec1
Equation: y = A1*exp(-x/t1) + y0
Weighting:
y   No weighting

Chi^2/DoF   = 0.07996
R^2   = 0.99974

y0   48.65674   ±0.28038
A1   50.9378   ±0.2852
t1   6227.26398   ±94.90461

Thermal racemisation of 2-aza[6]helicene at 461 K

Data: 2-aza[6]helicene at 461 K
Model: ExpDec1
Equation: y = A1*exp(-x/t1) + y0
Weighting:
y   No weighting

Chi^2/DoF   = 1.45058
R^2   = 0.995

y0   48.14578   ±1.19779
A1   50.17445   ±1.18601
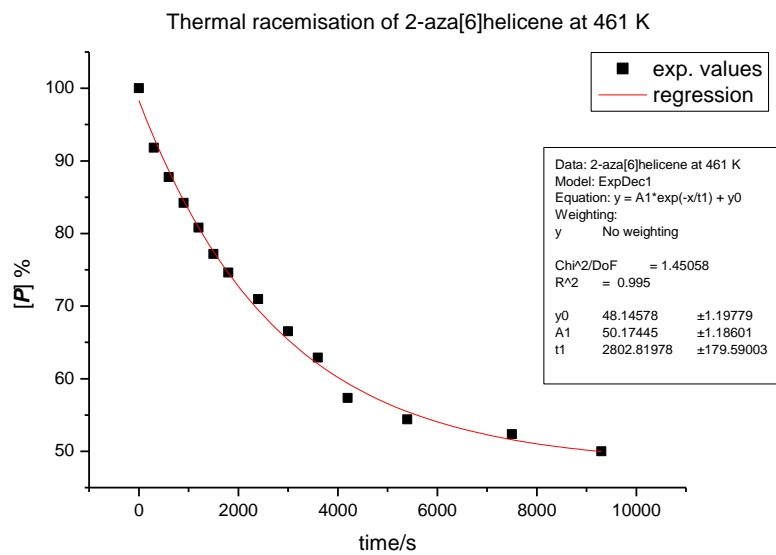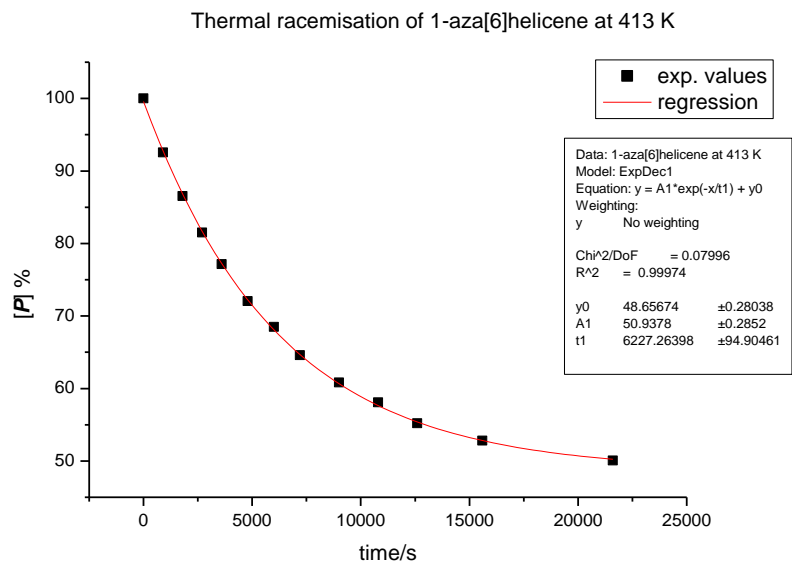t1   2802.81978   ±179.59003

Figure 3.6 Racemisation kinetics for 1-aza[6]helicene **84** and 2-aza[6]helicene **85**.
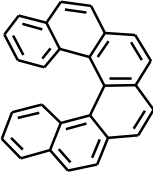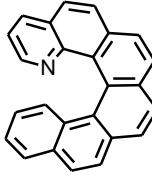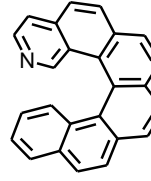
	73	**84**	**85**
temperature (in K)	461	413	461
k_i (in s^{-1})	3.08×10^{-5}	$8.03 \pm 0.12 \times 10^{-5}$	$1.80 \pm 0.12 \times 10^{-4}$
$\Delta G^{\neq}$ (in kcal/mol)	36.9	32.25 ± 0.02	35.33 ± 0.07
$t_{1/2}$ (in min)	187.5	71.9	32.4

Table 3.1 Kinetic parameters for [6]helicene **73**[52], 1-aza[6]helicene **84** and 2-aza[6]helicene **85**.

The comparison of parameters found with the known data for [6]helicene **73** is depicted in Table 4.1. It is evident that 1-aza[6]helicene **84** has racemisation barrier significantly lower than two other representatives (regardless the lower temperature since $\Delta G^{\neq}$ for [6]helicene **73** at 413 is 36.7 kcal/mol). As mentioned in the introductory part, substitution in the position 1 is supposed to be the most important factor affecting barrier. Transition states are schematically showed in Figure 1.4. It can be clearly deduced that while [6]helicene **73** and 2-aza[6]helicene **85** has the same C(1)-H...C(16)-H interaction, in 1-aza[6]helicene **84** it is N(1)…C(16)-H interaction (Figure 3.7). Based on this fact one might speculate that the electron lone pair of on nitrogen is less sterically demanding than hydrogen on sp^2 carbon and, therefore the racemisation barrier of 1-aza[6]helicene **84** is lower. Opposed to that the valence shell electron pair repulsion theory (VSEPR) consider a lone electron pair as more "sterically" demanding (molecule of water is an archetypical example). This theory is however based rather on electrostatic interaction of lone and bonding electron pairs than on steric demands of atoms. VSEPR considers magnitude of repulsion in the following order: Lone pair-lone pair > lone pair-bonding pair > bonding pair-bonding pair. It would suggest the opposite trend than the experimental data. To shed light upon this problem, quantum chemical calculations were carried out[54]. First, using high level calculations (B3LYP/cc-pVTZ), experimental data were

reasonably well reproduced allowing further investigation of this phenomenon. The computed TSs **111**, **112** and **113** for all three helicenes are shown in Figure 3.7. [6]helicene **73** exhibits a C_s symmetric (or "meso") TS **111** (dihedral angle (*abcd*)=0°). There is a tiny difference in geometry of TS **112** for 2-aza[6]helicene **85** (dihedral angle (*abcd*)=2°). However, the distortion from C_s symmetry of TS **113** for 1-aza[6]helicene **84** is significant (dihedral angle (*abcd*)=12°) (Figure 3.7).
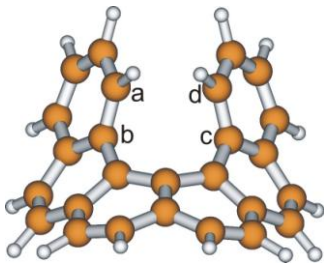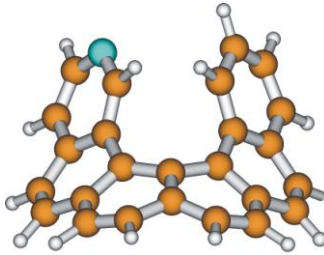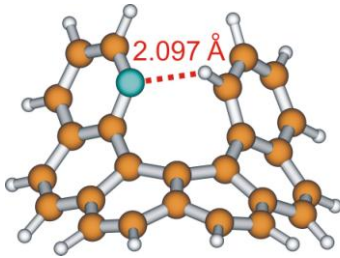
	experimental $\Delta G^{\neq}$ in kcal/mol	calculated $\Delta G^{\neq}$ in kcal/mol	dihedral angle (*abcd*)
a) **111**	36.9	36.4	0°
b) **112**	35.3	34.3	2°
c) **113**	32.3	31.9	12°

Figure 3.7

The lower symmetry of TS **113** for 1-aza[6]helicene **84** might also be considered as a factor reducing the barrier. Nevertheless, an alternative

explanation for the lower racemisation barrier might be hydrogen bonding between the nitrogen electron lone pair and the hydrogen atom on the pseudoparallel terminal benzene ring. (Figure 3.7 c). The distance of hydrogen from nitrogen is 2.097 Å which fits well to the theoretical and experimental data regarding hydrogen bonds. The calculated angle of C-H...:N atoms in TS shows the value of 113° whwhich is at the first glance too bended since hydrogen bond tends to be considered as highly directional having a usual value 180°. Nevertheless, recent studies indicate that directionality of the hydrogen bonding is not so strict and relatively strong hydrogen bonds with considerably bended angles can exist[90, 91].

To further support the mentioned explanation, experimental racemisation of protonated azahelicenes was carried out. It was expected the racemisation barrier of 1-aza[6]helicene **84** should increase upon protonation whereas at 2-aza[6]helicene **85** should be influenced much less. Indeed, upon protonation of 1-aza[6]helicene **84**, its racemisation barrier rose substantially by 2.3 kcal/mol. Surprisingly, barrier of 2-aza[6]helicene **85** dropped by 1.1 kcal/mol (Table 3.2). Nevertheless, protonation experiments support the general mechanistic picture outlined for racemisation of azahelicenes.

Thermal racemisation of 1-aza[6]helicenium BF_4 at 461 K

■ exp. values
— regression

Data: 1-aza[6]helicenium BF4 at 461K
Model: ExpDec1
Equation: y = A1*exp(-x/t1) + y0
Weighting:
y   No weighting

Chi^2/DoF   = 0.414
R^2   = 0.99866

y0   49.67399   ±0.48599
A1   50.84464   ±0.62669
t1   1187.00456   ±36.03533

[*M*] %

time/s

Thermal racemisation of 2-aza[6]helicenium BF_4 at 461 K

Data: (-)-2-aza[6]helicenium BF4 at 461K
Model: ExpDec1
Equation: y = A1*exp(-x/t1) + y0
Weighting:
y   No weighting

Chi^2/DoF   = 0.21712
R^2   = 0.99937

y0   50.6601   ±0.43623
A1   49.14354   ±0.5239
t1   823.61824   ±22.86104

Figure 3.8 Racemisation kinetics for protonated 1-aza[6]helicene **84** and 2-aza[6]helicene **85.**
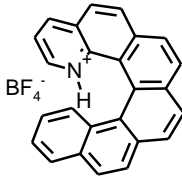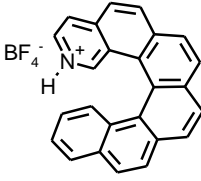
	[**84**-H$^+$][BF$_4^-$]	[**85**-H$^+$][BF$_4^-$]
temperature (in K)	461	461
k_i (in s^{-1})	4.21 ± 0.13 × 10^{-4}	6.08 ± 0.17 × 10^{-4}
$\Delta G^{\neq}$ (in kcal/mol)	34.55 ± 0.03	34.21 ± 0.03
$t_{1/2}$ (in min)	13.7	9.5

Table 3.2 Kinetic parameters for protonated 1-aza[6]helicene **84** and 2-aza[6]helicene **85**.

3.2.3 Azahelicenes as ligands for transition metals

Investigation of azahelicenes ability to serve as ligands for transition metals started with electrospray-mass spectrometry (ESI-MS) experiments. Azahelicenes **83**, **84** and **85** with AgOTf were sprayed from acetone under the mild ionization conditions[92] to observe a formation of corresponding complex ions. Both 1-aza[6]helicene **84** and 2-aza[6]helicene **85** form intensive doublets at 766 Da representing silver ion bound dimers of azahelicenes. Surprisingly, no such dimers or oligomers were observed for diaza[5]helicene **83**. A cationic complex with the highest mass in the spectrum corresponded to the silver cation bearing one diaza[5]helicene **83** and one molecule of acetone. X-ray analysis was performed in order to provide the detailed insight into the silver complexes. Single crystals of silver complexes with both hexacyclic azahelicenes **84** and **85** were successfully grown and subjected to X-ray analysis. The structure of the complexes is shown in Figure 3.9 and 3.10. The notable feature of both complexes is that homochiral dimers are exclusively formed when starting from racemic azahelicenes. Only the (*P,P*) and (*M,M*) pairs are found in the crystals. In the silver complex **114** (CCDC 664674) two molecules of 2-aza[6]helicene **85** are placed in (slightly bended) linear arrangement that is typical for silver(I) complexes with nitrogen containing ligands. Moreover, the coordination sphere of silver is supplemented with the triflate anion. The similar T-shaped arrangement is seen in the silver complex **115** (CCDC 664673). 1-aza[6]helicene **84** are placed in almost perfect linear arrangement and a molecule of propanol make up the T-shaped ligand surroundings of silver. However, more careful inspection of bonding connections reveals that the distances between the silver atom and centroids of the C(6a)-C(16b) and C(6a′)-C(16b′) bonds are 2.901 Å and 2.916 Å, respectively, and thus fall well below the sum of their van der Waals radii ($\sum_{Ag,C}$ =3.42 Å). It can be undoubtedly considered as another coordination sites of 1-aza[6]helicene **84**. Hence, the coordination sphere can be better described as a trigonal bipyramid in which each azahelicene binds as an N,C bidentate ligand with the nitrogen atom and C=C bond occupying axial and equatorial positions, respectively. Consequently, the selected azahelicenes might join the family of novel chiral olefin-type ligands and might attract attention in the asymmetric catalysis community[93].
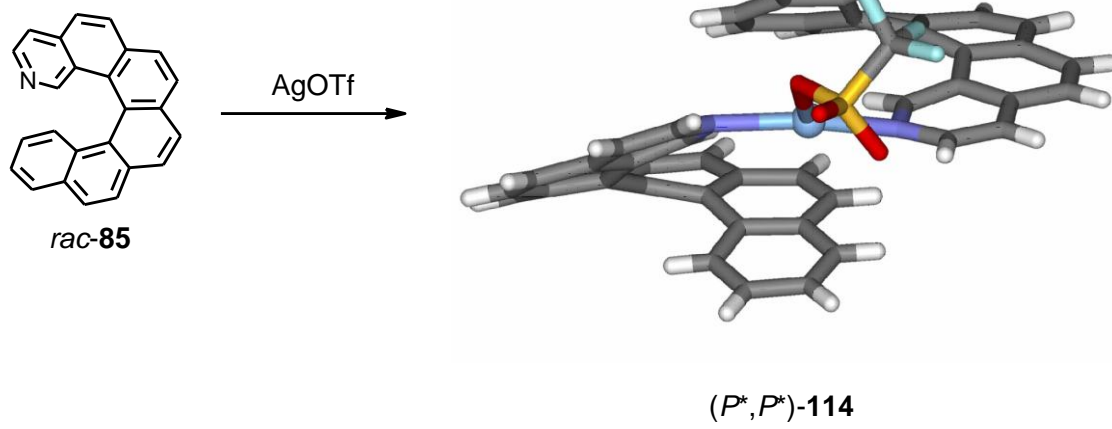
Figure 3.9 X-ray crystal structure of silver(I) complex **114**.
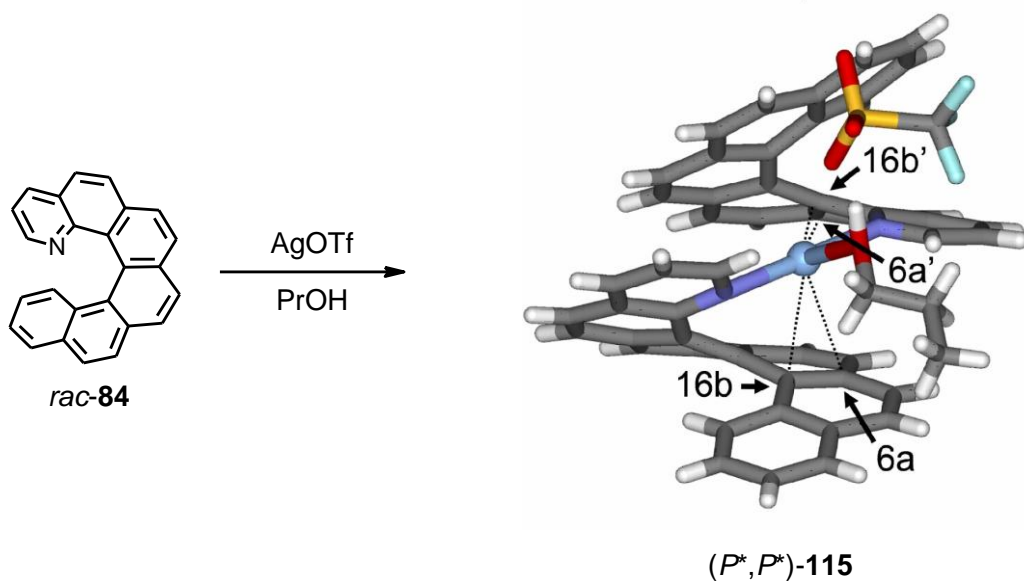
Figure 3.10 X-ray crystal structure of silver(I) complex **115**.

3.2.4 Complexation and chiral recognition in gas phase

Mass spectrometry (MS) in chemistry is a powerful tool particularly for the structure and mechanisms elucidation. However, it is considered as "achiral" meaning that the differentiation of enantiomers is not accessible using this technique. Nonetheless, when individual enantiomers are mass labeled chiral information might be reflected by MS measurement and, for instance, a stereochemical outcome of a reaction can be monitored[94]. For these purposes doubly deuterated azahelicene [7,8-d_2]-**84** was synthesized and resolve into enantiomers (*P*)-(+)-[7,8-d_2]-**84** and (*M*)-(-)-[7,8-d_2]-**84**. An original intention was to probe if the above mentioned solid phase self recognition of enantiomers also occurs in the gas phase where no additional solution or solid phase effects can be taken into account. (*P*)-(+)-[7,8-d_0]-**84** and (*M*)-(-)-[7,8-d_2]-**84** were mixed (roughly 1:1) and the ESI MS spectrum was aquired in order to determine the exact ratio of both pseudoenantiomers. Then AgOTf was added and the second spectrum was measured. As deuteration of [7,8-d_2]-**84** is not absolute, the mass difference of the pseudoenentiomers is only 2 amu and the isotope distributions of both labeled and unlabeled [7,8-d_2]-**84** and [7,8-d_0]-**84** are partially overlapped. Therefore, the statistical treatment of the isotope patterns is necessary to extract the desired information about the ratios and the stereochemical effect (SE = K_{homo}/K_{hetero} = K_{PP}/K_{PM} = K_{MM}/K_{PM}). Figure 3.11 shows an example of the experimental isotope pattern of such mixtures prepared. Linear combination of the isotope distribution of the corresponding components allows determining the exact mixing ratio.
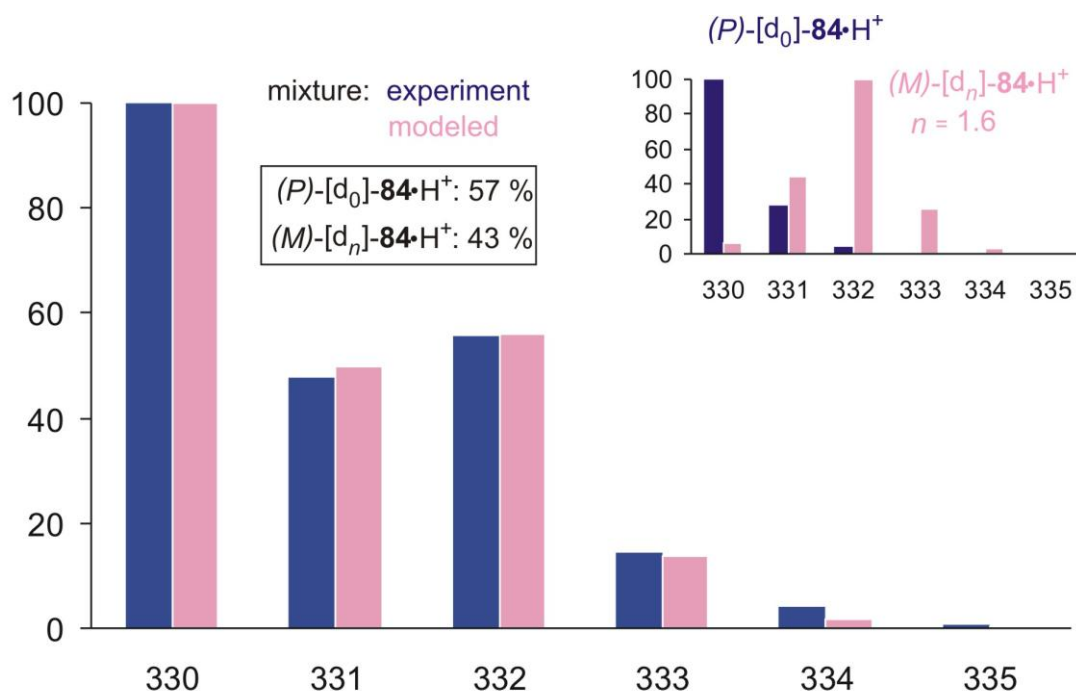
Figure 3.11 Normalized ion abundances of the mass region of the protonated 1-aza[6]helicenes **84**.

Knowing the ratio of pseudoenantiomers, SE in the silver bound dimer can be modeled in a similar manner. Silver exist in two almost equally abundant isotopes 107 and 109 which makes the isotope distribution of the azahelicene dimer even more complex. Figure 3.12a shows the experimental isotope pattern (blue bars) of the silver complex resulting from the mixture of (*P*)-(+)-[7,8-d_0]-**84,** (*M*)-(-)-[7,8-d_2]-**84** and AgOTf. The pink bars represent the purely statistical distribution. From comparison with the experiment it is clear that the experimental isotope pattern contains a higher abundance of low and high mass ions which corresponds to homochiral complexes [((+)-(*P*)-[d_0]-**84**)+Ag+((+)-(*P*)-[d_0]-**84**)]$^+$ (*m/z* 765 for the ^{107}Ag and *all*-^{12}C isotope) and [((-)-(*M*)-[d_2]-**84**)+Ag+((-)-(*M*)-[d_2]-**84**)]$^+$ (*m/z* 769 for the ^{107}Ag and *all*-^{12}C isotope). The red bars in the Figure 3.12a represent a model that satisfactory fits the experimental data providing the value of the stereochemical effect (SE) 5.4. It indicates large preference of bisligation of silver with azahelicenes of the same chirality. A control experiment was done with the labeled and unlabeled **84** of the same chirality ((*M*)-(-)-[7,8-d_0]-**84**, (*M*)-(-)-[7,8-d_2]-**84**) and AgOTf, where no stereochemical discrimination is expected. Indeed,

the experimental isotope distribution is almost identical with the statistical distribution and the model fits best with the value of SE equal to 1 (Figure 3.12b).
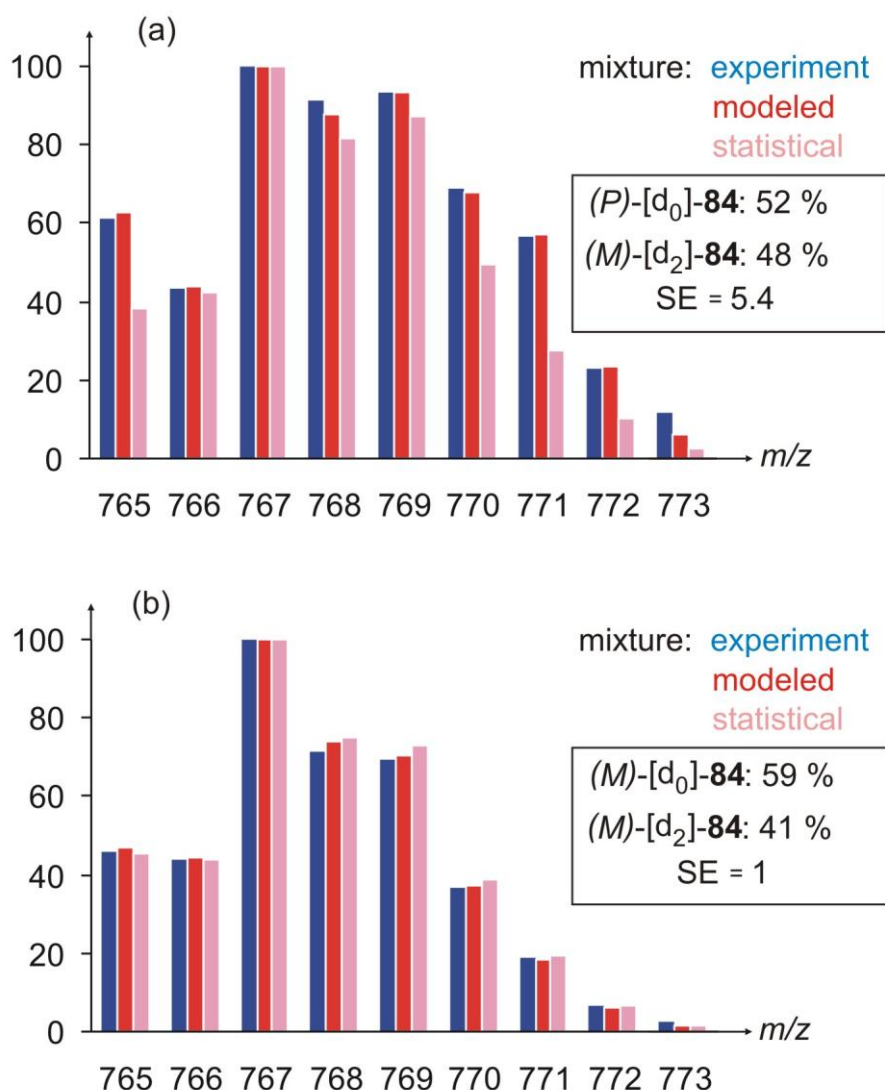
Figure 3.12 Normalized ion abundances of the mass region of the silver(I)-bound dimers of 1-aza[6]helicenes **84**.

Similar set of experiments was performed but without using silver. Electrospray ionization (ESI) of a methanolic solution of 1-aza[6]helicene **84** gives rise to an intense signal corresponding to the protonated molecule [**84**+H]$^+$. Furthermore, upon the adjustment of mild ionization conditions, the ESI process can also lead to larger associates such as the proton bound dimer [**84**$_2$+H]$^+$. These proton bound dimers were investigated in the same fashion as silver complexes of

azahelicenes. The proton bound dimers of a mixture of above mentioned pseudoenantiomers were generated and isotope patterns were analysed. The results are summarised in Figure 3.13. SE is again very remarkable and even larger than in the case of silver complexes. The SE value was assigned to be 13. The higher value of SE for the proton bound dimer than for the silver bound dimer can be ascribed to the larger ionic radius of silver and thus to a smaller repulsion of the sterically demanding helical backbones.
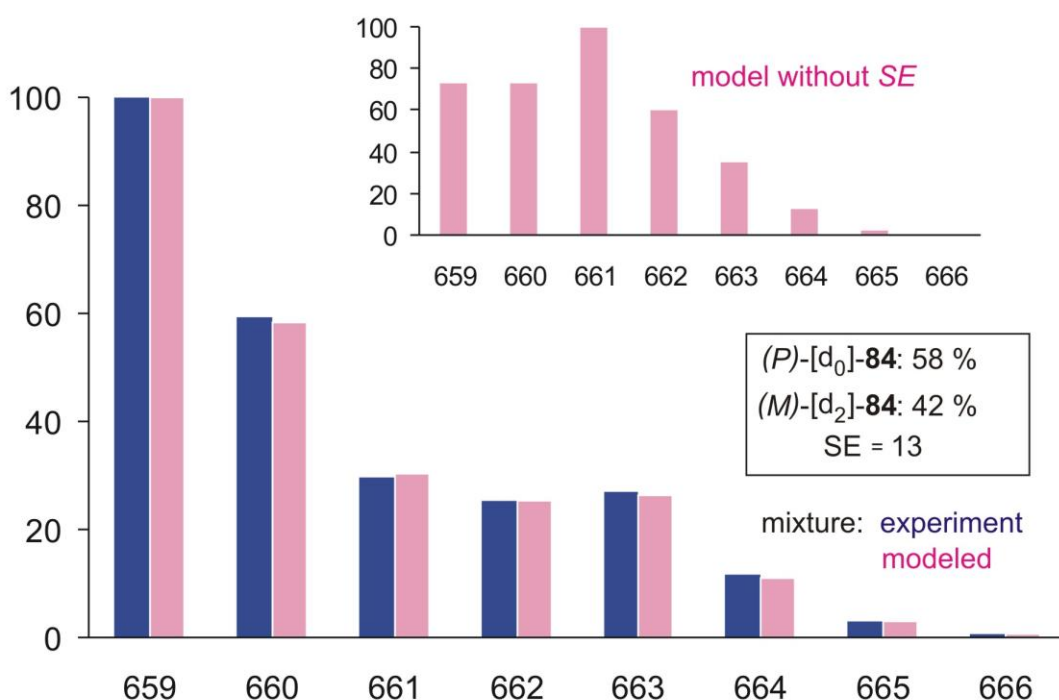
Figure 3.13 Normalized ion abundances of the mass region of the proton-bound dimers of 1-aza[6]helicenes **84**.
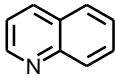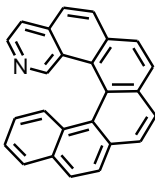
Both X-ray analysis and MS gas phase experiments revealed that self recognition and tendency to form homochiral associates is an important feature of azahelicenes. These results together with previous studies of Branda[37] indicate that a longing of helicene enantiomers for partners of the same chirality is a general feature for this type of molecules.

3.2.5 Basicity of azahelicenes

Already mentioned diaza[5]helicene **83** was previously prepared by Staab et al. in order to study it as a proton sponge[95]. X-ray analysis of its single crystals (crystallised from the solution with an excess of a strong acid) afforded only a monocationic salt, which contains acidic proton in between two basic nitrogen atoms. The estimation of pK_a by the NMR transprotonation experiment gave the value of 10.3 ± 0.2 (in DMSO). This interesting fact drove us to examine also the basicities of the hexacyclic monoazahelicenes **84** and **85**, which have not been determined yet. First, the determination of the gas phase basicities (proton affinities) was carried out using a kinetic method[96]. This method is based on the collision induced dissociation (CID) of proton bound dimers. As mentioned above, ESI MS give rise to the proton bound dimers (PBD). When two different bases (A and B) are used, mixed PBD [A-H-B]$^+$ can be generated. Using ESI MS/MS technique the desired mixed PBD can be mass selected and dissociated into [A-H]$^+$, [B-H]$^+$ and corresponding neutral molecules. In other words, upon the collision induced dissociation two molecules of different basicity (proton affinity) are competing for one proton and, obviously, the more basic wins. This lead to a different ratio of protonated molecules [A-H]$^+$ and [B-H]$^+$ depending on their basicities. A relative abundance of protonated molecules (*I*) after CID can be treatedby the equation of ΔH = -$RTln[I(AH^+)/I(BH^+)]$. When a reference base of known proton affinity (PA) is used, proton affinity (ΔH) of an unknown base can be determined. In principle, this method is very similar to NMR based transprotonation experiments, which use a reference base or acid to estimate pK_a of an unknown base or acid.

Applying the MS methodology, gas phase proton affinities of 1-aza[6]helicene **84** and 2-aza[6]helicene **85** were assigned. The exact values of proton affinities are depicted in Table 3.3. Hence, it is evident that both aza[6]helicenes are considerably more basic in the gas phase than common pyridine-type or ammonia-type nitrogen organic bases. This increased PAs can probably be attributed to the effective delocalisation of the positive charge along the extended π-system. A slightly higher value of PA for 1-aza[6]helicene **84** than for 2-aza[6]helicene **85** might be attributed to stabilising through-space interaction

of proton with the aromatic skeleton. This explanation is also supported by DFT calculations[97].

	NH$_3$			NEt$_3$	**85**
PA (in kJ/mol)	854	930	953	982	992
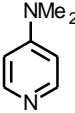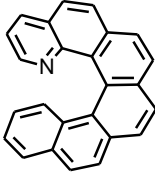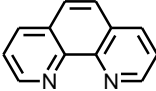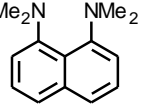
	NMe$_2$	**84**		Me$_2$N NMe$_2$
PA (in kJ/mol)	998	1000	1004	1028

Table 3.3 Proton affinities of 1-aza[6]helicene **84**, 2-aza[6]helicene **85** and some other common organic bases[98].

The gas phase and solution phase acidity/basicity, however, might differ notably. As the largest area of azahelicene applications is expected to be in a solution, information about basicity in the solution is needed. A variety of methods is available to determine acid-base dissociation constant (pK_a). The most commonly used are potentiometric and spectrophotometric titrations. Whereas spectrophotometric titrations are employed for measuring pK_a values of water-soluble compounds, potentiometry is extensively used also for the pK_a determination which requires the use of organic solvents[99]. Azahelicenes are molecules with large aromatic backbone and therefore insoluble in water. A drawback of the titration methods mentioned is a need of relatively large quantities of high-purity compounds. Alternatively, capillary zone electrophoresis (CZE) is powerful method widely used for determination of physico-chemical properties including pK_a [100–102]. This method is routinely applied to determine dissociation constants of compounds in water but can be adapted to nonaqueous solvents. The

amount of a sample necessary for an analysis is negligible in comparison with titration methods (it is at least three orders of magnitude lower).

CZE was utilised for the pK_a determination of diaza[5]helicene **83**, 1-aza[6]helicene **84** and 2-aza[6]helicene **85** in methanol. Methanol has the most similar properties to water among common organic solvents and shows a good ability to dissolve azahelicenes. The core of this method is based on the relation of the effective electrophoretic mobility (m$_{eff}$) of an ionisable compound depending on pH of the solution. In practice, m$_{eff}$ of a sample is measured in buffered solutions of different pH. Then, the dependence of pH on m$_{eff}$ is plotted, a regression curve is fitted and pK_a is derived. pH of buffered solutions was calculated according to the Handerson-Hasselbalch equation, where activity coefficients of ionic species were calculated from the Debey-Hückel equation reflecting the solvent properties. The recalculation of methanol based pK_a to water based ^{w}pK_a is possible[103]. Results of these measurements for all three azahelicenes are summarized in Table 3.4[104]. These results show that the order of the basicity in methanol for 1-aza[6]helicene **84** and 2-aza[6]helicene **85** is reverse than in the gas phase. However, in contrast to the gas phase, no significantly higher basicity is observed in solution and basicity of aza[6]helicenes **84** and **85** is not strongly affected by the extended aromatic scaffold since quinoline and isoquinoline have the same trend of basicity with regard to the nitrogen position and have very similar values of pK_a. Conversely, the extended aromatic system might be the reason of a bit lower pK_as in comparison with quinolines, since solvation of the bulky helicene skeleton is more difficult[105]. As far as diaza[5]helicene **83** is concerned, its relatively high basicity is in agreement with the reported proton sponge properties[95].The lower value of the determined p$K_{a,2}$ in comparison with the reported value (8.9 vs. 10.3) can be probably attributed to solvation properties of different solvents (MeOH vs. DMSO).
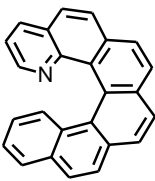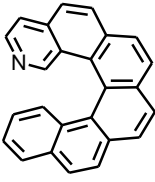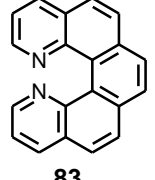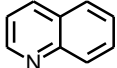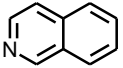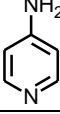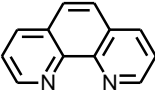
	$pK_{a,1}$	$pK_{a,2}$	$^{w}pK_{a,1}$	$^{w}pK_{a,2}$
84	4.94 ± 0.05	-	4.55 ± 0.25	-
85	5.68 ± 0.05	-	5.28 ± 0.25	-
83	7.56 ± 0.38	8.85 ± 0.26	7.12 ± 0.58	8.39 ± 0.46

	-	-	5.25	-
	-	-	4.90	-
	-	-	5.42	-
	-	-	9.11	-
NEt$_3$	-	-	11.01	-
	-	-	4.84	-

Table 3.4 Dissociation constants of of 1-aza[6]helicene **84**, 2-aza[6]helicene **85,** diaza[5]helicene **83** and some other common organic bases[106] in methanol (pK_a) and in water ($^{w}pK_a$).

3.3 Application of azahelicenes in asymmetric catalysis

This field is totally unexplored and many asymmetric transformations to utilise azahelicenes might be envisioned. After the literature search and basic molecular modeling, enantioselective kinetic resolution (KR) of alcohols was selected as a model reaction. Asymmetric KR is based on a prerequisite that one enantiomer reacts faster than the other and, at certain degree of conversion the remaining starting material is optically highly enriched or pure[107]. The ability of chiral catalyst to react exclusively with one enantiomer can be expressed with selectivity (s), which is defined as a ratio of rate constants for faster reacting and slower reacting enantiomer. In practice, selectivity is calculated from the degree of conversion and the enantomeric excess (ee) of remaining substrate.

$$s = \frac{k_R}{k_S} = \frac{\ln(1-c)(1-ee_s)}{\ln(1-c)(1+ee_s)},$$

k_R – rate constatnt for faster reacting enantiomer
k_S – rate constatnt for slower reacting enantiomer
c – conversion
ee_s – enantiomeric excess of remaining substrate

In general, the enantioselective reactions can be divided into two categories - enzymatic[108] and chemical[107]. Enzymatic kinetic resolution relies on enzymes that are isolated from natural material or produced by recombinant techniques. Enzymes often show high values of selectivity, however, their substrate specifity is usually very high even though the recent progress in enzymatic evolution brings some promising results[109]. Nevertheless, the development of enzymes for a specific substrate or an enzyme with the broad substrate specifity (while keeping selectivity) can be laborious and high-cost. Chemical kinetic resolution uses either transition metal complexes or small organic molecules as chiral catalysts. This allows relatively rapid optimization and broad substrate specifity. Three chiral nucleophilic catalysts that belong up to date to the most selective catalysts are shown in Figure 3.14 together with their selectivity achieved for 1-phenylethanol as a substrate[110–112].

116
s = 42

117
s = 14

118
s = 26
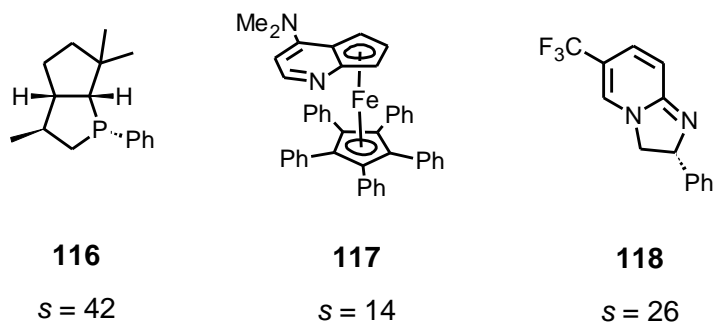
Figure 3.14 Structures of the most successful catalysts in chemical kinetic resolution of secondary alcohols.

1-phenylethanol was also used as model substrate for KR using aza[6]helicenes as catalysts. Following the Birman's protocol, isobutyric anhydride as an acylating agent, diisopropylethylamine as a base and chloroform as a solvent were chosen [112]. Scheme 3.15 depicts preliminary results obtained for (-)-(*M*)-1-aza[6]helicene **84** and (-)-(*M*)-2-aza[6]helicene **85** as nucleophilic catalysts. Reaction with (-)-(*M*)-1-aza[6]helicene **84** catalyst was sluggish and less then 5% conversion was achieved after 48 hours. In contrast to that, the reaction with (-)-(*M*)-2-aza[6]helicene **85** catalyst was significantly faster and 65 % conversion was achieved after 68 hours. Enantiomeric excess of remaining alcohol was determined to be 92 % with absolute configuration (*R*) for the major enantiomer.

.(*M*)-(-)-**84**   (*M*)-(-)-**85**

conversion <5 %

92% ee   50% ee

conversion 65 %

s = 9
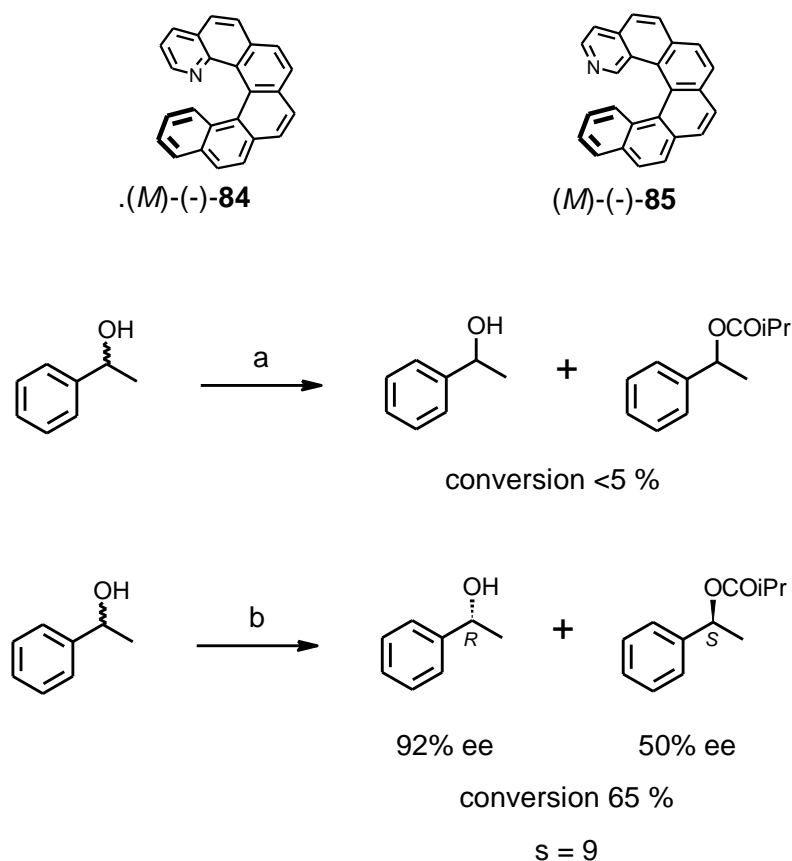
Scheme 3.15   Reagents and conditions:

(a) (-)-(*M*)-**84** (cat.), (i-PrCO)$_2$O, i-Pr$_2$NEt, CHCl$_3$, rt, <5 %.

(b) (-)-(*M*)-**85** (cat.), (i-PrCO)$_2$O, i-Pr$_2$NEt, CHCl$_3$, rt, 65 %.

This stereochemical outcome can be rationalised using the TS1 and TS2 models (Figure 3.15). A previously proposed mechanism of asymmetric induction suggests that an aromatic core of the substrate is stacked to the pyridinium ring of the catalyst via cation-π and π-π interactions[112]. Then the favored TS model might be TS1, where methyl in the benzylic position is pointing away from the helicene skeleton. On the contrary, in the TS2 model the steric clash of methyl with the helicene backbone might be responsible for lower reactivity.

TS1   **TS2**
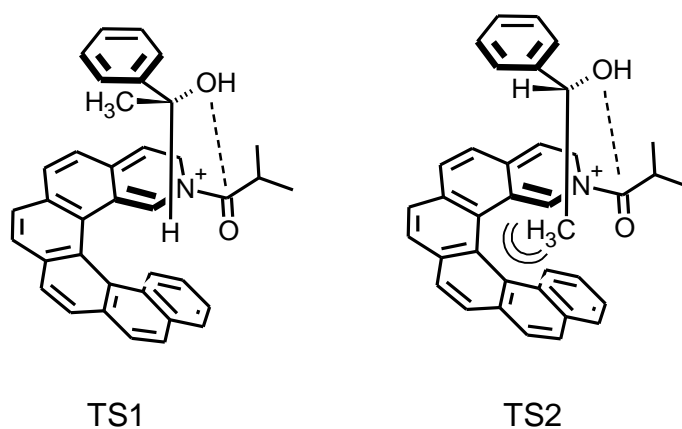
Figure 3.15 Proposed transition state models for asymmetric induction.

To the best of our knowledge this is the first successful application of azahelicenes in asymmetric catalysis.

4   Summary

- The novel modular and practical syntheses of azahelicenes **83**, **84** and **85** have been developed.

- The hexacyclic derivatives **84** and **85** have been resolved into enantiomers for the first time and helicity has been assigned.

- The sufficient configurational stability of azahelicenes **84** and **85** has been confirmed and the influence of the nitrogen position on the racemisation barrier has been described.

- The ability of azahelicenes to form the transition-metal complexes has been proven.

- The interesting aspects of chiral self-recognition of the azahelicenes have been described.

- The gas phase and solution phase basicities have been determined.

- The first utilisation of azahelicenes in enantioselective catalysis has been described.

5 Experimental Section

General. ^{1}H NMR spectra were measured at 200.04 MHz, 499.8 MHz and 500.13 MHz, ^{13}C NMR spectra at 125.7 MHz, in $CDCl_3$ with TMS as an internal standard and DMSO. Chemical shifts are given in δ-scale, coupling constants J are given in Hz. HMBC experiments were set up for J_{C-H} = 5 Hz. For correct assignment of both ^{1}H and ^{13}C NMR spectra of key compounds, the COSY, ROESY, HMQC, HMBC, and CIGAR-HMBC experiments were performed. For all the other compounds, the general semiempirical equations were applied to the chemical shift assignments. IR spectra were measured in $CHCl_3$ or CCl_4. EI MS spectra were determined at an ionizing voltage of 70 eV, m/z values are given along with their relative intensities (%). FAB MS spectra were measured using the thioglycerol-glycerol 3:1 matrix, m/z values are given. HR MS spectra were obtained by the EI or FAB. CD and UV spectra were measured in CH_3CN. Commercially available reagent grade materials were used as received. Decane, piperidine, diisopropylamine ant triethylamine were degassed by three freeze-pump-thaw cycles before use; toluene and $(CH_2Cl)_2$ were distilled from calcium hydride under argon; THF and diethyl ether were freshly distilled from sodium/benzophenone under nitrogen. Commercial pure solvents were used directly when growing crystals for the X-ray analysis. TLC was performed on Silica gel 60 F_{254}-coated aluminium sheets (Merck) and spots were detected by the solution of $Ce(SO_4)_2$. 4 H_2O (1 %) and $H_3P(Mo_3O_{10})_4$ (2 %) in sulfuric acid (10 %). Flash chromatography was performed on Silica gel 60 (0.040-0.063 mm or <0.063 mm, Merck) or on Biotage KP-Sil® Silica cartridges (0.040-0.063 mm) used in Horizon® HPFC system (Biotage, Inc.). The HPLC analyses of chiral azahelicenes **84** and **85** were performed on a Chiralcel OD-H column (250 × 4.6 mm, 5 μm) in heptane–isopropanol 3:1, flow rate 0.8 ml/min, simultaneous UV detection at 254 nm (Varian) and polarimetric detection (Chiralizer, Knauer).

Cyclisation Procedure. A Schlenk flask was charged with the starting triyne, triphenylphosphine (40 mol %), and filled with argon. Degassed decane was added and the mixture was warmed to 140 °C to dissolve. $CpCo(CO)_2$ (20 mol %) was added via Hamilton syringe and the reaction mixture was heated to 140 °C with concomitant irradiation with a halogen lamps (Halo Star 64480, Osram, or

KANDOlite JDD E27, placed outside the reaction vessel) for 1 h. Solvent was removed *in vacuo* (80 ^{o}C, 20 mbar) and the crude product was chromatographed on silica gel (hexane-acetone 85:15) to provide the cyclised product.

Aromatisation Procedure. A glass vial was charged with a solution of the starting tetrahydroazahelicene in toluene and MnO_2 (30 equiv.). The vial was tightly capped and heated by microwave irradiation (Biotage microwave oven system). The resulting reaction mixture was directly chromatographed on silica gel (hexane-acetone-triethylamine 80:20:1) to provide the desired product.
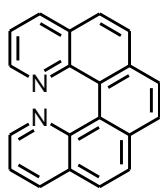
Benzo[1,2-*h*:4,3-*h'*]diquinoline (1,14-diaza[5]helicene) 83. Method A (by reaction with MnO_2): Tetrahydro-azahelicene **92** (60 mg, 0.21 mmol), MnO_2 (0.55 g, 6.33 mmol, 29.98 equiv.), toluene (18 ml), 150 °C, 20 min. The aromatisation procedure afforded azahelicene **83** (24 mg, 41 %) as an amorphous yellowish solid.

Method B (by reaction with DDQ): A 10 ml glass vial was charged with a solution of the starting tetrahydroazahelicene **92** (19 mg, 67 µmol) in $(CH_2Cl)_2$ (8 ml) and DDQ (152 mg, 670 µmol, 10.0 equiv.). The vial was tightly capped and heated by microwave irradiation (Biotage microwave oven system) to 200°C for 40 min. The solvent was removed *in vacuo* and the crude product was chromatographed on silica gel (hexane-acetone-triethylamine 80:20:1) to provide azahelicene **83** (7 mg, 37 %) as an amorphous yellowish solid.

Method C (by reaction with TfOH on silica gel) Helicenediacetate **106** (90 mg, 225 µmol) was dissolved in CH_2Cl_2 (10 ml) and TfOH coated silica gel (10 w % of TfOH on silica gel, 5.5 g, 36.7 mmol to TfOH) was added. The solvent was evaporated *in vacuo*, the resulting solid was put under argon and stirred for 2 h at 120°C. The resulting reaction mixture was directly chromatographed on silica gel (hexane-acetone-triethylamine 80:20:1) to provide the desired product **83** (42 mg, 67 %) as an amorphous yellowish solid.

Mp 260-264 °C (toluene)

^{1}H NMR (500 MHz, DMSO-d_6): 7.59 (2 H, dd, *J* = 8.1, 4.1), 8.10 (2 H, d, *J* = 8.5), 8.12 (2 H, d, *J* = 8.5), 8.19 (2 H, s), 8.44 (2 H, dd, *J* = 8.1, 1.8), 8.56 (2 H, dd, *J* = 4.1, 1.8).

¹³C NMR (125 MHz, DMSO-d₆): 122.11 (d), 126.08 (s), 126.31 (d), 127.11 (d), 127.64 (s), 127.98 (d), 133.70 (s), 134.95 (d), 145.95 (d), 146.70 (s).

IR (CCl₄): 3046 w, 1616 w, 1596 w, 1588 w, 1551 w, 1506 w, 1484 w, 1475 w, 1468 w, 1435 w, 1399 w, 1342 w, 1280 w, 1261 w, 1198 w, 1149 w, 1128 w, 1086 w, 1070 m, 1039 w, 1012 w, 864 vw, 843 vs, 827 w, 818 w, 720 w, 651 m, 618 m, 537 vw, 512 w, 408 vw.

IR (CHCl₃): 3360 w, br, 3204 w, br, 2937 vs, br, 2463 w, br, 1636 w, 1616 w, 1596 w, 1589 w, 1553 w, 1507 w, 1475 m, 1439 w, 1399 m, 1389 m, 1362 m, 1343 w, 1330 w, 1280 w, sh, 1270 w, 1246 m, br, 1187 w, 1174 w, 1157 m, 1129 w, 1099 w, 1087 w, 1031 w, 1008 w, 975 w, 938 w, 899 w, 864 vw, 846 s, 830 w, 820 w, 810 w, 719 w, 661 s, 652 m, 639 w, 618 w, 537 vw, 514 w.

EI MS: 280 (M⁺·, 100), 279 (48), 252 (49), 227 (5), 149 (13), 129 (10), 111 (10), 97 (19), 83 (25), 71 (51), 57 (50), 43 (45).

HR EI MS: calculated for $C_{20}H_{12}N_2$ 280.1000; found 280.0996.
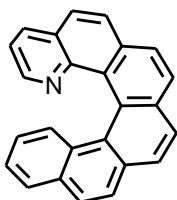
Benzo[5,6]phenanthro[3,4-*h*]quinoline (1-aza[6]helicene) 84. Tetrahydroazahelicene **96** (200 mg, 0.60 mmol) in toluene (18 ml), MnO_2 (1.57 g, 18.08 mmol, 30.13 equiv.), 150 °C, 80 min. The aromatisation procedure afforded azahelicene **84** (128 mg, 65 %) as an amorphous yellowish solid.

Mp 184-186 °C (heptane).

¹H NMR (500 MHz, CDCl₃): 6.59 (1 H, ddd, *J* = 8.5, 6.8, 1.4), 7.10 (1 H , dd, *J* = 8.0, 4.2), 7.18 (1 H, ddd, *J* = 8.0, 6.8, 1.2), 7.56 (1 H, ddt, *J* = 8.5, 1.2, 0.6, 0.6), 7.84 (1 H, ddd, *J* = 8.0, 1.4, 0.7), 7.86 (1 H, dd, *J* = 8.5, 0.5), 7.92 (1 H, dd, *J* = 4.2, 1.8), 7.98 (1 H, dd, *J* = 8.2, 0.5), 8.00 (2 H, s), 8.01 (1 H, d, *J* = 8.2), 8.03 (2 H, bd, *J* = 8.5), 8.11 (1 H, dd, *J* = 9.0, 0.5), 8.11 (1 H, ddd, *J* = 8.0, 1.8, 0.6).

¹³C NMR (125 MHz, CDCl₃): 120.56 (d), 124.12 (d), 124.20 (s), 124.66 (d), 125.98 (d), 126.05 (d), 126.23 (d), 126.29 (d), 126.34 (d), 126.53 (d), 127.20 (d), 127.48 (d), 127.83 (d), 128.12 (d), 128.57 (d), 128.69 (s), 129.78 (s), 130.96 (s), 131.15 (s), 131.83 (s), 133.07 (s), 133.27 (s), 135.08 (d), 145.83 (s), 146.72 (d).

IR (CCl$_4$): 3049 m, 1622 w, 1606 w, 1599 w, 1583 w, 1553 w, 1519 w, 1512 w, 1497 w, 1438 w, 1426 w, 1411 w, 1391 w, 1368 w, 1308 w, 1262 w, 1133 m, 1114 m, 1104 m, 1097 m, 1072 m, 1054 m, 1040 m, 1027 m, 1019 m, 844 vs, 828 m, 819 m, 631 m, 618 m, 517 m.

FAB MS : 330 ((M+H)$^+$), 302, 289, 279.

HR FAB MS: calculated for C$_{25}$H$_{16}$N 330.1283; found 330.1297.
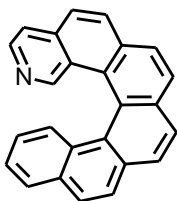
Benzo[5,6]phenanthro[3,4-*h*]isoquinoline (2-aza[6]helicene) 85. Tetrahydroazahelicene **102** (200 mg, 0.60 mmol) in toluene (18 ml), MnO$_2$ (1.57 g, 18.08 mmol, 30.13 equiv.), 130 °C, 30 min. The aromatisation procedure afforded azahelicene **85** (105 mg, 53 %) as an amorphous yellowish solid.

Mp 233-235 °C (heptane-CH$_2$Cl$_2$).

^{1}H NMR (500 MHz, CDCl$_3$): 6.73 (1 H, ddd, *J* = 8.4, 6.8, 1.4), 7.26 (1 H, ddd, *J* = 8.0, 6.8, 1.1), 7.54 (1 H, ddt, *J* = 8.4, 1.1, 0.6, 0.6), 7.61 (1 H, dd, *J* = 5.4, 1.1), 7.86 (1 H, dt, *J* = 8.5, 0.6, 0.6), 7.87 (1 H, ddd, *J* = 8.0, 1.4, 0.6), 7.93 (1 H, d, *J* = 8.5), 7.95 (1 H, bd, *J* = 8.5), 8.02 (1 H, d, *J* = 8.1), 8.02 (1 H, d, *J* = 8.2), 8.04 (1 H, d, *J* = 8.1), 8.08 (1 H, d, *J* = 8.2), 8.14 (1 H, d, *J* = 8.5), 8.24 (1 H, d, *J* = 5.4), 8.91 (1 H, t, *J* = 0.9).

^{13}C NMR (125 MHz, CDCl$_3$): 119.88 (d), 123.39 (s), 124.50 (s), 124.82 (d), 125.82 (d), 125.88 (d), 126.04 (d), 126.84 (d), 126.88 (s), 127.08 (d), 127.76 (d), 127.82 (d), 127.90 (s), 128.15 (d), 128.29 (d), 128.56 (d), 128.99 (s), 130.95 (d), 131.35 (s), 131.63 (s), 132.31 (s), 133.48 (s), 134.64 (s), 143.15 (d), 150.51 (d).

IR (CHCl$_3$): 3058 w, 3033 w, 1618 w, sh, 1607 m, 1599 w, sh, 1582 w, 1568 w, 1551 w, 1509 w, 1496 w, 1431 w, 1418 w, 1408 w, 1396 w, 1309 w, 1300 w, 852 vs, 523 s.

FAB MS : 330 ((M+H)$^+$), 314, 300, 287, 277, 250, 224, 181, 149, 93, 73, 69, 57, 55.

HR FAB MS: calculated for C$_{25}$H$_{16}$N 330.1283; found 330.1293.
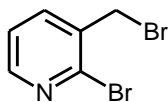
2-Bromo-3-(bromomethyl)pyridine 87. 2-Bromo-3-methypyridine **86** (15.44 g, 89.8 mmol) was dissolved in CCl_4 (150 ml) and NBS (17.70 g, 99.4 mmol, 1.11 equiv.), AIBN (147 mg, 0.90 mmol, 0.01 equiv.), K_2CO_3 (125 mg, 0.90 mmol, 0.01 equiv.) were added. Flask with reaction mixture was connected to condenser, washed with nitrogen and heated to reflux with irradiation with a infra lamp for a further 1.5 h under positive pressure of nitrogen. Reaction mixture was filtered through paper filter, solvent was removed *in vacuo* and the crude product was chromatographed on silica gel to provide tribromide **88** (6.81 g, 23 %, ^{1}H NMR spectrum identical with tribromide previously reported[79]) and desired dibromide **87** (11.00 g, 49 %) as an oil.

^{1}**H NMR** (500 MHz, $CDCl_3$): 4.56 (1 H, s), 7.28 (1H, dd, $J = 7.6, 4.7$), 7.78 (1 H, dd, $J = 7.6, 2.0$), 8.32 (1 H, dd, $J = 4.7, 2.0$).

^{13}**C NMR** (125 MHz, $CDCl_3$): 31.39 (t), 123.21 (d), 139.19 (d), 134.67 (s), 143.69 (s), 149.72 (d).

IR ($CHCl_3$): 1580 m, 1562 s, 1450 w, 1436 m, 1407 vvs, 1276 m, 1108 s, 1065 m, 870 m, 828 m, 803 m, 570 w, 492 w, 442 w.

EI MS: 253 ($M^{+\cdot}$ with 2x ^{81}Br, 10), 251 ($M^{+\cdot}$ with ^{81}Br and ^{79}Br, 10), 249 ($M^{+\cdot}$ with 2x ^{79}Br, 10), 172 (99), 170 (100).

HR EI MS: calculated for $C_6H_5N^{81}Br_2$ 252.8748; found 252.8737, calculated for $C_6H_5N^{79}Br^{81}Br$ 250.8768; found 250.8772, calculated for $C_6H_5N^{79}Br_2$ 248.8789; found 248.8777.
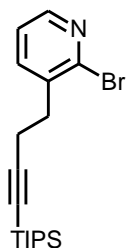
2-Bromo-3-{4-[tris(1-methylethyl)silyl]but-3-yn-1-yl}pyridine 89. A 250 ml flask was charged with tris(1-methylethyl)(prop-1-yn-1-yl)silane (6.56 g, 33.40 mmol, 1.10 equiv.) and flushed with argon. THF (30 ml) was added and the solution was cooled to −78 °C. n-BuLi (1.6 M solution in hexanes, 21 ml, 33.60 mmol, 1.11 equiv.) was added and the mixture was stirred for 2 h at −78 °C. The resulted organolithium was added dropwise to the solution of bromopyridine **87** (7.63 g, 30.39 mmol) in THF (30 ml) precooled to −78 °C. The reaction mixture was stirred at −78°C for 30 min. Solvents were removed *in vacuo* and the crude product was chromatographed on

silica gel (hexane-ether 93:7) to provide alkyne **89** (9.0 g, 81 %) as an amorphous solid.

^{1}H NMR (500 MHz, CDCl$_3$): 0.97-1.07 (21 H, m), 2.65 (2 H, t, J = 6.9), 2.94 (2 H, t, J = 6.9), 7.19 (1 H, dd, J = 7.5, 4.7), 7.64 (1 H, dd, J = 7.5, 2.0), 8.24 (1 H, dd, J = 4.7, 2.0).

^{13}C NMR (125 MHz, CDCl$_3$): 11.24 (d), 18.59 (q), 19.49 (t), 34.36 (t), 82.28 (s), 106.60 (s), 122.58 (d), 136.82 (s), 139.07 (d), 144.23 (s), 148.04 (d).

IR (CHCl$_3$): 2866 vs, 2171 m, 1581 w, 1560 m, 1464 m, 1451 m, 1429 m, 1407 vs, 1383 m, 1367 w, 1119 m, 1069 m, 996 m, 884 m, 800 w, 679 s, 660 s, 618 w.

EI MS: 324 ((M-C$_3$H$_7$)$^{+\cdot}$ with ^{81}Br, 100), 322 ((M-C$_3$H$_7$)$^{+\cdot}$ with ^{79}Br, 100), 282 (40), 280 (40), 254 (12), 252 (10), 240 (12), 238 (12), 172 (16), 170 (15), 158 (44), 156 (40), 130 (23), 109 (7), 83 (10), 66 (20), 59 (25), 43(27).

HR EI MS: calculated for C$_{15}$H$_{21}$^{79}BrNSi 322.0627; found 322.0622, calculated for C$_{15}$H$_{21}$^{81}BrNSi 324.0606; found 324.0605.
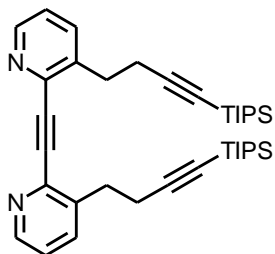
2,2'-Ethyne-1,2-diylbis(3-{4-[tris(1-methylethyl)silyl]but-3-yn-1-yl}pyridine) 90. A Schlenk flask was charged with Pd(PPh$_3$)$_4$ (116 mg, 0.10 mmol, 5 mol %), CuI (52 mg, 0.27 mmol, 15 mol %) and filled with acetylene. A solution of bromopyridine **89** (666 mg, 1.85 mmol) in piperidine (10 ml) was added and reaction mixture was stirred for 30 min at 80 °C. The solvent was removed *in vacuo* and the crude product was chromatographed on silica gel (hexane-ether 90:10) to provide triyne **90** (467 mg, 86 %) as a pale amorphous solid.

^{1}H NMR (500 MHz, CDCl$_3$): 0.95 – 1.03 (42 H, m), 2.74 (4 H, t, J = 6.9), 3.12 (4 H, t, J = 6.9), 7.21 (2 H, dd, J = 7.8, 4.7), 7.71 (2 H, bdd, J = 7.8, 1.7), 8.52 (2 H, dd, J = 4.7, 1.7).

^{13}C NMR (125 MHz, CDCl$_3$): 11.26 (d), 18.56 (q), 20.34 (t), 32.39 (t), 82.13 (s), 89.87 (s), 107.03 (s), 123.03 (d), 137.05 (d), 138.66 (s), 142.11 (s), 148.21 (d).

IR (CHCl$_3$): 3055 w, 2866 vs, 2171 m, 1581 w, 1567 m, 1463 m, 1442 s, 1383 w, 1367 w, 1341 w, 1326 w, 1104 w, 1073 w, 997 m, 884 s, 799 w, 678 s, 662 s, 620 w.

EI MS: 596 (M$^{+\cdot}$, 12), 581 (4), 553 (76), 511 (4), 439 (12), 425 (5), 397 (7), 357 (5), 298 (5), 273 (19), 255 (8), 234 (6), 213 (6), 183 (9), 149 (20), 98 (12), 87 (25), 73 (47), 59 (100), 41 (59).

HR EI MS: calculated for C$_{38}$H$_{56}$N$_2$Si$_2$ 596.3982; found 596.4000.
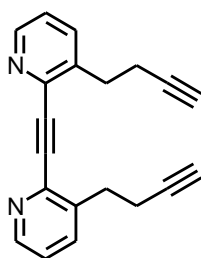
2,2'-Ethyne-1,2-diylbis(3-but-3-yn-1-ylpyridine) 91. A Schlenk flask was charged with triyne **90** (467 mg, 0.782 mmol) and filled with argon. THF (20 ml) was added and the resulting solution was treated with a solution of n-Bu$_4$NF • 3 H$_2$O (608 mg, 1.93 mmol, 2.47 equiv.) in THF (10 ml). After stirring at room temperature for 1 h, the solvent was removed *in vacuo* and the crude product was chromatographed on silica gel (hexane-acetone 60:40) to provide the unprotected triyne **91** (171 mg, 77 %) as a pale yellow solid.

^{1}H NMR (500 MHz, CDCl$_3$): 1.98 (2 H, t, J = 2.6), 2.65 (4 H, dt, J = 7.1, 7.1, 2.6), 3.15 (4 H, t, J = 7.1), 7.25 (2 H, dd, J = 7.8, 4.8), 7.68 (2 H, dd, J = 7.8, 1.7), 8.54 (2 H, dd, J = 4.8, 1.7).

^{13}C NMR (125 MHz, CDCl$_3$): 19.03 (t), 32.02 (t), 69.82 (d), 82.89 (s), 89.77 (s), 123.22 (d), 136.76 (d), 138.45 (s), 142.17 (s), 148.37 (d).

IR (CHCl$_3$): 3309 s, 3055 w, 2965 m, 2934 w, 2857 w, 2120 vw, 1582 w, 1568 m, 1443 vs, 1343 vw, 1328 vw, 1311 w, 1105 w, 1061 vw, 803 w, 643 m, br.

EI MS: 284 (M$^{+\cdot}$, 26), 283 (100), 268 (23), 257 (9), 243 (25), 231 (9), 205 (9), 191 (6), 178 (5), 167 (3), 151 (5), 141 (5), 127 (3), 116 (5), 101 (8), 83 (9), 69 (12), 59 (50).

HR EI MS: calculated for C$_{20}$H$_{16}$N$_2$ 284.1313; found 284.1316.
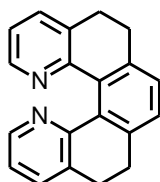
5,6,9,10-Tetrahydrobenzo[1,2-*h*:4,3-*h'*]diquinoline 92. Triyne **91** (148 mg, 0.52 mmol), PPh$_3$ (55 mg, 0.210 mmol, 40 mol %),

CpCo(CO)$_2$ (14 µl, 0.11 mmol, 21 mol %), decane (6 ml). The cyclisation procedure afforded tetrahydrohelicene **92** (89 mg, 60 %) as an amorphous yellowish solid.

¹H NMR (500 MHz, CDCl$_3$): 2.81 (4 H, m), 2.96 (4 H, m), 7.00 (2 H, dd, *J* = 7.5, 4.8), 7.19 (2 H, s), 7.52 (2 H, ddt, *J* = 7.5, 1.8, 0.8, 0.8), 8.14 (2 H,dd, *J* = 4.8, 1.8).

¹³C NMR (125 MHz, CDCl$_3$): 29.13 (t), 29.23 (t), 121.51 (d), 127.55 (d), 133.10 (s), 133.96 (s), 134.63 (d), 140.23 (s), 146.39 (d), 154.19 (s).

IR (CHCl$_3$): 3057 w, 2945 vs, 2845 m, 1587 m, 1575 s, 1568 s,1507 vw, 1455 s, 1448 s, 1435 vs, 1426 vs, 1402 s, 1349 w, 1319 w, 1292 w, 1239 m, 1181 w, 1170 w, 1154 w, 1133 w, 1110 m, 1092 w, 971 w, 943 w, 920 w, 872 w, 829 s, 814 w, 807 m, 641 m, 624 s, 600 w, 585 w, 532 w, 523 w, 512 w, 499 w, 468 w.

EI MS: 284 (M$^{+\cdot}$, 13), 97 (12, 83 (16), 69 (34), 55 (62), 43 (100), 29 (47).

HR EI MS: calculated for C$_{20}$H$_{16}$N$_2$ 284.1313; found 284.1309.
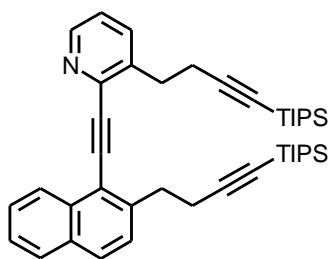
3-{4-[Tris(1-methylethyl)silyl]but-3-yn-1-yl}-2-[(2-{4-[tris(1-methylethyl)silyl]but-3-yn-1-yl}naphthalen-1-yl)ethynyl]-pyridine 94. A 100 ml flask was charged with bromopyridine **89** (2.00 g, 5.46 mmol), diyne **93** (2.00 g, 5.55 mmol, 1.02 equiv.), Pd(PPh$_3$)$_4$ (315 mg, 0.27 mmol, 5 mol %), CuI (105 mg, 0.55 mmol, 10 mol %), and filled with argon. Diisopropylamine (40 ml) and toluene (20 ml) were added and the reaction mixture was stirred at room temperature for 80 min. Solvents were removed *in vacuo* and the crude product was chromatographed on silica gel (hexane-ether 80:20) to provide triyne **94** (3.19 g, 90 %) as a white solid.

¹H NMR (500 MHz, CDCl$_3$): 0.96-1.05 (21 H, m), 2.79 (2 H, t, *J* = 7.0), 3.19 (2 H, t, *J* = 7.0), 7.21 (1 H, dd, *J* = 7.8, 4.8), 7.49 (1 H, ddd, *J* = 8.1, 6.8, 1.2), 7.51 (1 H, d, *J* = 8.4), 7.51 (1 H, ddd, *J* = 8.4, 6.8, 1.5), 7.73 (1 H, dd, *J* = 7.8, 1.7), 7.80 (1 H, bd, *J* = 8.4), 7.83 (1 H, ddt, *J* = 8.1, 1.5, 0.8, 0.8), 8.53 (1 H, dq, *J* = 8.4, 1.0, 1.0, 1.0), 8.58 (1 H, dd, *J* = 4.8, 1.7).

^{13}C NMR (125 MHz, CDCl$_3$): 11.28 (d), 18.57 (q), 20.69 (t), 32.80 (t), 82.12 (s), 89.08 (s), 96.48 (s), 107.00 (s), 118.45 (s), 122.55 (d), 125.94 (d), 126.31 (d), 127.18 (d), 127.41 (d), 128.03 (d), 129.08 (d), 137.10 (d), 137.90 (s), 142.35 (s), 143.08 (s), 148.31 (d).

IR (CHCl$_3$): 2866 vs, 2205 w, 2171 m, 1621 vw, 1593 w, 1582 w, 1566 w, 1508 w, 1464 m, 1436 s, 1430 m, 1383 w, 1367 w, 1103 w, 1072 w, 1040 w, 1026 w, 997 m, 884 s, 868 w, sh, 817 m, 678 s, 661 s, 619 m.

EI MS: 645 (M$^{+\cdot}$, 11), 602 (47), 560 (3), 488 (15), 450 (26), 436 (5), 408 (7), 394 (3), 322 (8), 157 (13), 129 (8), 115 (39), 87 (45), 73 64), 59 (100), 41 (43).

HR EI MS: calculated for C$_{43}$H$_{59}$NSi$_2$ 645.4186; found 645.4205.
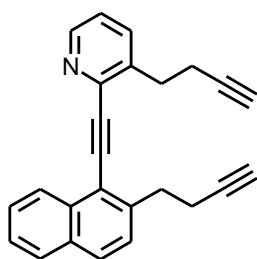
3-But-3-yn-1-yl-2-[(2-but-3-yn-1-ylnaphthalen-1-yl)ethynyl]-pyridine 95. A 100 ml flask was charged with triyne **94** (3.02 g, 4.67 mmol) and filled with argon. THF (30 ml) was added and the solution was treated with n-Bu$_4$NF (0.964 M in THF, 23.2 ml, 23.28 mmol, 2.40 equiv.). The reaction mixture was stirred at room temperature for 30 h. The solvent was removed *in vacuo* and the crude product was chromatographed on silica gel (hexane-ether 50:50) to provide unprotected triyne **95** (1.43 g, 92 %) as a pale yellow solid.

^{1}H NMR (500 MHz, CDCl$_3$): 1.99 (1 H, t, *J* = 2.6), 2.02 (1 H, t, *J* = 2.6), 2.70 (2 H, dt, *J* = 7.5, 7.5, 2.6), 2.70 (2 H, dt, *J* = 7.3, 7.3, 2.6), 3.22 (2 H, t, *J* = 7.3), 3.36 (2 H, t, *J* = 7.5), 7.26 (1 H, dd, *J* = 7.8, 4.8), 7.47 (1 H, d, *J* = 8.4), 7.50 (1 H, ddd, *J* = 8.1, 6.8, 1.2), 7.61 (1 H, ddd, *J* = 8.4, 6.8, 1.3), 7.70 (1 H, ddt, *J* = 7.8, 1.7, 0.6, 0.6), 7.84 (1 H, bd, *J* = 8.4), 7.84 (1 H, ddt, *J* = 8.1, 1.3, 0.6, 0.6), 8.52 (1 H, ddt, *J* = 8.4, 1.2, 0.9, 0.9), 8.60 (1 H, dd, *J* = 4.8, 1.7).

^{13}C NMR (125 MHz, CDCl$_3$): 19.32 (t), 19.88 (t), 32.46 (t), 34.37 (t), 69.31 (d), 69.81 (d), 82.90 (s), 83.55 (s), 89.02 (s), 96.35 (s), 118.52 (s), 122.78 (d), 126.07 (d), 126.29 (d), 127.12 (d), 127.29 (d), 128.11 (d), 129.26 (d), 131.96 (s), 133.81 (s), 136.76 (d), 137.72 (s), 142.07 (s), 143.10 (s), 148.44 (d).

IR (CHCl$_3$): 3309 vs, 3058 w, 2205 w, 2119 w, 1620 vw, 1592 w, 1582 m, 1566 m, 1556 w (sh), 1508 w, 1453 w, sh, 1436 vs, 1430 s, 1103 m, 1067 w, 1026 w, 867 w, 820 m, 642 s.

EI MS: 333 (M$^+$, 33), 332 (100), 318 (19), 317 (19), 294 (32), 278 (21), 254 (12), 226 (8), 142 (11), 73 (5).

HR EI MS: calculated for C$_{25}$H$_{19}$N 333.1518; found 333.1512.
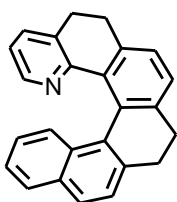
5,6,9,10-Tetrahydrobenzo[5,6]phenanthro[3,4-*h*]quinoline 96. Triyne **95** (50 mg, 0.15 mmol), PPh$_3$ (16 mg, 59 μmol, 39 mol %), CpCo(CO)$_2$ (4 μl, 30 μmol, 20 mol %), decane (7 ml). The cyclisation procedure afforded tetrahydrohelicene **96** (41 mg, 82 %) as an amorphous yellowish solid.

Mp 225-227 °C (dioxane).

^{1}H NMR (500 MHz, CDCl$_3$): 2.65-2.74 (1 H, m), 2.83-2.91 (2 H, m), 2.96 (1 H, ddd, *J* = 15.1, 4.6, 1.9), 3.07-3.12 (2 H, m), 6.65 (1 H, dd, *J* = 7.5, 4.8), 6.75 (1 H, ddd, *J* = 8.7, 6.7, 1.4), 7.07 (1 H, ddd, *J* = 8.0, 6.8, 1.2), 7.20 (1 H, ddt, *J* = 7.4, 1.3, 0.6, 0.6), 7.33 (1 H, bdd, *J* = 7.4, 1.3), 7.37 (1 H, dq, *J* = 8.7, 1.0, 1.0, 1.0), 7.40 (1 H, ddt, *J* = 7.5, 1.8, 0.8, 0.8), 7.46 (1 H, bdd, *J* = 8.2, 0.2), 7.65 (1 H, ddt, *J* = 8.0, 1.4, 0.6, 0.6), 7.67 (1 H, bdd, *J* = 8.2, 0.8).

^{13}C NMR (125 MHz, CDCl$_3$): 29.24 (t), 29.25 (t), 30.46 (t), 30.93 (t), 120.86 (d), 123.52 (d), 124.47 (d) (two carbon atoms), 125.94 (d), 126.41 (d), 127.17 (d), 127.64 (d), 127.72 (d), 130.29 (s), 132.11 (s), 132.55 (s), 132.78 (s), 133.02 (s), 133.88 (s), 134.29 (d), 137.19 (s), 138.64 (s), 140.90 (s), 146.50 (d), 154.18 (s).

IR (CHCl$_3$): 3056 m, 3009 s, 2944 vs, 2839 m, 1586 m, 1569 m, 1509 w, 1451 s, 1436 vs, 1410 m, 1377 m, 1159 w, 1111 w, 1028 w, 865 w, 834 s, 822 s, 813 m.

EI MS: 333 (M$^+$, 100), 300 (8), 277 (8), 167 (6), 149 (42), 83 (7), 71 (10), 57 (23).

HR EI MS: calculated for C$_{25}$H$_{19}$N 333.1518; found 333.1526.
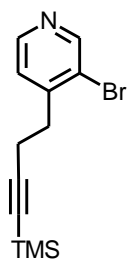
3-Bromo-4-[4-(trimethylsilyl)but-3-yn-1-yl]pyridine 98. A 100 ml flask was charged with diisopropylamine (1.23 g, 12.13 mmol, 1.05 equiv.) in THF (20 ml) under argon and cooled to 0°C. n-BuLi (1.6 M solution in hexanes, 7.30 ml, 11.68 mmol, 1.01 equiv.) was added dropwise and the mixture was stirred at 0 °C for 30 min. Bromopyridine **97** (1.99 g, 11.57 mmol) in THF (10 ml) was added and the reaction mixture was stirred at 50°C for 45 min.   After cooling to 0 °C, a solution of (3-bromoprop-1-yn-1-yl)(trimethyl)silane (2.55 g, 13.34 mmol, 1.15 equiv.) in THF (10 ml) was added. The mixture was stirred at 0 °C for 3 h and then allowed to reach the room temperature. Solvents were removed *in vacuo* and the crude product was chromatographed on silica gel (hexane-acetone 90:10) to provide alkyne **98** (3.02 g, 93 %) as a yellowish oil.

^{1}H NMR (500 MHz, CDCl$_3$): 0.13 (9 H, s), 2.57 (2 H, t, J = 7.2), 2.94 (2 H, t, J = 7.2), 7.23 (1 H, d, J = 4.9), 8.43 (1 H, bd, J = 4.9), 8.67 (1 H, bs).

^{13}C NMR (125 MHz, CDCl$_3$): -0.02 (q), 19.23 (t), 34.26 (t), 86.55 (s), 104.71 (s), 123.00 (s), 125.66 (d), 148.03 (d), 148.21 (s), 151.90 (d).

IR (CHCl$_3$): 3057 w, 2902 m, 2175 m, 1587 m, 1477 w, 1468 w, 1402 s, 1339 w, 1320 w, 1252 s, 845 vs, 698 m, 604 w.

EI MS: 283 (M$^{+\cdot}$ with ^{81}Br, 3), 281 (M$^{+\cdot}$ with ^{79}Br, 3), 268 (98), 266 (100), 202 (60), 196 (8), 186 (61), 144 (99).

HR EI MS: calculated for C$_{12}$H$_{16}$^{79}BrNSi 281.0235; found 281.0244; calculated for C$_{12}$H$_{16}$^{81}BrNSi 283.0214; found 283.0188.
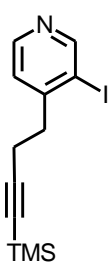
3-Iodo-4-[4-(trimethylsilyl)but-3-yn-1-yl]pyridine 99.

Method A (by halogen-lithium exchange reaction): A Schlenk flask was charged with bromopyridine **98** (709 mg, 2.51 mmol) and filled with argon. Diethyl ether (30 ml) was added, the solution was cooled to -78 °C, and n-BuLi (1.6 M solution in hexanes, 2.77 mmol, 1.10 equiv.) was added dropwise. The reaction mixture was stirred at -78 °C for 30 min. Then, a solution of iodine (959 mg, 3.79 mmol, 1.51 equiv.) in diethylether (7 ml) was

added and the mixture was stirred at -78°C for 1.5 h. After reaching room temperature, the resulting mixture was poured into cold water (50 ml) and the product was extracted with diethyl ether (2 × 50 ml). The combined organic fractions were washed with aqueous sodium thiosulfate (2 × 50 ml), solvents were evaporated *in vacuo*, and the crude product was chromatographed on silica gel (hexane-acetone 90:10) to provide iodopyridine **99** (678 mg, 82 %) as an yellowish oil.

Method B (by Finkelstein-like iodine-to-bromine exchange reaction): A 10 ml glass vial was charged with NaI (322 mg, 2.15 mmol, 2.01 equiv.), bromopyridine **98** (303 mg, 1.07 mmol), CuI (67 mg, 0.35 mmol, 33 mol %) and trans-N,N'-dimethylcyclohexane-1,2-diamine (108 mg, 0.76 mmol, 71 mol %) under argon. The vial was tightly capped, dioxane (10 ml) was added and the mixture was heated by microwave irradiation (Biotage microwave oven system) to 150 °C for 3 h and then to 170 °C for 2 h. Further heating did not bring any progress of the reaction.Thus, the solvent was removed *in vacuo* and the crude product was chromatographed on silica gel (hexane-acetone 90:10) to provide mixture of unseparable iodopyridine **99** (214 mg, 61 %) and recovery of bromopyridine **98** (46 mg, 15 %) as an yellowish oil.

^{1}H NMR (500 MHz, CDCl$_3$): 0.13 (9 H, s), 2.55 (2 H, t, *J* = 7.2), 2.91 (2 H, t, *J* = 7.2), 7.25 (1 H, d, *J* = 5.0), 8.48 (1 H, bd, *J* = 5.0), 8.93 (1 H, bs).

^{13}C NMR (125 MHz, CDCl$_3$): -0.01 (q), 19.44 (t), 38.72 (t), 86.66 (s), 99.85 (s), 104.53 (s), 125.42 (d), 148.90 (d), 151.69 (s), 157.61 (d).

IR (CHCl$_3$): 2174 w, 1580 w, 1468 w, 1399 w, 1252 m, 845 vs, 700 w, 602 vw.

EI MS: 329 (M$^{+\cdot}$, 14), 314 (57), 202 (100), 186 (44), 144 (54).

HR EI MS: calculated for C$_{12}$H$_{16}$INSi 329.0097; found 329.0104.
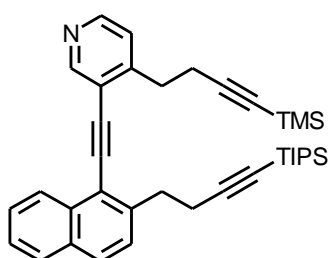
4-[4-(Trimethylsilyl)but-3-yn-1-yl]-3-[(2-{4-[tris(1-methyl-ethyl)silyl]but-3-yn-1-yl}naphthalen-1-yl)ethynyl]pyridine 100. A Schlenk flask was charged with diyne **93** (420 mg, 1.16 mmol, 1.14 equiv.), Pd(PPh$_3$)$_4$ (59 mg, 0.051 mmol, 5 mol %), CuI (23 mg,

0.121 mmol, 12 mol %) and filled with argon. The solution of iodopyridine **99** (335 mg, 1.02 mmol) in diisopropylamine (30 ml) was added and the reaction was stirred at room temperature for 40 min. The solvent was removed *in vacuo* and the crude product was chromatographed on silica gel (hexane-acetone 80:20) to provide triyne **100** (520 mg, 91 %) as an off-white solid.

^{1}H NMR (500 MHz, CDCl$_3$): 0.12 (9 H, s), 0.96-1.04 (21 H, m), 2.72 (2 H, t, *J* = 7.3), 2.76 (2 H, t, *J* = 7.3), 3.16 (2 H, t, *J* = 7.3), 3.32 (2 H, t, *J* = 7.3), 7.29 (1 H, d, *J* = 5.1), 7.51 (1 H, d, *J* = 8.3), 7.51 (1 H, ddd, *J* = 8.1, 6.8, 1.2), 7.61 (1 H, ddd, *J* = 8.4, 6.8, 1.3), 7.80 (1 H, bd, *J* = 8.3), 7.85 (1 H, ddt, *J* = 8.1, 1.3, 0.6, 0.6), 8.40 (1 H, dq, *J* = 8.4, 1.0, 1.0, 1.0), 8.51 (1 H, bd, *J* = 5.1), 8.86 (1 H, bs).

^{13}C NMR (125 MHz, CDCl$_3$): -0.02 (q), 11.28 (d), 18.57 (q), 20.24 (t), 21.32 (t), 33.41 (t), 34.81 (t), 81.60 (s), 86.40 (s), 92.94 (s), 93.62 (s), 105.08 (s), 107.59 (t), 118.65 (s), 120.59 (s), 123.92 (d), 125.88 (d), 125.94 (d), 127.14 (d), 127.49 (d), 128.22 (d), 128.95 (d), 132.02 (s), 133.49 (s), 142.00 (s), 148.51 (d), 150.17 (s), 152.75 (d).

IR (CHCl$_3$): 3059 w, 2960 vs, 2944 vs, 2866 s, 2200 w, 2172 m, 1620 w, 1600 m, sh, 1589 m, 1568 w, sh, 1508 w, 1487 w, 1464 m, 1450 m, sh, 1406 m, 1383 m, 1366 m, 1252 s, 1173 w, 1074 m, 1026 m, 996 m, 884 s, 845 vs, 821 m, 698 w, 679 m, 662 m.

EI MS: 561 (M$^{+\cdot}$, 11), 518 (86), 451 (20), 408 (64), 366 (6), 266 (36), 254 (8), 223 (5), 202 (22), 186 (20), 149 (59), 144 (36), 115 (10), 87 (17), 73 (100), 59 (56).

HR EI MS: calculated for C$_{37}$H$_{47}$NSi$_2$ 561.3247; found 561.3225.
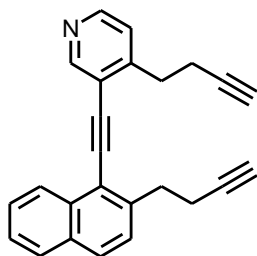
4-But-3-yn-1-yl-3-[(2-but-3-yn-1-ylnaphthalen-1-yl)ethynyl]-pyridine 101. The Schlenk flask was charged with triyne **100** (520 mg, 0.926 mmol) and filled with argon. THF (20 ml) was added and the resulting solution was treated with solution of n-Bu$_4$NF • 3 H$_2$O (731 mg, 2.32 mmol, 2.50 equiv.) in THF (10 ml). After stirring at room temperature for 1 h, the solvent was removed *in vacuo* and the crude product was chromatographed on silica gel (hexane-acetone 80:20) to provide unprotected triyne **101** (260 mg, 84 %) as a pale yellow solid.

¹H NMR (500 MHz, CDCl₃): 2.02 (1 H, t, J = 2.6), 2.04 (1 H, t, J = 2.6), 2.68 (2 H, dt, J = 7.6, 7.6, 2.6), 2.71 (2 H, dt, J = 7.4, 7.4, 2.6), 3.20 (2 H, t, J = 7.4), 3.33 (2 H, t, J = 7.6), 7.31 (1 H, dd, J = 5.1, 0.8), 7.46 (1 H, d, J = 8.4), 7.52 (1 H, ddd, J = 8.1, 6.8, 1.2), 7.62 (1 H, ddd, J = 8.5, 6.8, 1.4), 7.84 (1 H, bd, J = 8.4), 7.86 (1 H, ddt, J = 8.1, 1.4, 0.7, 0.7), 8.41 (1 H, ddt, J = 8.5, 1.2, 0.9, 0.9), 8.52 (1 H, d, J = 5.1), 8.88 (1 H, d, J = 0.8).

¹³C NMR (125 MHz, CDCl₃): 18.72 (t), 19.88 (t), 33.16 (t), 34.55 (t), 69.32 (d), 69.83 (d), 82.59 (s), 83.43 (s), 92.72 (s), 93.68 (s), 118.71 (s), 120.42 (s), 123.63 (d), 125.84 (d), 126.08 (d), 127.20 (d), 127.25 (d), 128.27 (d), 129.11 (d), 131.98 (s), 133.42 (s), 141.66 (s), 148.72 (d), 149.86 (s), 152.87 (d).

IR (CHCl₃): 3309 vs, 3059 w, 2203 w, 2119 w, 1620 vw, 1588 m, 1568 w, 1552 w, 1510 w, 1488 w, 1432 w, 1260 w, 1046 w, 1026 w, 962 vw, 891 vw, 867 w, 820 m, 642 vs, 435 w.

EI MS: 333 (M⁺·, 50), 332 (100), 318 (45), 305 (31), 292 (41), 278 (50), 265 (19), 254 (26), 239 (17), 226 (36), 215 (13), 202 (33), 189 (24), 178 (13), 165 (17), 139 (13), 115 (8), 97 (11), 83 (15), 71 (28), 55 (34), 43 (35).

HR EI MS: calculated for $C_{25}H_{19}N$ 333.1518; found 333.1514.
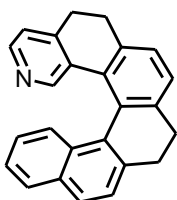
5,6,9,10-Tetrahydrobenzo[5,6]phenanthro[3,4-*h*]isoquinoline 102.

Method A (general cyclisation procedure): Triyne **101** (108 mg, 0.32 mmol), PPh₃ (31 mg, 0.118 mmol, 37 mol %), CpCo(CO)₂ (8 μl, 0.060 mmol, 19 mol %), decane (8 ml). The cyclisation procedure afforded tetrahydroazahelicene **102** (96 mg, 89 %) as an amorphous yellowish solid.

Method B (cyclisation using microwave irradiation): A 20 ml glass vial was charged with triyne **101** (400 mg, 1.20 mmol) and PPh₃ (126 mg, 0.48 mmol, 40 mol %), tightly capped and put under argon. THF (15 ml), 1-butyl-2,3-dimethylimidazolium tetrafluoroborate (200 μl) and CpCo(CO)₂ (32 μl, 0.24 mmol, 20 mol %) were added and the vial was heated by microwave irradiation (Biotage microwave oven system) to 150 °C for 14 min. The solvent was removed *in vacuo* and the crude

product was chromatographed on silica gel (hexane-acetone 85:15) to provide tetrahydroazahelicene **102** (347 mg, 87 %) as an amorphous yellowish solid.

Mp 201-205 °C (hexane-acetone).

^{1}H NMR (500 MHz, CDCl$_3$): 2.65-2.78 (5 H, m), 2.85-3.05 (3 H, m), 6.87 (1 H, ddd, J = 8.6, 6.7, 1.4), 7.07 (1 H, bd, J = 4.5), 7.12 (1 H, ddd, J = 8.0, 6.7, 1.2), 7.22 (1 H, dd, J = 7.4, 1.1), 7.31 (1 H, dd, J = 7.4, 1.2), 7.42 (1 H, dq, J = 8.6, 1.0, 1.0, 1.0), 7.47 (1 H, d, J = 8.1), 7.52 (1 H, bd, J = 4.5), 7.67 (1 H, ddt, J = 8.0, 1.4, 0.7, 0.7), 7.72 (1 H, bd, J = 8.1), 7.97 (1 H, bs).

^{13}C NMR (125 MHz, CDCl$_3$): 29.04 (t), 29.13 (t), 30.50 (t), 30.96 (t), 121.99 (d), 124.34 (d), 124.98 (d), 125.36 (d), 126.26 (d), 126.51 (d), 127.01 (s), 128.25 (d), 128.25 (d), 128.44 (s), 128.88 (s), 130.88 (s), 131.10 (s), 131.20 (s), 133.30 (s), 137.71 (s), 138.42 (s), 140.97 (s), 145.74 (s), 146.71 (d), 148.18 (d).

IR (CHCl$_3$): 3056 m, 3011 s, 1622 w (sh), 1600 m, 1583 w, 1571 w (sh), 1555 w, 1509 m, 1491 m, 1467 m, 1458 m, 1437 s, 1406 s, 1378 m, 1351 w, 1328 w, 1322 w, 1240 m, 1159 w, 1051 w, 1027 w, 885 m, 866 w, 835 vs, 820 s, 813 s, 688 m.

EI MS: 333 (M$^{+\cdot}$, 100), 305 (8), 277 (11), 159 (7), 85 (7), 71 (10), 57 (15), 43 (9).

HR EI MS: calculated for C$_{25}$H$_{19}$N 333.1518; found 333.1510.
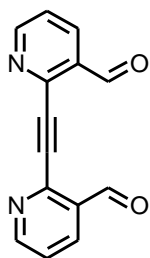
2,2'-Ethyne-1,2-diyldipyridine-3-carbaldehyde 104. A Schlenk flask was charged with bromide **103** (300 mg, 1.61 mmol), Pd(PPh$_3$)$_2$Cl$_2$ (45 mg, 0.06 mmol, 4%), CuI (6 mg, 0.03 mmol, 2%) and filled with acetylene. A mixture of Et$_3$N (8 ml) and THF (2 ml) was added and reaction mixture was stirred for 2 h at 50 °C. The solvents were removed *in vacuo* and the crude product was chromatographed on silica gel (hexane-acetone 80:20) to provide dialdehyde **104** (143 mg, 75 %) as a pale amorphous solid.

^{1}H NMR (500 MHz, CDCl$_3$): 7.53 (1 H, ddd, J = 7.9, 4.7, 0.9), 8.29 (1 H, dd, J = 7.9, 1.8), 8.90 (1 H, dd, J = 4.7, 1.8), 10.71 (1 H, d, J = 0.9).

^{13}C NMR (125 MHz, CDCl$_3$): 89.73 (s), 124.45 (d), 132.75 (s), 135.20 (d), 144.23 (s), 154.64 (d), 189.94 (d).

IR (CHCl$_3$): 3054 w, 2805 w, 2743 w, 2230 vw, 1701 vs, 1578 s, 1566 s, 1440 s, 1390 m.

EI MS: 236 (M$^{+\cdot}$, 64), 208 (24), 179 (100), 153 (37), 126 (13), 99 (14), 87 (6), 75 (17), 69 (8), 62 (11), 55 (11), 51 (29). 41 (15).

HR EI MS: calculated for C$_{14}$H$_8$N$_2$O$_2$ 236.0586; found 236.0581.
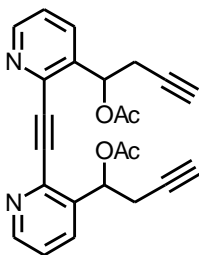
Ethyne-1,2-diylbis(pyridine-2,3-diylbut-1-yne-4,4-diyl) diacetate 105. A solution of propargyl magnesiumbromide (freshly prepared from magnesium turnings (83 mg, 3.41 mmol, 2.40 equiv.) and propargyl bromide (441 mg, 3.71 mmol,2.61 equiv.) in Et$_2$O (15 ml) was placed in the Schlenk flask under argon and cooled to -78°C. Dialdehyde **104** (336 mg, 1.42 mmol) in THF (40 ml) was added dropwise to the solution of Grignard reagent and resulting mixture was stirred for 20 min at -78 °C. Then acetic anhydride (432 mg, 4.23 mmol, 2.98 equiv.) was added and the mixture was stirred for 1 h at room temperature. After quenching the reaction with EtOH (5 ml) ethyl acetate (50 ml) was added and mixture was washed with brine (3 × 20 ml) and dried over MgSO$_4$. Solvents were removed *in vacuo* and the crude product was chromatographed on silica gel (hexane-acetone 80:20) to provide desired triyne **105** (200 mg, 35 %) as a yellowish oil.

^{1}H NMR (500 MHz, CDCl$_3$): 2.01 (2 H, t, *J* = 2.7), 2.15 (2 H, s), 2.93 (2 H, ddd, *J* = 17.1, 5.4, 2.7), 3.01 (2 H, ddd, *J* = 17.1, 5.7, 2.7), 6.40 (1 H, bt, *J* = 5.6), 6.43 (1 H, bt, *J* = 5.6), 7.35 (2 H, ddd, *J* = 8.0, 4.8, 0.5), 7.88 (2 H, dd, *J* = 8.0, 1.7), 8.62 (2 H, bdd, *J* = 4.8, 1.7).

^{13}C NMR (125 MHz, CDCl$_3$): 20.90 (q) (two carbon atoms), 25.30 (t), 25.31 (t), 69.92 (d), 70.00 (d), 71.65 (d), 71.68 (d), 78.42 (s), 78.45 (s), 89.90 (s), 89.93 (s), 123.42 (d) (two carbon atoms), 134.22 (d) (two carbon atoms), 137.29 (s), 137.31 (s), 140.02 (s) (two carbon atoms), 149.72 (d), 149.75(d), 169.46 (s), 169.48 (s).

IR (CHCl$_3$): 3309 s, 3055 w, 2234 vw, sh, 2124 w, 1746 vs, 1583 m, 1569 s, 1444 vs, 1420 m, sh, 1373 s, 1341 w, sh, 1236 vs, 1044 s, 1029 s, 651 s, 640 s, 604 w.

EI MS: 400 (M$^{+\cdot}$, 1), 357 (11), 341 (11), 319 (14), 297 (43), 281 (68), 269 (31), 259 (43), 247 (13), 231 (36), 209 (11), 181 (17), 149 (10), 128 (9), 112 (6), 97 (8), 71 (26), 57 (24), 43 (100).

HR EI MS: calculated for $C_{24}H_{20}N_2O_4$ 400.1423; found 400.1427.
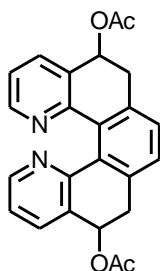
5,6,9,10-Tetrahydrobenzo[1,2-*h*:4,3-*h'*]diquinoline-5,10-diyl diacetate 106. Triyne **105** (150 mg, 0.38 mmol), PPh$_3$ (39 mg, 0.15 mmol, 40 mol %), CpCo(CO)$_2$ (10 μl, 0.08 mmol, 20 mol %), decane (7 ml). The cyclisation procedure afforded helicenediacetate **106** (114 mg, 76 %) as an amorphous yellowish solid.

^{1}H NMR (500 MHz, CDCl$_3$): 2.14 (1 H, s), 2.18 (1 H, s), 2.98 - 3.10 (1 H, m), 3.16 (1 H, dd, *J* = 15.1, 4.9), 3.19 (1 H, dd, *J* = 15.1, 4.9), 6.15 (1 H, m), 6.17 (1 H, bdd, *J* = 8.8, 4.9), 7.13 (2 H, dd, *J* = 7.6, 4.7), 7.26 (2 H, s), 7.73 (1 H, ddd, *J* = 7.6, 1.7, 0.9), 7.75 (1 H, bdd, *J* = 7.6, 1.7), 8.24 (1 H, ddd, *J* = 4.7, 1.8, 0.5), 8.25 (1 H, bdd, *J* = 4.7, 1.7).

^{13}C NMR (125 MHz, CDCl$_3$): 21.28 (q), 21.32 (q), 34.69 (t), 34.77 (t), 69.66 (d), 69.73 (d), 121.95 (d) (two carbon atoms), 128.95 (d) (two carbon atoms), 130.08 (s) (two carbon atoms), 132.97 (s) (two carbon atoms), 133.21 (d) (two carbon atoms), 135.05 (s), 135.09 (s), 147.72 (d), 147.96 (d), 152.77 (s), 153.08 (s), 170.70 (s), 170.83 (s).

IR (CHCl$_3$): 3060 w, 1732 s, 1587 w, 1571 m, 1461 m, 1435 m, 1374 s, 1241 vs, 1035 s, 614 w.

EI MS: 400 (M$^{+\cdot}$, 17), 297 (6), 280 (100), 269 (13), 252 (17), 178 (23), 161 (12), 149 (15), 140 (27), 97 (9), 81 (12), 69 (32), 57 (29), 41 (36).

HR EI MS: calculated for $C_{24}H_{20}N_2O_4$ 400.1423; found 400.1426.
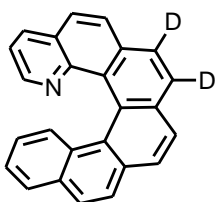
(7,8-^{2}H$_2$)Benzo[5,6]phenanthro[3,4-*h*]quinoline-[7,8-d_2]-84. A 20 ml glass vial was charged with diisopropylamine (20.2 mg, 200 μmol, 2.20 equiv.) in THF (5 ml) under argon and cooled to 0°C. n-BuLi (1.6 M solution in hexanes, 124 μl, 200 μmol, 2.20

equiv.) was added dropwise and the mixture was stirred at 0°C for 30 min. The solution was cooled to -78°C, the triyne precursor **95** (30 mg, 90 μmol) in THF (5 ml) was added and the reaction mixture was stirred at -78 °C for 30 min. Then, D_2O (10 mg, 500 μmol, 5.60 equiv.) was added and the mixture was allowed to warm to room temperature. Subsequently, $CpCo(CO)_2$ (2.7 mg, 15 μmol, 17 mol %) and PPh_3 (9.4 mg, 36 μmol, 40 mol %) in THF (5 ml) were added and the reaction mixture was heated to 150 °C for 14 min using microwave irradiation. Then, the volatile components were removed *in vacuo* to yield crude **96**. Without further work-up the glass vial was charged with MnO_2 (235 mg, 2.70 mmol, 29.7 equiv.) and toluene (10 ml), tightly capped and heated by microwave irradiation to 150 °C for 80 min. The resulting reaction mixture was directly chromatographed on silica gel (hexane-acetone-triethylamine 80:20:1) to provide the azahelicene [7,8-d_2]-**84** (13 mg, 45 %) as an amorphous yellowish solid.

^{1}H NMR (500 MHz, $CDCl_3$): 6.58 (1 H, ddd, J = 8.5, 6.8, 1.5), 7.10 (1 H, dd, J = 8.0, 4.2), 7.18 (1 H, ddd, J = 8.0, 6.8, 1.2), 7.56 (1 H, ddd, J = 8.6, 1.2, 0.6), 7.84 (1 H, ddd, J = 8.0, 1.5, 0.6), 7.85 (1 H, d, J = 8.5), 7.90 (2 H, s), 7.92 (1 H, dd, J = 4.2, 1.8), 7.98 (1 H, d, J = 8.2), 8.00 (1 H, d, J = 8.2), 8.02 (1 H, d, J = 8.5), 8.11 (1 H, dd, J = 8.0, 1.8).

^{13}C NMR (125 MHz, $CDCl_3$): 120.56 (d), 124.13 (d), 124.20 (s), 124.66 (d), 125.99 (d), 126.01 (d), 126.23 (d), 126.29 (s), 126.35 (d), 127.15 (d), 127.48 (d), 127.83 (d), 128.11 (d), 128.69 (s), 129.80 (s), 130.96 (s), 131.15 (s), 131.85 (s), 133.01 (s), 133.21 (s), 135.07 (d), 145.84 (s), 146.73 (d).

IR ($CHCl_3$): 3050 w, 2279 vw, 1613 w, 1598 w, 1574 w, 1553 w, 1515 w, 1496 w, 1397 w, 1366 w, 1304 w, 1262 w, 1134 m, 1115 m, 1096 m, 1076 m, 1040 m, 1027 m, 834 vs.

EI MS: 331 (M$^{+\cdot}$, 100), 330 (89), 329 (35), 304 (27), 303 (21), 302 (28), 256 (7), 164 (17), 151 (10), 111 (8), 97 (12), 83 (15), 69 (27), 57 (30), 43 (27). Electrospray ionization mass spectra imply a deuterium incorporation of (80.5 ± 1.5) atom-% D in the 7- and 8-positions.

HR EI-MS: calculated for $C_{25}H_{13}D_2N$, *m/z* = 331.1330; found, *m/z* = 331.1335.
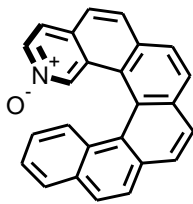
Benzo[5,6]phenanthro[3,4-*h*]isoquinoline 2-oxide 107. The Schlenk flask was charged with azahelicene (*P*)-(+)-**85** (30 mg, 125 μmol) and filled with argon. CH$_2$Cl$_2$ (3 ml) was added, the solution was cooled to 0°C and MCPBA (40 mg, 232 μmol, 1.9 equiv.) in CH$_2$Cl$_2$ (3 ml) was added dropwise. The reaction mixture was stirred at room temperature for 24 h. The resulting solution was washed with saturated NaHCO$_3$ (3 x 10 ml) and brine (10 ml). After drying over MgSO$_4$, the solvent was removed *in vacuo* and the crude product was chromatographed on silica gel (CH$_2$Cl$_2$-methanol 80:20) to provide desired N-oxide (+)-**107** (25 mg, 80 %) as a yellow solid.

^{1}H NMR (500 MHz, CDCl$_3$): 6.90 (1 H, ddd, *J* = 8.5, 6.8, 1.4), 7.40 (1 H, ddd, *J* = 8.0, 6.8, 1.1), 7.63 (1 H, ddt, *J* = 8.5, 1.1, 0.7, 0.7), 7.69 (1 H, dt, *J* = 6.9, 0.6, 0.6), 7.83 (1 H, bd, *J* = 8.5), 7.91 (1 H, dd, *J* = 6.9, 1.7), 7.95 (1 H, d, *J* = 8.6), 7.95 (1 H, ddt, *J* = 8.0, 1.3, 0.6, 0.6), 7.99 (1 H, dd, *J* = 8.1, 0.4), 8.01 (1 H, dt, *J* = 8.6, 0.7, 0.7), 8.02 (1 H, dd, *J* = 8.1, 0.6), 8.05 (1 H, dd, *J* = 8.1, 0.4), 8.06 (1 H, dd, *J* = 8.5, 0.5), 8.11 (1 H, dd, *J* = 8.1, 0.5), 8.45 (1 H, dt, *J* = 1.7, 0.7, 0.7).

^{13}C NMR (125 MHz, CDCl$_3$): 123.36 (s), 123.61 (d), 124.50 (s), 125.01 (d), 125.20 (d), 126.15 (d), 126.65 (d) (two carbon atoms), 126.84 (d), 126.99 (d), 126.99 (s), 127.53 (s), 128.59 (d), 128.63 (s), 128.67 (d), 129.12 (d), 129.31 (d), 129.85 (d), 132.26 (s), 132.49 (s), 132.52 (s), 133.53 (s), 135.65 (d), 137.26 (d).

IR (CHCl$_3$): 3050 w,1604 w, 1579 w, 1548 w, 1507 w, 1496 w, 1475 w, 1439 w, 1408 w, 1399 w, 1249 w, 1143 m, 1120 m, 1095 m, 1049 m, 1037 m, 846 w.

EI MS: 345 (M$^{+\cdot}$, 10), 329 (100), 300 (76), 287 (6), 164 (8), 150 (22), 137 (5), 109 (6), 97 (14), 83 (16), 69 (30), 55 (36), 43 (39).

HR EI MS: calculated for C$_{25}$H$_{15}$NO 345.1154; found 345.1157.

Optical rotation: [α]$^{25}_D$ +3 139 (c 0.002, CH$_2$Cl$_2$).
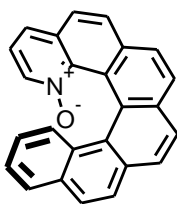
Benzo[5,6]phenanthro[3,4-*h*]quinoline 1-oxide 108. The Schlenk flask was charged with azahelicene (*M*)-(-)-**84** (30 mg, 125 μmol) and filled with argon. CH$_2$Cl$_2$ (3 ml) was added, the solution was cooled to 0°C and MCPBA (40 mg, 232 μmol, 1.9 eq.) in CH$_2$Cl$_2$ (3 ml) was added dropwise. The reaction mixture was stirred at

room temperature for 24 h. The resulting solution was washed with saturated NaHCO$_3$ (3 x 10 ml) and brine (10 ml). After drying over MgSO$_4$, the solvent was removed *in vacuo* and the crude product was chromatographed on silica gel (CH$_2$Cl$_2$-methanol 80:20) to provide desired N-oxide (-)-**108** (11 mg, 35%) as a yellow solid and recovery of azahelicene (*M*)-(-)-**84** (14 mg, 47 %).

^{1}H NMR (500 MHz, CDCl$_3$): 6.57 (1 H, ddd, *J* = 8.4, 6.9, 1.4), 6.98 (1 H, ddt, *J* = 8.5, 1.2, 0.7, 0.7), 7.07 (1 H, dd, *J* = 7.9, 6.2), 7.18 (1 H, ddd, *J* = 8.0, 6.9, 1.2), 7.52 (1 H, dd, *J* = 6.2, 1.4), 7.82 (1 H, dd, *J* = 7.9, 1.4), 7.89 (1 H, ddt, *J* = 8.0, 1.4, 0.5, 0.5), 7.91 (1 H, dd, *J* = 8.6, 0.6), 7.98 (1 H, dd, *J* = 8.5, 0.5), 8.00 (1 H, d, *J* = 8.5), 8.01 (1 H, dd, *J* = 8.0, 0.5), 8.04 (1 H, d, *J* = 8.2), 8.06 (1 H, d, *J* = 8.2), 8.10 (1 H, d, *J* = 8.6), 8.24 (1 H, dd, *J* = 8.0, 0.5).

^{13}C NMR (125 MHz, CDCl$_3$): 119.70 (s), 120.71 (d), 123.41 (d), 123.74 (s), 123.88 (d), 124.61 (d), 125.23 (d), 125.61 (d) (two carbon atoms), 125.67 (d), 126.40 (d), 127.85 (d), 127.87 (d), 128.40 (d), 129.15 (s), 129.53 (d), 129.92 (d), 130.07 (s) (two carbon atoms), 130.90 (s), 131.66 (s), 131.72 (s), 133.69 (s), 135.48 (d), 140.15 (s).

IR (CHCl$_3$): 3050 w, 1554 w, 1512 w, 1494 w, 1466 w, 1409 w, 1246 m, 1125m, 1076 m, 1040 m, 1020 m, 845 m.

EI MS: 345 (M$^{+\cdot}$, 1), 329 (9), 256 (9), 178 (11), 161 (7), 149 (20), 136 (8), 129 (12), 111 (14), 97 (28), 83 (38), 69 (91), 55 (89), 41 (100).

HR EI MS: calculated for C$_{25}$H$_{15}$NO 345.1154; found 345.1165.

Optical rotation: [α]$^{25}_D$ -3 035 (c 0.002, CH$_2$Cl$_2$).

Asymmetric kinetic resolutions

Asymmetric kinetic resolution of (±)-1-phenylethanol with (*M*)-(-)-1-aza[6]helicene 84 as a catalyst.

The Schlenk flask was charged with *M*)-(-)-**84** (8 mg, 24 µmol, 10 mol %) and put under argon atmosphere. CDCl$_3$ (1 ml), (±)-1-phenylethanol (30 mg, 30 µl, 0.250 mmol) and i-Pr$_2$NEt (24 mg, 18 µl, 0.188 mmol, 0.75 equiv.) were added in turn to the flask and the resulting solution was stirred for 15 min. Then the reaction was started with addition of isobutyric anhydride (27 mg, 28 µl, 0.188 mmol, 0.75 equiv.). The progress of acylation was checked periodically by withdrawing a small

aliquot of the reaction mixture, diluting it with $CDCl_3$ and analyzing by ^1H NMR (integrating benzylic protons of alcohol and ester)[112]. After 48 h conversion of the reaction was <5 %.

Asymmetric kinetic resolution of (±)-1-phenylethanol with (*M*)-(-)-2-aza[6]helicene 85 as a catalyst.

The Schlenk flask was charged with (*M*)-(-)-**85** (8 mg, 24 µmol, 10 mol %) and put under argon atmosphere. $CDCl_3$ (1 ml), (±)-1-phenylethanol (30 mg, 30 µl, 0.250 mmol) and i-Pr$_2$NEt (24 mg, 18 µl, 0.188 mmol, 0.75 equiv.) were added in turn tothe flask and resulting solution was stirred for 15 min. Then the reaction was started with addition of isobutyric anhydride (27 mg, 28 µl, 0.188 mmol, 0.75 equiv.). The progress of acylation was checked periodically by withdrawing a small aliquot of the reaction mixture, diluting it with $CDCl_3$ and analyzing by ^1H NMR (integrating benzylic protons of alcohol and ester)[112]. After 24 h the reaction stopped at 21 % conversion. Another portion of (*M*)-(-)-**85** (8 mg, 24 µmol, 10 mol %), i-Pr$_2$NEt (24 mg, 18 µl, 0.188 mmol, 0.75 equiv.) and isobutyric anhydride (27 mg, 28 µl, 0.188 mmol, 0.75 equiv.) was added. Another addition of i-Pr$_2$NEt (24 mg, 18 µl, 0.188 mmol, 0.75 equiv.) and isobutyric anhydride (27 mg, 28 µl, 0.188 mmol, 0.75 equiv.) was carried out after 48 h. After 68 h conversion of the reaction was 65 %. The reaction mixture was worked up and analysed according to the reported procedure[112]. Enantiomeric excess of remaining alkohol was 92 % with the preference for (*R*) optical isomer. Acylated product's enantiomeric excess was determined after basic hydrolysis to be 50 % with the preference for (*S*) optical isomer.

X-ray single crystal analyses

X-Ray Analysis of 1-Aza[6]helicene 84. Racemic azahelicene **84** (4 mg) was refluxed in heptane (2 ml) until dissolved. The resulting solution in a capped vial was placed in a Dewar flask filled with hot water. The sample was allowed to cool to room temperature over the period of 3 days. Single crystals of **84** were separated; $C_{25}H_{15}N$, M_r = 329.38; orthorhombic, space group *Pbca*, a = 9.8414 (4) Å, b = 15.8948 (7) Å, c = 21.6929 (9) Å; Z = 8, D_{calc} 1.289 Mgm^{-3}; dimensions of yellow crystal 0.61 × 0.58 × 0.47 mm^3; X-ray data were measured on CCD

detector with MoK$_\alpha$ radiation, T=150(2) K; θ_{max} = 26.7°; 36819 diffractions collected, 3574 independent (R$_{int}$ = 0.110); an absorption neglected (μ = 0.08 mm^{-1}). Refinement method: full matrix least squares based on F^2, 235 parameters, goodness of fit 1.08, final R indices [I > 2σ(I)] R1=0.059, wR2(all data) = 0.191, maximal/minimal residual electron density 0.33/-0.27 eÅ^{-3}.

X-Ray Analysis of 2-Aza[6]helicene 85. Dichloromethane was added dropwise to a slurry of racemic azahelicene **85** (4 mg) in refluxing heptane (2 ml) until the solid was dissolved. The resulting solution in a capped vial was placed in a Dewar flask filled with hot water. The sample was allowed to cool to room temperature over the period of 3 days. Single crystals of **85** were separated; C$_{25}$H$_{15}$N, M_r = 329.38; monoclinic, space group $P2_1/c$, a = 16.542 (2) Å, b = 15.035 (5) Å, c = 14.245 (2) Å, ψ = 112.793 (14)° ; Z = 8, D$_{calc}$ 1.340 Mgm^{-3}; dimensions of yellow crystal 0.34 × 0.14 × 0.03 mm^3; X-ray data were measured on CCD detector with MoKα radiation, T=150(2) K; θ_{max} = 25.1°; 20975 diffractions collected, 5809 independent (R$_{int}$ = 0.066); an absorption neglected (μ = 0.08 mm^{-1}). Refinement method: full matrix least squares based on F^2, 469 parameters, goodness of fit 0.64, final R indices [I > 2σ(I)] R1=0.034, wR2(all data) = 0.067, maximal/minimal residual electron density 0.13/-0.16 eÅ^{-3}.

X-Ray Analysis of [Ag(1-aza[6]helicene)$_2$(PrOH)][OTf] 112. A solution of racemic azahelicene **84** (2 mg, 6.08 µmol) in toluene (1 ml) was added to a solution of AgOTf (1 mg, 3.89 µmol, 0.64 equiv.) in toluene (1 ml) at room temperature. Immediate precipitation of a complex occurred. The solvent was removed *in vacuo* and heptane (2 ml) was added. Propanol was added dropwise to a refluxing mixture of the complex in heptane until the solid was dissolved. The resulting solution in a capped vial was placed in a Dewar flask filled with hot water. The sample was allowed to cool to room temperature over the period of 3 days. Single crystals of **112** were separated; C$_{53}$H$_{38}$AgN$_2$O·CF$_3$O$_3$S, M_r = 975.79; monoclinic, space group $P\,2_1/n$,, a = 18.174 (2) Å, b = 12.728 (2) Å, c = 18.724 (3) Å, ψ = 103.738 (12)°; Z = 4, D$_{calc}$ 1.541 Mgm^{-3}; dimensions of colourless crystal 0.3 × 0.19 × 0.08 mm^3; X-ray data were measured on CCD detector with MoKα

radiation, T=150(2) K; θ_{max} = 26.6°; 55741 diffractions collected, 8781 independent (R_{int} = 0.025); an absorption neglected (μ = 0.60 mm^{-1}). Refinement method: full matrix least squares based on F^2, 587 parameters, goodness of fit 1.10, final R indices [I > 2σ(I)] R1= 0.027, wR2(all data) = 0.077, maximal/minimal residual electron density 1.21/-0.50 eÅ^{-3}.

X-Ray Analysis of Ag(2-aza[6]helicene)₂][OTf] 111. A solution of racemic azahelicene **85** (2 mg, 6.08 µmol) in toluene (1 ml) was added to a solution of AgOTf (1 mg, 3.89 µmol, 0.64 equiv.) in toluene (1 ml) at room temperature. Immediate precipitation of a complex occurred. The heterogeneous mixture was refluxed until the solid dissolved. The resulting solution in a capped vial was placed in a Dewar flask filled with hot water. The sample was allowed to cool to room temperature over the period of 3 days. Single crystals of **111** were separated; $C_{51}H_{30}AgF_3N_2O_3S \cdot C_7H_8$, M_r = 1007.83; monoclinic, space group $P 2_1/n$,, a = 12.5583 (3) Å, b = 12.9296 (4) Å, c = 28.3045 (14) Å, $\mathcal{V}$ = 101.716 (3)°; Z = 4, D_{calc} 1.488 Mgm^{-3}; dimensions of colourless crystal 0.31 × 0.19 × 0.07 mm^3; X-ray data were measured on CCD detector with MoKα radiation, T=150(2) K; θ_{max} = 26.0°; 27399 diffractions collected, 8920 independent (R_{int} = 0.038); an absorption neglected (μ = 0.56 mm^{-1}). Refinement method: full matrix least squares based on F^2, 587 parameters, goodness of fit 1.07, final R indices [I > 2σ(I)] R1= 0.056, wR2(all data) = 0.159, maximal/minimal residual electron density 1.15/-0.66 eÅ^{-3}. The correction for twinning (matrix -1 0 0, 0 -1 0, 1 0 1) were applied during refinement. The solvating toluene molecule is disordered over two possitions.

Optical resolutions of azahelicenes

Optical resolution of 1-aza[6]helicene 84. Optical resolution of racemic azahelicene **84** via diastereoisomeric salts was attempted using mandelic, malic, tartaric, di-O-toluoyltartaric, 10-camphorsulfonic, and Mosher acids without success. Eventually, we succeeded with (+)-di-O-benzoyltartaric acid, applied in large excess. Under these conditions, the acid formed with racemic **84** a yellow, diastereoisomerically enriched solid. It contained the respective components in a

2:1 ratio. Crystallisation of this adduct was not practical and thus it was purified only by boiling in diethyl ether (liberated (+)-**84** exhibited about 95 % ee). After basification, (+)-**84** was crystallised from diethyl ether-pentane to give optically pure (+)-**84**. The laevorotatory enantiomer was obtained from the mother liquors using the enantiomeric (-)-di-O-benzoyltartaric acid and the above-mentioned procedure.

For more experimental details on 1-aza[6]helicene **84** resolution see[113].

(+)-1-Aza[6]helicene 84. Mp 209-211 °C (the pure enantiomer completely racemized at the melting point), $[\alpha]^{25}_D$ +3 615 (c 0.001, CH_2Cl_2), retention time 10.5 min (Chiralcel OD-H column).

(-)-1-Aza[6]helicene 84. Mp 212-213 °C (the pure enantiomer completely racemized at the melting point). $[\alpha]^{25}_D$ -3 631 (c 0.001, CH_2Cl_2), retention time 9.1 min (Chiralcel OD-H column).

Optical resolution of 2-aza[6]helicene 85. In HPLC on a Chiralcel OD-H column both enantiomers of racemic azahelicene **85** differed significantly in their retention times and, therefore, they were separated in a semipreparative way on an overloaded analytical column or semipreparative (Eurocel 01).

For more experimental details on 2-aza[6]helicene **85** resolution see[113].

(-)-2-Aza[6]helicene 85:   Mp 251-252 °C (the pure enantiomer completely racemized at the melting point). $[\alpha]^{25}_D$ -3 840 (c 0.001, CH_2Cl_2), retention time 9.4 min (Chiralcel OD-H column).

(+)-2-Aza[6]helicene 85:   Mp 250-252 °C (the pure enantiomer completely racemized at the melting point). $[\alpha]^{25}_D$ +3 825 (c 0.001, CH_2Cl_2), retention time 20.1 min (Chiralcel OD-H column).

Optical resolution of [7,8-d_2]-**84**. In HPLC on a Eurocel 01 column, both enantiomers of 1-aza[6]helicene differ enough in their retention times to be separated in a semipreparative way. Racemic azahelicene [7,8-d_2]-**84** (4 mg) was resolved by repeated HPLC separations using an Agilent 1100 Series preparative instrument (heptane-isopropanol 3:1, 19 ml/min flow rate, 0.5 mg injections of the racemate in 600 μl eluent). Evaporation of the solvents afforded (*M*)-(-)-[7,8-d_2]-**84** (1 mg, >99 % ee, retention time 9.2 min.) and (*P*)-(+)-[7,8-d_2]--**84** (1.5 mg, >99 % ee, retention time 10.7 min) as yellowish crystals.

Racemisation kinetics experiments

Racemisation of 1-aza[6]helicene 84. Optically pure (+)-**84** (2 mg, >99 % ee) in 1-decanol (2 ml) was distributed in 20 vials, that were heated to a constant temperature (413 K) using a thermostat (Block-Heater H 250, Rotilabo). The content of (+)-**84** (*P*, %) was monitored by HPLC (Chiralcel OD-H column) in the course of time (s).

Data: 1-aza[6]helicene at 413 K
Model: ExpDec1
Equation: y = A1*exp(-x/t1) + y0
Weighting:
y   No weighting

Chi^2/DoF   = 0.07996
R^2   = 0.99974

y0   48.65674   ±0.28038
A1   50.9378   ±0.2852
t1   6227.26398   ±94.90461
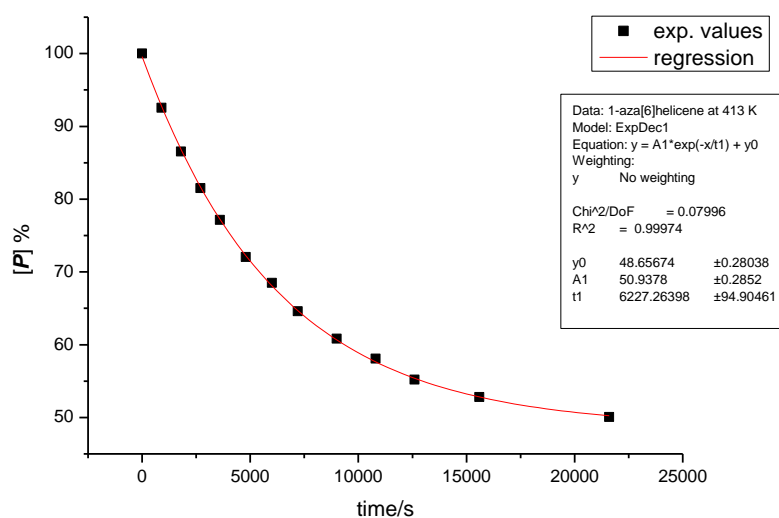
T (in K)	413
solvent	1-decanol
$\Delta G^{\neq}$ (in kJ/mol)	134.8 ± 0.1
$t_{1/2}$ (in min)	71.9
k_i (in s^{-1})	8.03 ± 0.12 × 10^{-5}

Racemisation of 2-aza[6]helicene 85. Optically pure (+)-**85** (2 mg, >99 % ee) in 1-decanol (2 ml) was distributed in 20 vials, that were heated to a constant temperature (461 K) using a thermostat (Block-Heater H 250, Rotilabo). The

content of (+)-**85** (*P*, %) was monitored by HPLC (Chiralcel OD-H column) in the course of time (s).

Data: 2-aza[6]helicene at 461 K
Model: ExpDec1
Equation: y = A1*exp(-x/t1) + y0
Weighting:
y   No weighting

Chi^2/DoF   = 1.45058
R^2   = 0.995

y0	48.14578	±1.19779
A1	50.17445	±1.18601
t1	2802.81978	±179.59003
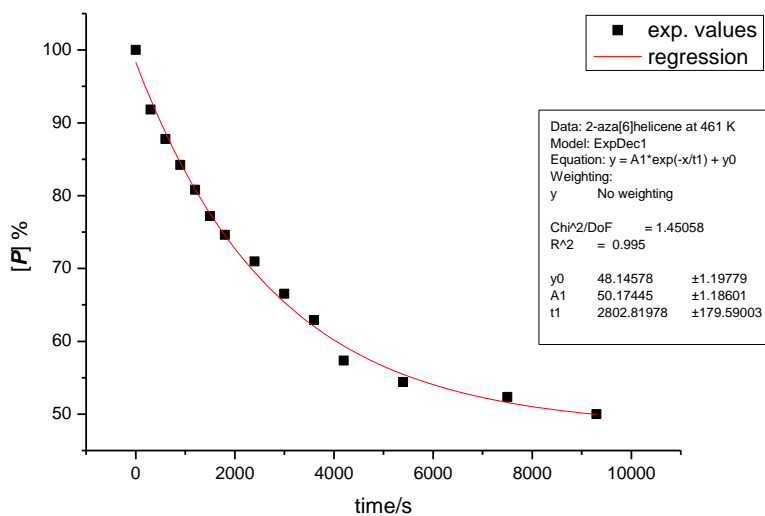
T (in K)	461
solvent	1-decanol
$\Delta G^{\neq}$ (in kJ/mol)	147.7 ± 0.3
$t_{1/2}$ (in min)	32.4
k_i (in s^{-1})	$1.80 \pm 0.12 \times 10^{-4}$

Racemisation of 1-aza[6]helicenium BF$_4$ - [84-H$^+$][BF$_4^-$]. Optically pure (-)-1-aza[6]helicene **84** (0.5 mg, 1.52 µmol, >99 % ee) was dissolved in 1-butyl-2,3-dimethylimodazolium tetrafluoroborate (2 ml) and HBF$_4$ (54 wt. % in Et$_2$O, 230 µl, 1.67 mmol, 1099 equiv.)   was added. The resulting solution was distributed in 12 vials, that were heated to a constant temperature (461 K) using a thermostat (Block-Heater H 250, Rotilabo). The content of (-)-1-aza[6]helicene **84** (*M*, %) was monitored by HPLC (Chiralcel OD-H column) in the course of time (s) after basic work-up.

Data: 1-aza[6]helicenium BF4 at 461K
Model: ExpDec1
Equation: y = A1*exp(-x/t1) + y0
Weighting:
y   No weighting

Chi^2/DoF   = 0.414
R^2   = 0.99866

y0   49.67399   ±0.48599
A1   50.84464   ±0.62669
t1   1187.00456   ±36.03533
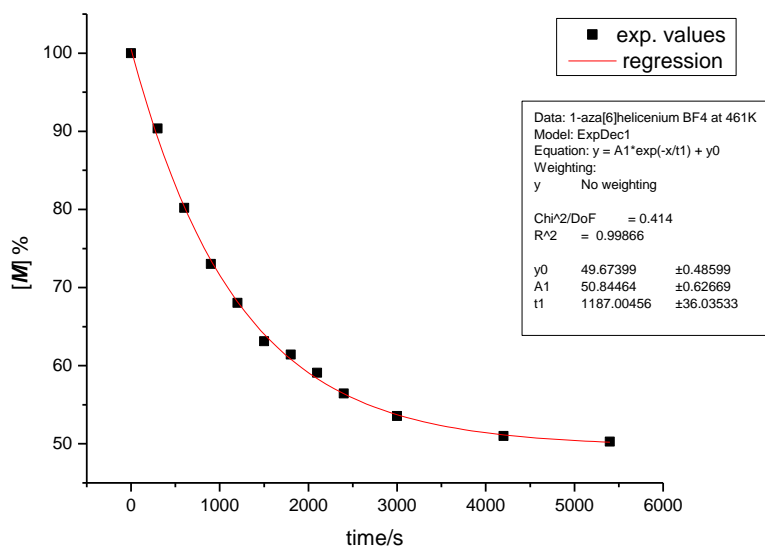
T (in K)	461
$\Delta G^{\neq}$ (in kJ/mol)	144.4 ± 0.1
$t_{1/2}$ (in min)	13.7
k_i (in s^{-1})	4.21 ± 0.13 × 10^{-4}

Racemisation of 2-aza[6]helicenium BF$_4$ - [85-H$^+$][BF$_4^-$]. Optically pure (-)-2-aza[6]helicene **85** (0.5 mg, 1.52 µmol, >99 % ee) was dissolved in 1-butyl-2,3-dimethylimodazolium tetrafluoroborate (2 ml) and HBF$_4$ (54 wt. % in Et$_2$O, 230 µl, 1.67 mmol, 1099 equiv.)   was added. The resulting solution was distributed in 12 vials, that were heated to a constant temperature (461 K) using a thermostat (Block-Heater H 250, Rotilabo). The content of (-)-2-aza[6]helicene **85** (*M*, %) was monitored by HPLC (Chiralcel OD-H column) in the course of time (s) after basic work-up.

Data: (-)-2-aza[6]helicenium BF4 at 461K
Model: ExpDec1
Equation: y = A1*exp(-x/t1) + y0
Weighting:
y   No weighting

Chi^2/DoF   = 0.21712
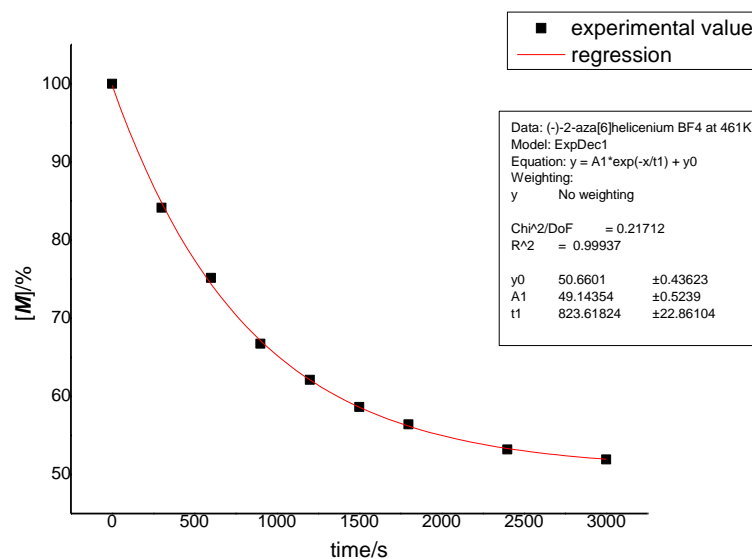R^2   = 0.99937

y0   50.6601   ±0.43623
A1   49.14354   ±0.5239
t1   823.61824   ±22.86104

T (in K)	461
$\Delta G^{\neq}$ (in kJ/mol)	143.0 ± 0.1
$t_{1/2}$ (in min)	9.5
k_i (in s^{-1})	$6.08 \pm 0.17 \times 10^{-4}$

Gas phase complexation study. The mass spectrometric experiments were performed with a Waters Micromass ZQ mass spectrometer equipped with an ESI source. The silver(I)-bound dimers of the azahelicene ligands, i.e., compounds **84**, **85**, or [7,8-d_2]-**84**, were generated from mmolar acetone solutions of the azahelicenes and silver(I) triflate, which were introduced to the ESI source via a syringe pump (ca. 5 μl/min) using nitrogen as a sheath gas. The ionization conditions were kept soft in order to enhance the formation of bisligated metal-cation complexes. For the evaluation of possible stereochemical effects in the formation of silver(I)-bound dimers of the azahelicenes, the ion intensities of the corresponding mass region in the source spectra were modeled in a stepwise procedure as detailed elsewhere[94, 114]. To this end, acetone solutions of the pure azahelicenes were subjected ESI as a first step in order to establish the isotope

envelopes of the signals due to the protonated bases and for the determination of the deuterium content of the labeled samples. Next, a mixture of a chiral, non-labeled azahelicene with one enantiomer of [7,8-d_2]-**84** was prepared and the mixing ratio was determined by numerical fitting of the overlapping isotope clusters of the protonated molecules. Finally, silver(I) triflate was added to the solution and the resulting isotope cluster of the silver(I)-bound ions of the type [LAgL']$^+$ (L, L' = azahelicenes) was analyzed by numerical modeling of the experimentally observed isotope patterns. Additional collision-induced dissociation experiments of the ions described below were recorded using a TSQ Classic mass spectrometer in order to confirm their assignment as genuine silver(I)-bound dimers.

Gas phase proton bound dimers study. For exact experimental details see[115].

Gas phase proton affinities study. For exact experimental details see[97].

Basicities of azahelicenes in methanol. For exact experimental detail see[104].

Abbreviations

Ac	acetyl
AIBN	azobisisobutyronitrile
BOP	[2'-(benzyloxy)-1,1'-binaphthalen-2-yl](diphenyl)phosphane
CAN	cerium(IV) ammonium nitrate
CD	circular dichroism
COD	1,5-cyclooctadiene
Cp	cyclopentadienyl
DBTA	*O,O*'-dibenzoyltartaric acid
DDQ	1,2-dicyano-4,5-dichlorobenzoquinone
de	diastereomeric excess
DFT	density functional theory
DNA	deoxyribonucleic acid
ee	enantiomeric excess
Et	ethyl
Grubbs 2nd	benzylidene[1,3- bis(2,4,6-trimethylphenyl)-2-imidazolidinylidene]dichloro(tricyclohexylphosphine)ruthenium
GS	ground state
HMPA	hexamethylphosphoramide
HPLC	high-performance liquid chromatography
hv	irradiation
i-Pr	isopropyl
KHMDS	potassium hexamethyldisilazane
LDA	lithium diisopropylamide
LiHMDS	lithium hexamethyldisilazane
MCPBA	*m*-chloroperoxybenzoic acid
Me	methyl
Me-Duphos	1,1'-benzene-1,2-diylbis(2,5-dimethylphospholane)
Mp	melting point
NBS	*N*-bromosuccinimide
n-Bu	n-butyl
NMR	nuclear magnetic resonance
op	optical purity

rt	room temperature
TAPA	2-(2,4,5,7-tetranitro-9*H*-fluoren-9-ylideneamino-oxy)propanoic acid
Tf	trifluoromethanesulfonyl
THF	tetrahydrofuran
TIPS	triisopropylsilyl
TLC	thin layer chropmatography
TMS	trimethylsilyl
TS	transition state
UV	ultra violet
VAZO	1,1'-azobis-(cyclohexanecarbonitrile)

Reference List

1. Watson, J. D.; Crick, F. H. C. *Nature* **1953,** *171* (4356), 737.

2. Iwaura, R.; Hoeben, F. J. M.; Masuda, M.; Schenning, A. P. H. J.; Meijer, E. W.; Shimizu, T. *J. Am. Chem. Soc.* **2006,** *128* (40), 13298.

3. Jonkheijm, P.; van der Schoot, P.; Schenning, A. P. H. J.; Meijer, E. W. *Science* **2006,** *313* (5783), 80.

4. Onouchi, H.; Okoshi, K.; Kajitani, T.; Sakurai, S. I.; Nagai, K.; Kumaki, J.; Onitsuka, K.; Yashima, E. *J. Am. Chem. Soc.* **2008,** *130* (1), 229.

5. Maeda, T.; Furusho, Y.; Sakurai, S. I.; Kumaki, J.; Okoshi, K.; Yashima, E. *J. Am. Chem. Soc.* **2008,** *130* (25), 7938.

6. Goto, H.; Furusho, Y.; Yashima, E. *J. Am. Chem. Soc.* **2007,** *129* (29), 9168.

7. Katz, T. J. *Angew. Chem. Int. Ed.* **2000,** *39*, 1921.

8. Schmuck, C. *Angew. Chem. Int. Ed.* **2003,** *42*, 2448.

9. Martin, R. H. *Angew. Chem. Int. Ed.* **1974,** *13*, 649.

10. Newman, M. S.; Lednicer, D. *J. Am. Chem. Soc.* **1956,** *78* (18), 4765-.

11. Wood, C. S.; Mallory, F. B. *J. Org. Chem.* **1964,** *29* (11), 3373.

12. Flammang, M.; Nasielsk, J.; Martin, R. H. *Tetrahedron Lett.* **1967,** (8), 743.

13. Liu, L. B.; Yang, B. W.; Katz, T. J.; Poindexter, M. K. *J. Org. Chem.* **1991,** *56* (12), 3769.

14. Phillips, K. E. S.; Katz, T. J.; Jockusch, S.; Lovinger, A. J.; Turro, N. J. *J. Am. Chem. Soc.* **2001,** *123* (48), 11899.

15. Paruch, K.; Vyklicky, L.; Katz, T. J.; Incarvito, C. D.; Rheingold, A. L. *J. Org. Chem.* **2000,** *65* (25), 8774.

16. Dreher, S. D.; Paruch, K.; Katz, T. J. *J. Org. Chem.* **2000,** *65* (3), 806.

17. Nuckolls, C.; Katz, T. J.; Katz, G.; Collings, P. J.; Castellanos, L. *J. Am. Chem. Soc.* **1999,** *121* (1), 79.

18. Katz, T. J.; Liu, L. B.; Willmore, N. D.; Fox, J. M.; Rheingold, A. L.; Shi, S. H.; Nuckolls, C.; Rickman, B. H. *J. Am. Chem. Soc.* **1997,** *119* (42), 10054.

19. Dai, Y. J.; Katz, T. J.; Nichols, D. A. *Angew. Chem. Int. Ed.* **1996,** *35* (18), 2109.

20. Willmore, N. D.; Hoic, D. A.; Katz, T. J. *J. Org. Chem.* **1994,** *59* (7), 1889.

21. Liu, L. B.; Katz, T. J. *Tetrahedron Lett.* **1990,** *31* (28), 3983.

22. Gingras, M.; Dubois, F. *Tetrahedron Lett.* **1999,** *40* (7), 1309.

23. Dubois, F.; Gingras, M. *Tetrahedron Lett.* **1998,** *39* (28), 5039.

24. Rajca, A.; Wang, H.; Pink, M.; Rajca , S. *Angew. Chem. Int. Ed.* **2000,** *39*, 4481.

25. Harrowven, D. C.; Nunn, M. I. T.; Fenwick, D. R. *Tetrahedron Lett.* **2002,** *43* (41), 7345.

26. Tepl7, F.; Star8, I. G.; Star7, I.; Kollarovi4, A.; Šaman, D.; Rulíšek, L.; Fiedler, P. *J. Am. Chem. Soc.* **2002,** *124* (31), 9175.

27. Nakano, K.; Hidehira, Y.; Takahashi, K.; Hiyama, T.; Nozaki, K. *Angew. Chem. Int. Ed.* **2005,** *44* (43), 7136.

28. Collins, S. K.; Grandbois, A.; Vachon, M. P.; Cote, J. *Angew. Chem. Int. Ed.* **2006,** *45* (18), 2923.

29. Zhang, Y. Z.; Petersen, J. L.; Wang, K. K. *Org. Lett.* **2007,** *9* (6), 1025.

30. Ichikawa, J.; Yokota, M.; Kudo, T.; Umezaki, S. *Angew. Chem. I nt. Ed.* **2008,** *47* (26), 4870.

31. Martin, R. H. *Chimia* **1975,** *29* (3), 137.

32. Rau, H.; Schuster, O. *Angew. Chem. Int. Ed.* **1976,** *15* (2), 114.

33. Staab, H. A.; Diehm, M.; Krieger, C. *Tetrahedron Lett.* **1994,** *35* (45), 8357.

34. Deshayes, K.; Broene, R. D.; Chao, I.; Knobler, C. B.; Diederich, F. *J. Org. Chem.* **1991,** *56* (24), 6787-6795.

35. Bazzini, C.; Brovelli, S.; Caronna, T.; Gambarotti, C.; Giannone, M.; Macchi, P.; Meinardi, F.; Mele, A.; Panzeri, W.; Recupero, F.; Sironi, A.; Tubino, R. *Eur. J. Org. Chem.* **2005,** (7), 1247.

36. Caronna, T.; Gabbiadini, S.; Mele, A.; Recupero, F. *Helv. Chim. Acta* **2002,** *85* (1), 1.

37. Murguly, E.; McDonald, R.; Branda, N. R. *Org. Lett.* **2000,** *2* (20), 3169.

38. Field, J. E.; Hill, T. J.; Venkataraman, D. *J. Org. Chem.* **2003,** *68* (16), 6071.

39. Aloui, F.; El Abed, R.; Marinetti, A.; Hassine, B. *Tetrahedron Lett.* **2008,** *49* (26), 4092.

40. Harrowven, D. C.; Guy, I. L.; Nanson, L. *Angew. Chem. Int. Ed.* **2006,** *45* (14), 2242.

41. Stará, I. G.; Starý, I.; Tichý, M.; Závada, J.; Hanuš, V. *J. Am. Chem. Soc.* **1994,** *116* (12), 5084.

42. Carreno, M. C.; Garcia-Cerrada, S.; Sanz-Cuesta, M. J.; Urbano, A. *Chem. Comm.* **2001,** (16), 1452.

43. Carreno, M. C.; Garcia-Cerrada, S.; Urbano, A. *J. Am. Chem. Soc.* **2001,** *123* (32), 7929.

44. Carreno, M. C.; Garcia-Cerrada, S.; Urbano, A. *Chem. -Eur. J.* **2003,** *9* (17), 4118.

45. Ogawa, Y.; Toyama, M.; Karikomi, M.; Seki, K.; Haga, K.; Uyehara, T. *Tetrahedron Lett.* **2003,** *44* (10), 2167.

46. Tanaka, K.; Suzuki, H.; Osuga, H. *J. Org. Chem.* **1997,** *62* (13), 4465.

47. Stará, I. G.; Alexandrová, Z.; Teplý, F.; Sehnal, P.; Starý, I.; Šaman, D.; Budešínský, M.; Cvačka, J. *Org. Lett.* **2005,** *7* (13), 2547.

48. Stará, I. G.; Starý, I.; Kollarovič, A.; Teplý, F.; Vyskočil, S.; Šaman, D. *Tetrahedron Lett.* **1999,** *40* (10), 1993.

49. Tanaka, K.; Kamisawa, A.; Suda, T.; Noguchi, K.; Hirano, M. *J. Am. Chem. Soc.* **2007,** *129* (40), 12078.

50. Laleu, B.; Mobian, P.; Herse, C.; Laursen, B. W.; Hopfgartner, G.; Bernardinelli, G.; Lacour, J. *Angew. Chem. Int. Ed.* **2005,** *44* (12), 1879.

51. Goedicke, C. *Tetrahedron Lett.* **1970,** (12), 937.

52. Martin, R. H.; Marchant, M. J. *Tetrahedron Lett.* **1972,** (35), 3707.

53. Martin, R. H.; Marchant, M. J. *Tetrahedron* **1974,** *30* (2), 347.

54. Janke, R. H.; Haufe, G.; Wurthwein, E. U.; Borkent, J. H. *J. Am. Chem. Soc.* **1996,** *118* (25), 6031.

55. Lindner, H. J. *Tetrahedron* **1975,** *31* (3), 281.

56. Yamada, K.; Nakagawa, H.; Kawazura, H. *Bull. Chem. Soc. Jpn.* **1986,** *59* (8), 2429.

57. Benhassine, B.; Gorsane, M.; Pecher, J.; Martin, R. H. *Bull. Soc. Chim. Belg.* **1986,** *95* (7), 557.

58. Reetz, M. T.; Beuttenmuller, E. W.; Goddard, R. *Tetrahedron Lett.* **1997,** *38* (18), 3211.

59. Sato, I.; Yamashima, R.; Kadowaki, K.; Yamamoto, J.; Shibata, T.; Soai, K. *Angew. Chem. Int. Ed.* **2001,** *40* (6), 1096.

60. Dreher, S. D.; Katz, T. J.; Lam, K. C.; Rheingold, A. L. *J. Org. Chem.* **2000,** *65* (3), 815.

61. Boersma, A. J.; Klijn, J. E.; Feringa, B. L.; Roelfes, G. *J. Am. Chem. Soc.* **2008,** *130* (35), 11783.

62. Coquiere, D.; Feringa, B. L.; Roelfes, G. *Angew. Chem. Int. Ed.* **2007,** *46* (48), 9308.

63. Roelfes, G.; Feringa, B. L. *Angew. Chem. Int. Ed.* **2005,** *44* (21), 3230.

64. Roelfes, G.; Boersma, A. J.; Feringa, B. L. *Chem. Comm.* **2006,** (6), 635.

65. Hasegawa, T.; Furusho, Y.; Katagiri, H.; Yashima, E. *Angew. Chem. Int. Ed.* **2007,** *46* (31), 5885.

66. Reetz, M. T.; Sostmann, S. *Tetrahedron* **2001,** *57* (13), 2515.

67. Weix, D. J.; Dreher, S. D.; Katz, T. J. *J. Am. Chem. Soc.* **2000,** *122* (41), 10027.

68. Yamamoto, K.; Ikeda, T.; Kitsuki, T.; Okamoto, Y.; Chikamatsu, H.; Nakazaki, M. *J. Chem. Soc. -Perkin Trans. 1* **1990,** (2), 271.

69. Nakazaki, M.; Yamamoto, K.; Ikeda, T.; Kitsuki, T.; Okamoto, Y. *J. Chem. Soc. -Chem. Comm.* **1983,** (14), 787.

70. Xu, Y.; Zhang, Y. X.; Sugiyama, H.; Umano, T.; Osuga, H.; Tanaka, K. *J. Am. Chem. Soc.* **2004,** *126* (21), 6566.

71. Schwartz, T.; Rould, M. A.; Lowenhaupt, K.; Herbert, A.; Rich, A. *Science* **1999,** *284* (5421), 1841.

72. Eaton, D. F. *Science* **1991,** *253* (5017), 281.

73. Epstein, A. J.; Miller, J. S. *Synthetic Met.* **1996,** *80* (2), 231.

74. Zhang, Q. M.; Li, H. F.; Poh, M.; Xia, F.; Cheng, Z. Y.; Xu, H. S.; Huang, C. *Nature* **2002,** *419* (6904), 284.

75. Pendry, J. B. *Science* **2004,** *306* (5700), 1353.

76. Verbiest, T.; Van Elshocht, S.; Kauranen, M.; Hellemans, L.; Snauwaert, J.; Nuckolls, C.; Katz, T. J.; Persoons, A. *Science* **1998,** *282* (5390), 913.

77. Field, J. E.; Muller, G.; Riehl, J. P.; Venkataraman, D. *J. Am. Chem. Soc.* **2003,** *125* (39), 11808.

78. Rebek, J.; Costello, T.; Wattley, R. *J. Am. Chem. Soc.* **1985,** *107* (25), 7487.

79. Mandal, A. B.; Augustine, J. K.; Quattropani, A.; Bombrun, A. *Tetrahedron Lett.* **2005,** *46* (36), 6033.

80. Teplý, F.; Stará, I. G.; Starý, I.; Kollarovič, A.; Šaman, D.; Vyskočil, S.; Fiedler, P. *J. Org. Chem.* **2003,** *68* (13), 5193.

81. Fu, P. P.; Harvey, R. G. *Chem. Rev.* **1978,** *78* (4), 317.

82. Stará, I. G.; Starý, I.; Kollarovič, A.; Teplý, F.; Vyskočil, S.; Šaman, D. *Tetrahedron Lett.* **1999,** *40* (10), 1993.

83. Klapars, A.; Buchwald, S. L. *J. Am. Chem. Soc.* **2002,** *124* (50), 14844.

84. Vávra, J.; Streinz, L.; Vodička, P.; Budešínský, M.; Koutek, B. *Synlett* **2002,** (11), 1886.

85. Newman, M. S.; Darlak, R. S.; Tsai, L. *J. Am. Chem. Soc.* **1967,** *89* (24), 6191.

86. Lightner, D. A.; Powers, T. W.; Truebloo, K. N.; Frank, G. W.; Hefelfin, D. T. *J. Am. Chem. Soc.* **1972,** *94* (10), 3492.

87. Malkov, A. V.; Orsini, M.; Pernazza, D.; Muir, K. W.; Langer, V.; Meghani, P.; Kocovsky, P. *Org. Lett.* **2002,** *4* (6), 1047.

88. de Rango, C.; Tsoucaris, G. *Cryst. Struc. Comm.* **1973,** *2*, 189.

89. Beurskens, P. T.; Beurskens, G.; van den Hark, Th. E. M. *Cryst. Struc. Comm.* **1976,** *5*, 241.

90. Taylor, R.; Kennard, O.; Versichel, W. *J. Am. Chem. Soc.* **1983,** *105* (18), 5761.

91. Murrayrust, P.; Glusker, J. P. *J. Am. Chem. Soc.* **1984,** *106* (4), 1018.

92. Cech, N. B.; Enke, C. G. *Mass Spectrometry Reviews* **2001,** *20* (6), 362.

93. Glorius, F. *Angew. Chem. nt. Ed.* **2004,** *43* (26), 3364.

94. Schröder, D.; Schwarz, H. *Diastereoselective effects in gas-phase ion chemistry;* SPRINGER-VERLAG BERLIN: BERLIN, 2003.

95. Staab, H. A.; Zirnstein, M. A.; Krieger, C. *Angew. Chem. Int. Ed.* **1989,** *28* (1), 86.

96. Cooks, R. G.; Wong, P. S. H. *Acc. Chem. Res.* **1998,** *31* (7), 379.

97. Roithová, J.; Schröder, D.; Míšek, J.; Stará, I. G.; Starý, I. *J. Mass Spectrom.* **2007,** *42* (9), 1233.

98. *http://webbook. nist. gov/chemistry/* **2008**.

99. Garrido, G.; de Nogales, V.; Rafols, C.; Bosch, E. *Talanta* **2007,** *73* (1), 115.

100. Jia, Z. J. *Curr. Pharm. Anal.* **2005,** *1* (1), 41.

101. Koval, D.; Kašička, V.; Jiráček, J.; Collinsova, M. *Electrophoresis* **2006,** *27* (23), 4648.

102. Solinová, V.; Kašička, V.; Koval, D.; Česnek, M.; Holý, A. *Electrophoresis* **2006,** *27* (5-6), 1006.

103. Rived, F.; Roses, M.; Bosch, E. *Anal. Chim. Acta* **1998,** *374* (2-3), 309-.

104. Ehala, S.; Míšek, J.; Stará, I. G.; Starý, I.; Kašička, V. *J. Sep. Sci.* **2008,** *31* (14), 2686.

105. Tunon, I.; Silla, E.; Pascualahuir, J. L. *J. Am. Chem. Soc.* **1993,** *115* (6), 2226.

106. Weast, R. C. *CRC Handbook of Chemistry nad Physics* **1988**.

107. Kagan, H. B.; Fiaud, J. C. *Topics in Stereochemistry* **1988,** *18*, 249.

108. Sih, C. J.; Wu, S. H. *Topics in Stereochemistry* **1989,** *19*, 63.

109. Reetz, M. T.; Wang, L. W.; Bocola, M. *Angew. Chem. Int. Ed.* **2006,** *45* (8), 1236.

110. Vedejs, E.; Daugulis, O. *J. Am. Chem. Soc.* **1999,** *121* (24), 5813.

111. Ruble, J. C.; Latham, H. A.; Fu, G. C. *J. Am. Chem. Soc.* **1997,** *119* (6), 1492.

112. Birman, V. B.; Jiang, H. *Org. Lett.* **2005,** *7* (16), 3445.

113. Míšek, J.; Teplý, F.; Stará, I. G.; Tichý, M.; Šaman, D.; Císařová, I.; Vojtíšek, P.; Starý, I. *Angew. Chem. Int. Ed.* **2008,** *47* (17), 3188.

114. Schröder, D.; Wesendrup, R.; Hertwig, R. H.; Dargel, T. K.; Grauel, H.; Koch, W.; Bender, B. R.; Schwarz, H. *Organometallics* **2000,** *19* (13), 2608.

115. Míšek, J.; Stará, I. G.; Starý, I.; Roithová, J.; Schröder, D. *Croat. Chem. Acta* **2008,** submitted. (see appendix)

Appendix

The following appendix contains two manuscripts of submitted articles of the author.